UNIVERSITA' DEGLI STUDI DI MILANO-BICOCCA

Doctoral School of Sciences

PhD in Biology

Cycle XXVI

Genetic Mechanisms of Maize Development: from Gametophyte to Flowers

Supervisor: Dr. Massimo LABRA

PhD thesis by:

Silvia FEDERICI

Matr. N. 055175

Academic years 2011-2013

Alla mia famiglia

To my family

TABLE OF CONTENTS

ABSTRACT

Zea mays L. is one of the world's most agronomically important crop. The understanding of the molecular basis of inflorescences architecture and seed development may be useful for agronomic purposes. The major goal of this research is to investigate different aspect of maize development to shed light on the genetic mechanisms involved in the formation of maize inflorescences as well as seed development.

In the first part of my thesis, the mechanisms regulating inflorescences development have been investigated by studying a new *barren* mutant, *barren inflorescence173* (*bif173*). The recessive mutant *bif173* is affected in the formation of axillary meristems, showing defects in inflorescences development, such as a reduction in the number of spikelets and branches in the tassel and smaller and more disorganized ears. The phenotype of this mutant is not fully penetrant and its severity seems to be related to temperature or light changes. Also, we demonstrated that *bif173*, like other *barren* mutants, is involved in auxin biology and may play a role in auxin signaling. In order to identify the gene responsible of *bif173* mutation, a RNA-seq analysis was carried out to closely examine a mapping region previously identified and one SNP

present only in *bif173* mutant transcripts was found. This SNP represents a non-synonymous mutation in the coding region of the gene GRMZM2G038401, causing a change of a very conserved amino acid in the encoded protein. This gene encodes a metalloprotease, homologous to the FtsH ATP-dependent metalloproteases, a conserved family of membrane-bound proteases. The ubiquitous localization of the GRMZM2G038401 transcripts seems to be consistent with the numerous functions of these proteases. As evidence that GRMZM2G038401 gene is a good candidate for *bif173* mutation is the fact that the SNP found in the RNA-seq reads was not present in teosinte and other maize inbred lines, suggesting that it is not a polymorphism due to the genetic variability among maize background. In order to confirm that GRMZM2G038401 is the gene responsible for *bif173* mutation, plants homozygous for a transposon insertion are currently growing and if the phenotype resembles the *bif173* mutant phenotype, this gene will be confirmed as the causative gene. This finding will shed light on the molecular mechanisms regulating inflorescences development in maize and will increase our knowledge in auxin biology.

In the second part of my thesis, genetic mechanisms acting in

seed development have been investigated, particularly focusing on gametogenesis and embryogenesis. In *A. thaliana, DME* is a gene encoding a DNA glycosylase/lyase, active in the central cell of the female gametophyte before fertilization. The role of this enzyme is essential for the viability of the seed, in fact, acting as a demethylase, it activates the expression of maternal alleles, establishing imprinting in the endosperm. Here, two *DME* homologues in maize were identified: *ZmDME1* and *ZmDME2*. The proteins encoded by these genes showed a high homology with *A. thaliana* DME and a conserved protein structure characteristic of the DME family. A phylogenetic analysis also suggested that these proteins have a common evolutionary origin. The expression of these genes was found in different stages of gametogenesis, previously identified through a morphological analysis. *ZmDME1* and *ZmDME2* showed a different expression pattern compared to *A. thaliana DME*, i.e. the expression was not only found in the mature gametophyte containing the central cell, but also in the embryo and endosperm and in all the vegetative tissues tested. Furthermore, the localization of the expression of *ZmDME1* and *ZmDME2* in the mature gametophyte was detected not only in the central cell but also in the other cells of the embryo

sac and in the nucellus. In *A. thaliana dme* mutants produce non viable seeds, with enlarged endosperm and aborted embryos. A functional analysis using *zmdme1* mutant plants revealed no defects in vegetative and reproductive phases, producing all normal-shaped seeds. A morphological analysis of these mutants showed that gametogenesis and embryogenesis occur normally. Nevertheless, further analyses are needed to verify the function of these genes.

Even if the lack of DME orthologues in monocots has been previously hypothesized, recent findings suggest that a similar mechanism of DNA demethylation may take place in monocot gametophyte. Thus, we discuss about the possibility that ZmDME1 and ZmDME2 may be responsible of active demethylation in maize gametophyte, allowing the proper development of embryo and endosperm.

GENERAL INTRODUCTION

Zea mays L. ssp. *mays,* commonly referred to as maize, is a monocotyledonous species belonging to the tribe Andropogoneae of the family Poaceae. The grasses originated 55-70 million years ago (mya) and subsequently diversified to include all the major cereal crop species in addition to nearly 10,000 non-domesticated relatives (Kellogg, 2001; Bolot et al., 2009). The closest wild relatives of domesticated maize are the teosintes, the annual and perennial grasses of the genus *Zea* that are indigenous to Mexico and Central America (Fukunaga et al., 2005). Maize diverged from its teosinte ancestor between 6000 and 9000 years ago (Matsuoka et al., 2002).

Zea mays is one of the world's most agronomically important crop and has been also a keystone model organism for basic research for nearly a century (Strable and Scanlon, 2009). Several attributes of the maize plant, including a vast collection of mutant stocks, large heterochromatic chromosomes, extensive nucleotide diversity, and genic collinearity within related grasses, have positioned this species as a centerpiece for genetic, cytogenetic, and genomic research (Strable and Scanlon, 2009). Also, the fully sequenced maize genome and other genetic resources and molecular tools are now available.

Maize kernel morphology and composition are quantitative traits of immense agronomic and nutritional importance. A single-seeded fruit, the large and prominent maize kernel has been the focus of hundreds of genetic analyses of morphological and biochemical mutants (Strable and Scanlon, 2009). Inflorescence morphology is one of the major factors for controlling crops yield, bacause of its influence to seed number and ability to harvest (Satoh-Nagasawa et al., 2006). For this reason, the comprehension of genetic and molecular mechanisms that regulate inflorescence morphology, the development of reproductive structure and the reproduction are of paramount importance.

Maize inflorescences have unique features for developmental and morphological studies. Maize is a monoecious plant with unisexual male and female flowers borne on separate stems. This physical separation of flowers is particularly amenable to genetic analysis, facilitates controlled pollinations (Strable and Scanlon, 2009) and allows to study male and female development separately (Bortiri and Hake, 2007). Maize inflorescences are also unique due to their complex network of branching events, which is the result of different evolutionary mechanisms in grasses.

Since characters of inflorescences and flowers are closely associated with traits for grain yield, understanding the molecular basis of inflorescences architecture and seed development in maize may be useful for agronomic purposes. Also, elucidating the genetic control of maize inflorescences is important to understand mechanisms acting in grass developmental biology and to shed light on the evolutionary processes in monocots and angiosperms in general.

In my graduate project I analyzed different aspects of maize development. Because of the importance of both inflorescences and seeds in maize, the major goal of my research was to increase the understanding of the genetic mechanisms regulating the formation of maize inflorescences as well as gametogenesis and embyogenesis. In particular, in chapter I, I describe the characterization of a new *barren* mutant, *barren inflorescence173* (*bif173*). The recessive mutant *bif173* was originally identified in an EMS mutagenesis screen targeting mutants affected in the formation of axillary meristems. *bif173* mutants are characterized by defective inflorescence development, such as a reduction in the number of spikelets and branches in the tassel and smaller and more disorganized ears. Also, *bif173* mutant seems to be temperature-sensitive

and, like other *barren* mutants, *bif173* seems to be involved in auxin pathway. The identification of the causative gene of this mutation is pivotal to shed light on the genetic regulation of axillary meristems and the molecular mechanisms and pathways required for maize inflorescence development.

In chapter II, due to the agronomic and nutritional importance of maize kernels, I focus on maize reproduction and in particular on gametogenesis and embryogenesis. Genetic mechanisms acting in these specific stages of maize development and the morphology of both female gametophyte (embryo sac) and embryo have been studied. In particular, the presence and the role of *A. thaliana DEMETER* (*DME*) homologues in maize have been investigated.

DME is a gene encoding a DNA glycosylase/lyase, active in the central cell of the female gametophyte before fertilization and capable of activating the expression of maternal alleles through DNA active demethylation, establishing imprinting in the endosperm (Gehring et al., 2009a; Hsieh et al., 2009; Bauer and Fischer, 2011). In *A. thaliana dme* mutants produce non viable seeds, with enlarged endosperm and aborted embryos (Choi et al., 2002). Here I focus on the identification and characterization of *DME* homologues in maize.

REFERENCES

Bauer JM, Fischer RL. 2011. Genome demethylation and imprinting in the endosperm. *Current Opinion in Plant Biology* **14,** 1-6

Bolot S, Abrouk M, Masood-Quraishi U, Stein N, Messing J, Feuillet C, Salse J. 2009. The inner circle of the cereal genomes. *Current Opinion in Plant Biology* **12,** 119–125.

Bortiri E, Hake S. 2007. Flowering and determinacy in maize. *Journal of Experimental Botany* **58**(5) , 909-916.

Choi Y, Gehring M, Johnson L, Hannon M, Harada JJ, Goldberg RB, Jacobsen SE, Fischer RL. 2002. DEMETER, a DNA glycosylase domain protein, is required for endosperm gene imprinting and seed viability in *Arabidopsis. Cell* **110**, 33–42.

Fukunaga K, Hill J, Vigouroux Y, Matsuoka Y, Sanchez J, Liu K, Buckler ES, Doebley J. 2005. Genetic diversity and population structure of teosinte. *Genetics* **169,** 2241–2254.

Gehring M, Bubb KL, Henikoff S. 2009a. Extensive demethylation of repetitive elements during seed development underlies gene imprinting. *Science* **324**, 1447–51.

Hsieh TF, Ibarra CA, Silva P, Zemach A, Eshed-Williams L, et al. 2009. Genome-wide demethylation of *Arabidopsis* endosperm. *Science* **324**,1451–54

Kellogg EA. 2001. Evolutionary history of the grasses. *Plant Physiololy* **125,** 1198–1205.

Matsuoka Y, Vigouroux Y, Goodman MM, Sanchez GJ, Buckler E, Doebley J. 2002. A single domestication for maize shown by microsatellite genotyping. *Proceedings of the National Academy of Sciences* **99**, 6080–6084.

Satoh-Nagasawa N, Nagasawa N, Malcomber S, Sakai H, Jackson D. 2006. A trehalose metabolic enzyme controls inflorescence architecture in maize. *Nature* **441**, 227-230.

Strable J, Scanlon MJ. 2009. Maize (Zea mays): A model organism for basic and applied research in plant biology. *Cold Spring Harbor Protocols*, doi:10.1101/pdb.emo132.

CHAPTER I

GENETIC REGULATION OF MAIZE INFLORESCENCE DEVELOPMENT

1. INTRODUCTION

1.1 Inflorescence architecture in maize

An inflorescence is a cluster or group of flowers arranged on a stem that is composed of a main branch or a complicated arrangement of branches. Maize plants produce separate male and female inflorescences borne on the same plant, thus maize is a monoecious species (Kiesselbach, 1949) (Fig. 1.1). Both inflorescences have a peculiar architecture with many small spikelets organized in panicles. The spikelet is the basic unit of grass inflorescence architecture and is characterized by an outer and inner glumes that together enclose a variable number of florets (Vollbrecth and Schmidt, 2009) (Fig. 1.2).

The maize male inflorescence, the tassel, is situated at the apex of the mature plant, whereas the female inflorescence, the ear, is produced several nodes below the tassel at the apex of a

compressed branch originating in the axil of one or more leaves (Kiesselbach, 1949) (Fig. 1.1). The mature tassel consists of a symmetrical, many-rowed central axis and several asymmetrical long branches. Both the main spike and the lateral branches bear pairs of spikelets (McSteen et al., 2000). One spikelet is pedicellate and the other one is sessile. Each tassel spikelet consists of two glumes and two florets, an upper and a lower floret. The ear also has a symmetrical, many-rowed axis with paired spikelets, but no long, lateral branches. The presence of a variable number of long branches originating at the base of the typical tassel is the main morphological difference between the two inflorescences. Each ear spikelet produces a pair of glumes surrounding the florets (Fig. 1.2).

In both inflorescences each spikelet includes two florets. Each floret consists of a single lemma (external bract) and palea (internal bract), two lodicules (derived from petals), three stamens and a central pistil consisting of three fused carpels, surrounding a single ovule. The early development of both tassel and ear is similar. Subsequently, during floral development the developing pistil aborts in tassel florets, and the developing stamens undergo a similar fate in ear florets. Additionally, the entire lower floret of each ear spikelet aborts,

soon after initiating floral organ primordia, leaving one pistillate flower per spikelet (Bonnet, 1954; Dellaporta and Calderon-Urrea, 1994; Irish, 1996) (Fig. 1.2).

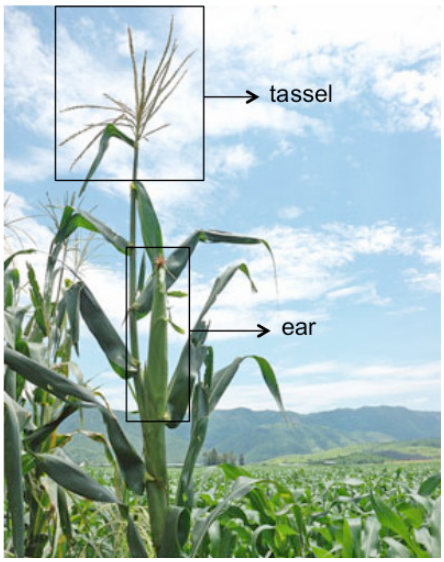

Fig. 1.1: Maize plant. Tassel (male inflorescence) is located at the top, whereas ear (female inflorescences) is located at mid-plant. (image from http://b4fa.org/)

1.2 Meristems in maize inflorescence development

The morphology of a mature plant reflects the activity of meristems, small groups of undifferentiated, self-regenerating cells (Steeves and Sussex, 1989; Weigel and Jurgens, 2002). Two main meristems, the shoot apical meristem (SAM) and the root apical meristem (RAM), establish the main axes of plant growth. The shoot apical meristem (SAM), located at the growing tip of the shoot, is the ultimate source for all aerial structures of the plant, including flowers. The SAM produces organs indeterminately, such that the number, timing and form of organs cannot be precisely predicted. This process is moderated by the environmental and genetic status of the plant, resulting in potentially limitless combinations of organs. This plastic potential is greatly enhanced by the production and activity of axillary meristems (AMs) (Bennet and Leyser, 2006).

The mechanisms regulating axillary meristem initiation in vascular plants are unclear. According to the detached-meristem theory, axillary meristems develop from cells that originate in the shoot apical meristem, while the *de novo* theory suggests that they develop from cells that acquire a meristematic identity. However, both forms of axillary

meristems seem to exist in the same plant (Long and Barton, 2000; Greb et al., 2003; Leyser, 2003; Bennett and Leyser, 2006).

Axillary meristems, formed in the axils of leaf primordia during both vegetative and reproductive development, are secondary meristems and they may be either quiescent or active. When active, they are directly responsible for the formation of secondary axes of growth (Bennet and Leyser, 2006). In maize, these include lateral vegetative branches called tillers, and several specialized axes producing the tassel and ear (Vollbrecht and Schmidt, 2009).

In maize, meristems undergo several distinct transitions in identity during the life of the plant (Irish and Nelson, 1991). The identity of a meristem is defined by the types of structures it produces (McSteen et al., 2000). A major change in the life of a plant occurs during the transition from vegetative to reproductive growth. The switch from vegetative to reproductive growth in maize entails an irreversible transition in which the SAM stops initiating leaves and becomes an inflorescence meristem (IM), committed to the formation of the inflorescences (Fig. 1.2). After the transition to flowering occurs, the maize inflorescences, the tassel and the ear, are

produced. The tassel is formed at the top of the plant, where the inflorescence meristem starts to produce axillary meristems called branch meristems (BMs), which develop into major branches at the base of the mature tassel. Only these first few axillary meristems are indeterminate and committed to form branches. Subsequent meristems are initiated in multiple rows at the top of the tassel and acquire a different identity, that of the spikelet-pair meristem (SPM) (Vollbrecht and Schmidt, 2009). Tassel branches form spikelet pair meristems as well. Branch meristems are considered to have less determinacy due to their capacity for continued growth of the main axis, whereas spikelet-pair meristems are determinate and thus originate short branches (McSteen et al., 2000; Vollbrecht et al., 2005). Each spikelet-pair meristem gives rise to a short branch that bears two spikelet meristems (SMs). The SM produces glume primordia, a distinguishing feature of this particular meristem and then forms two floral meristems, the upper and lower floral meristems (UFM and LFM). Each floral meristem subsequently forms the floral organs (Fig. 1.2).

Each ear also originates from a meristem at the tip of a shoot, in this case a lateral shoot in the axil of a leaf, several nodes below the tassel. The lateral SAM becomes an ear IM within a

few weeks after the floral transition at the tassel. One notable difference between the ear and tassel is that the ear's IM, while producing multiple rows of spikelet pair meristems, does not form any basal branches, because it does not produce BMs. The ear and tassel have distinct morphologies at maturity, but they appear similar at the early stages of their development, since they share common developmental processes and meristems types (Vollbrecht and Schmidt, 2009) (Fig. 1.2).

In conclusion, maize inflorescence development is the result of a hierarchical process. Four types of axillary meristems with different identity and fate, branch meristems (BMs), spikelet-pair meristems (SPMs), spikelet meristems (SMs) and floral meristems (FMs), give rise to structures in the maize inflorescence (Cheng et al., 1983; Irish, 1997; McSteen et al., 2000; Vollbrecht and Schmidt, 2009) (Fig. 1.2).

Thus, in maize, and in grasses in general, there are more classes of AMs than in, for instance, *A. thaliana*, which has only two types of axillary meristem: secondary inflorescence meristems (equivalent to branch meristems) and floral meristems (McSteen et al., 2000).

The complexity of axillary meristem development in maize makes this plant a unique model for inflorescence development

research.

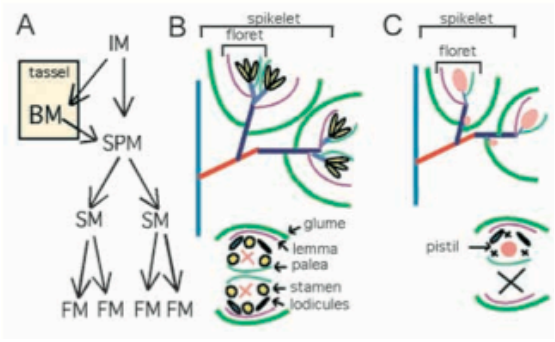

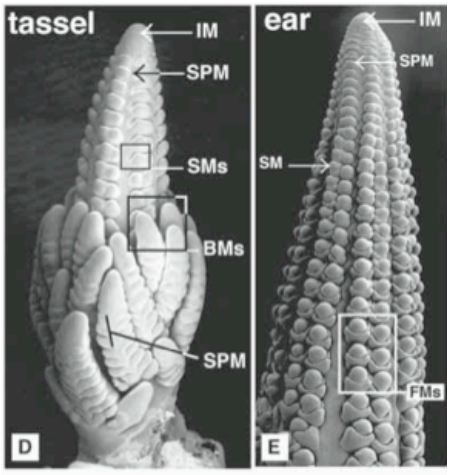

Fig. 1.2: Maize inflorescence development. A, Different meristem types in maize. The inflorescence meristem (IM) forms spikelet pair meristems (SPM) which form two spikelet meristems (SM), each of which forms two floral meristems (FM). Tassels also form branch meristems (BM) at the base. B and C, Schematic of a spikelet pair. Each spikelet contains two glumes and two florets. The mature floret comprises the lemma, a palea, three lodicules, three stamens and a pistil. The pistil aborts in male spikelets (B). All stamens and the lower floret abort in female spikelets (C). D and E, Male and female inflorescences, respectively. The different meristem types are indicated (Laudencia-Chingcuanco and Hake, 2002).

1.3 Genetic regulation of maize inflorescence development

Many genes are involved in the regulation of the inflorescence development and they are grouped in four different classes.

Class I: Genes that control meristem identity

This class includes genes involved in controlling the progressive specification of axillary meristem identity, defining the types of organs a meristem makes (McSteen et al., 2000).
Among these, there are *RAMOSA* genes (*RA1*, *RA2*, *RA3*) which have specific functions in maintaining the determinate identity of the SPMs, limiting branch outgrowth. When any of these three genes is mutated, the SPMs on both tassel and ear become indeterminate like BMs, leading to highly branched inflorescences (Vollbrecht et al., 2005; Bortiri et al., 2006; Satoh-Nagasawa et al., 2006; Bortiri and Hake, 2007).
The transition from spikelet pair meristems to spikelet meristem identity is controlled by *TASSEL SEED4* (*TS4*), while *TASSEL SEED6* (*TS6*) is required for the conversion of spikelet meristems to floret meristems. Both the tassel seed mutations *ts4* and *Ts6* cause irregular branching in tassel and ear (Irish, 1997).

Finally, *BRANCHED SILKLESS1* (*BD1*) is also required for the transition from spikelet to floral meristem identity (Colombo et al., 1998). In *bd1* mutants, the SMs on both inflorescences are indeterminate which led to extra spikelets and florets are absent in the ear. The *bd1* spikelet meristems cannot switch to floral meristem production and, instead, continue to reiterate the formation of glumes and spikelet-like meristems, demonstrating that *BD1* is required for floral meristem identity (Chuck et al., 2002).

Class II: Genes that control meristem determinacy

These are genes involved in meristem determinacy, which defines the number of structures a meristem will make. Indeterminate meristems make an indefinite number of structures, while determinate meristems make a specific number of organs (McSteen et al., 2000).

The best characterized of these genes involved in meristem determinacy is *INDETERMINATE SPIKELET1* (*IDS1*) which was cloned by homology to *APETALA2* (*AP2*) transcription factors. Although *IDS1* is expressed in multiple meristem types, the mutant phenotype affects only the determinacy of the spikelet meristem, and in the mutants multiple florets instead of

two are produced from one spikelet. *IDS1* is a recessive allele of *TS6* and the expression of *TS6*/*IDS1* is regulated by *TS4* post-transcriptionally. In both *ts4* and *Ts6*, *IDS* fails to be properly regulated, resulting in indeterminacy of the spikelet meristem (Chuck et al., 1998; Chuck et al., 2007).

The maize mutant *indeterminate floral apex1* (*ifa1*) affects determinacy of multiple meristem types within the inflorescence. In the *ifa1* mutants the SPMs become indeterminate and initiate extra SMs and the SMs produce more flowers. Although FM development is normal, the carpel becomes indeterminate and continues to proliferate (Laudencia-Chingcuanco and Hake, 2002).

Class III: Genes that control meristem maintenance

In addition to genes that give a meristem its identity, other genes are involved in creating and maintaining the structure of the meristem, allowing the formation of the right type and number of organs defined by the meristem (McSteen et al., 2000).

Alterations of the maintenance of the IM result in an abnormal inflorescence. In *A. thaliana*, *CLAVATA* (*CLV*) pathway genes function together with *WUSCHEL* in regulating stem cell

proliferation (Williams and Fletcher, 2005). In maize, genes related to *CLV* have been identified. *THICK TASSEL DWARF* (*TD1*) gene is orthologous to *CLV1* and mutants have a thicker central spike and ears variably fasciated, due to an enlarged IM (Bommert et al., 2005). The *FASCIATED EAR2* (*FEA2*) gene is homologous to *CLV2* and mutants result in enlarged IMs in both tassel and ear (Taguchi-Shiobara et al., 2001). Both these genes are important in regulating meristem maintenance in maize (Lunde and Hake, 2005).

Other genes control the initiation of axillary meristems and in maize these genes are known as the *barren inflorescence* loci. These genes include *BARREN INFLORESCENCE2* (*BIF2*), *BARREN INFLORESCENCE1* (*BIF1*), *SPARSE INFLORESCENCE1* (*SPI1*), *BARREN STALK1* (*BA1*), *BARREN STALK FASTIGIATE1* (*BAF1*) AND *VANISHING TASSEL2* (*VT2*). *bif2* , *Bif1* and *spi1* mutants have tassels with fewer branches, spikelets, florets and floral organs. All axillary meristems in the inflorescence (BM, SPM, SM, and FM) are affected in the mutants. *bif2* mutant plants produce fewer ears and with fewer kernel rows and total kernel numbers (McSteen and Hake, 2001; McSteen et al., 2007), while *Bif1* mutants do not have defects in the initiation of the axillary meristem that

gives rise to the ear shoot. Ears are produced in *Bif1* mutants as normal (Barazesh and McSteen, 2008). *spi1* loss of function mutants have a dramatic phenotype, with a significant reduction in the number of axillary meristems and lateral organs (Gallavotti et al., 2008).

barren stalk1 (*ba1*) mutant plants are unable to produce vegetative branches (tillers), female inflorescences (ears) and a normal apical male inflorescence, the tassel (Ritter et al., 2002). The tassel of *ba1* mutants is unbranched, shortened and predominantly sterile owing to the often complete lack of spikelets (Gallavotti et al., 2010).

Mutations in *BAF1* give rise to plants that either lack ears or produce fusion defects. The *baf1* mutants are distinct from other *barren* mutants because they are still capable of forming tassels with most branches, spikelets, and florets, whereas they often fail to produce ears (Gallavotti et al., 2011).

vt2 mutants in maize exhibit a severe *barren inflorescence* phenotype with smaller tassels at maturity, lacking lateral branches and functional spikelets. *vt2* mutant ears show obvious defects in length and kernel number with barren patches devoid of kernels often extending along the adaxial side of the ear (Phillips et al., 2011).

There are also other genes that regulate the initiation only of specific meristems, like *UNBRANCHED1* (*UB1*), *LIGULLESS2* (*LG2*), *SUPPRESSOR OF SESSILE SPIKELETS1* (*SOS1*) and *TASSELSHEATH4* (*TSH4*). *UB1*, *LG2* and *SOS1* are genes that affect initiation of specific meristem. *Ub1* mutants cannot initiate branch meristems, so they have tassels with no long branches but normal spikelet development along the central spike (Neuffer et al., 1997). *lg2* also have defects in BM initiation. They either produce no long branches on the tassel or only one or two normal branches (Walsh and Freeling, 1999). Both *ub1* and *lg2* have normal ears. *tsh4* is required in BM initiation and maintenance while *Sos1* only affects the sessile spikelet formation (Wu et al., 2009; Chuck et al., 2010).

Class IV: Genes that control floral organ identity

The final stages of reproductive development is the formation of floral organs. The morphology of maize floret is similar to eudicot flower, which is composed by four floral organs (sepal, petal, stamen and carpel). The maize floral meristem also forms four different types of organs. The leaf-like palea and the reduced lodicule are thought to be analogous to the sepal and

petal, respectively. The lodicules are reduced and hidden at the base of the stamens, where they swell and expand to expose the stamens for wind pollination. The reproductive organs are also similar to those of the eudicots in morphology and function. The male reproductive organ consists in three stamens, while the female one consists of a pistil, composed of three carpels, two of which fuse and elongate to form the silk (McSteen et al., 2000).

A model for the specification of floral organ identity has been proposed for *A. thaliana* and *Antirrhinum* (Bowman et al., 1991; Coen and Meyerowitz, 1991), and since the morphology between maize floret and eudicot flower is similar, the genetic mechanism involved in their development might be conserved in monocots and eudicots (McSteen et al., 2000). According to this model the identity of the floral organs is regulated by the action of three classes of homeotic genes: A, B and C. The A function alone specifies sepal identity, A and B together specify petals, B and C in combination result in stamen development, and C function alone specifies carpels.

In maize, isolation of functional homologues of B- and C-function genes has shown that the specification of organ identity has been conserved (McSteen et al., 2000).

ZAG1 is a MADS-box gene, homologous to the *A. thaliana* C-function gene *AGAMOUS* (*AG*), showing that some aspects of C function have been conserved in maize (Schmidt et al., 1993; Theissen et al., 1995). *zag1* mutants produces sterile silks, reducing the fertility of the ears (Mena et al., 1996).

The *silky1* (*si1*) mutant in maize has a phenotype that is similar to the B-function mutants of *A. thaliana.* The *si1* mutant transforms lodicules to palea-like organs and stamens to carpels (Ambrose, et al., 2000), whereas mutations in B-function genes of *A. thaliana* convert petals to sepals and stamens to carpels (Bowman et al., 1991). This gene is a MADS-box gene homologous to the B-function MADS-box gene *APETALA3* and *si1* mutant phenotype has extra silks on both tassel and ear spikelets (Ambrose et al., 2000).

Genes like *VESTIGIAL GLUME1* (*VG1*), *SILKLESS EARS1* (*SK1*) AND *INDETERMINATE FLORAL APEX1* (*IFA1*) also function in the determinacy of the floral meristem and the formation of floral organs. *Vg1* mutants have normal tassels and ears, but with very small glumes (Vollbrecht and Schmidt, 2009). *sk1* mutants have ears without silks (Parkinson et al., 2007) and *ifa1* mutants have a reduced number of spikelets and

flowers, and ovule primordia proliferate (Laudencia-Chinguanco and Hake, 2002).

To conclude, axillary meristems are initiated from the SAM and IM and are then maintained to guarantee a proper balance between the meristem itself and the initiation of the new organs of the inflorescence. Finally the identity and determinacy of each type of meristems are specified. Inflorescence development is a complex process which involves several genes, specific for the different steps of the development but working together in a precisely regulated network.

1.4 Role of the auxin hormon in axillary meristem initiation

Besides the genetic program of the inflorescence structure, also the surrounding environment plays a crucial role in the final developmental outcome (Gallavotti, 2013). Phytohormones are major determinants for the plant growth and they represent the first line of response to changes in environmental conditions (Vert and Chory, 2011).

One of the hormones that has a major influence of many aspects of plants development is auxin.

The biosyntesis, transport and signaling of auxin play a key role in the determination of plant architecture (Goldsmith, 1993; Benjamins and Scheres, 2008; Vanneste and Friml, 2009; Gallavotti, 2013).

Mutations in genes that are directly involved in auxin biology have been shown to have dramatic effects on the plant development in different species (Tobena-Santamaria et al., 2002; Cheng et al., 2006; Woo et al., 2007; Yamamoto et al., 2007; Gallavotti et al., 2008; Phillips et al., 2011).

In maize, several mutants showing defects in axillary meristem formation are known to be affected in auxin biology, confirming that a proper regulation of auxin pathways is necessary for normal inflorescence development.

The *barren* mutants *sparse inflorescence1* (*spi1*) and *vanishing tassel2* (*vt2*) demonstrate the need for auxin biosynthesis in axillary meristem initiation.

SPARSE INFLORESCENCE1 (*SPI1*) encodes a flavin monooxygenase with similarity to the *YUCCA (YUC)* genes of *A. thaliana,* which catalyze the conversion of indole pyruvic acid to indole acetic acid in the auxin biosynthetic pathway (Zhao et al., 2001). This gene has evolved a very specific and localized role in auxin biosynthesis during maize inflorescence

and vegetative development. *spi1* mutants show defects in the formation of branches, spikelets, florets, and floral organs (Gallavotti et al., 2008). *VANISHING TASSEL2* (*VT2*) encodes a co-ortholog of the TRYPTOPHAN AMINOTRANSFERASE 1 (TAA1) in *A. thaliana*, which converts tryptophan to indole pyruvic acid in auxin biosynthesis pathway. *vt2* mutants have dramatic effects on vegetative and reproductive development and they share many similarities with *spi1* mutants (Phillips et al., 2011).

Other *barren* mutants reveal that also a proper auxin transport is essential for normal inflorescence development.

BARREN INFLORESCENCE2 (*BIF2*) encodes a co-orthologue of the *A. thaliana* PINOID serine-threonine kinase, that is believed to regulate auxin transport in maize. The phenotype of *bif2* mutants is similar to the so-called *A. thaliana* "pinformed" phenotype, showing defects in inflorescence development (Okada et al., 1991; Galweiler et al., 1998). In *A. thaliana*, the "pinformed" inflorescence is generated by a mutation in the gene *PIN1*, encoding one of the members of the PIN family auxin transporters. Mutations in *PINOID* (Friml et al., 2004; Michniewicz et al., 2007) show a phenotype similar to *pin1*.

Barren inflorescence1 (*Bif1*) mutants share many phenotypic

similarities with *bif2* mutants and in *Bif1*;*bif2* double-mutant plants there is a dramatic enhancement of phenotype, indicating that *Bif1* plays a redundant role with *bif2* and they act together in the control of auxin transport in maize inflorescence. This is also demonstrated by the fact that *Bif1* mutants have reduced levels of auxin transport (Barazesh and McSteen, 2008).

Also, the transcription factor BARREN STALK1 (BA1) may function downstream of auxin transport (Wu and McSteen, 2007) and have a role in auxin signaling (Gallavotti et al., 2004). BA1 interacts with BIF2 (Gallavotti et al., 2004; Skirpan et al., 2008) and *ba1* mutants show a phenotype similar to *bif2* mutants, failing to initiate axillary meristems and resulting in plants composed only of a stem and leaves (Ritter et al., 2002).

Furthermore, *spi1*;*bif2* and *vt2*;*bif2* mutants completely lack branches and spikelets in the tassel and plants are severely reduced in size (Gallavotti et al., 2008; Phillips et al., 2011), revealing synergistic interactions between auxin transport and biosynthetic mutants.

This leads to the conclusion that auxin biosynthesis may act in concert with the activity of auxin transporters, as part of a

complex pathway necessary for the formation and activity of axillary meristem.

1.5 Aim of this work

Auxin biology plays a key role in several aspects of plant development. In maize, *barren* mutants demonstrate the crucial role of auxin in the determination of inflorescence architecture.
The identification of new *barren* mutants represents a great contribution to the understanding of molecular mechanisms regulating inflorescence development. Also, the study of these mutants is a potential source to identify new genes functioning in auxin biology.
Here, I introduce a new *barren* mutant, *barren inflorescence173* (*bif173*), a recessive mutant characterized by a classic *barren* phenotype in both the ear and tassel.
The aim of this work is to characterize *bif173* mutant and identify the gene responsible for this mutation, in order to increase our understanding of the molecular mechanisms and pathways required for maize inflorescence development.

2. MATERIALS AND METHODS

2.1 Plant material

Segregating F2 populations *bif173*xB73 as well as *bif173*/*bif173* homozygous mutants were planted in the field during summer 2013 in order to check the segregation of this mutant and the severity of its phenotype. To create *bif173*/*Bif1* double mutants, F1 +/*bif173*;+/*Bif1* plants were crossed to +/bif173 plants and the resulting seeds were grown in the field. A standard F2 population was generated for the analyis of the double *bif173*; *spi1* mutants. These plants were instead grown in the greenhouse. Double mutant phenotype was checked and compared to both single mutants and wild type plants of the same population. *bif173*/B73 plants were grown in the greenhouse during winter 2012-2013 to collect mutants and wild type samples for RNA-seq analysis. Seeds ordered from UniformMu were also planted in the greenhouse.

This part of my work was carried out in the Gallavotti lab at the Waksman Institute of Microbiology, Rutgers University, New Jersey (USA).

2.2 Genotyping

2.2.1 DNA isolation for PCR-genotyping

Fresh leaf tissue was collected and placed in tubes. Extraction buffer (100 mM Tris-HCl pH8, 50 mM EDTA pH8, 500 mM MaCl) was added and after adding metal beads in the tubes, samples were grinded using a SPEX/Sample prep 2000 Geno/grinder. With frozen tissues, the extraction buffer was added after grinding and tissue lyser blocks were kept frozen to prevent the tissue from thawing.

1% SDS and 1% β-Merchaptoethanol were added and samples were placed in waterbath at 65°C. Subsequenlty, 3M Na-acetate was added and samples were put on ice. After adding chloroform-isoamylalchool (24:1), samples were vortexed and kept at room temperature. After centrifuging, the supernatant was transferred to a new tube and isopropanol was added. Tubes were left at room temperature and later centrifuged. Supernatant was removed and pellets were washed with 70% ethanol. After centrifuging at14000 rpm, ethanol was removed and samples were dried and resuspended in water.

2.2.2 DNA isolation for 96-well plate genotyping

A piece of tissue was taken from each plant and placed in a single tube in a 96-well plate. Extraction buffer containing 100 mM Tris pH 8.0, 50 mM EDTA pH 8.0, and 500 mM NaCl solution was added to each tube and caps were securely placed on the plate. The plate was then put into a SPEX/Sample prep 2000 Geno/grinder and ground in 30 sec intervals until all the tissue was broken. 1%SDS and 1% β-Mercaptoethanol were then added to each tube. After incubation the incubation of the plates at 50 °C, cold 5M potassium acetate was added to each tube and the plate was inverted to mix and incubated on ice. The plates were then spun and the supernatant was put into new tubes in a new 96-well plate. Isopropanol was added to each tube and the tubes were inverted to mix. The plates were incubated for at least an hour at -20°C. After, the plates were spun and the supernatant was removed, ensuring that the pellet remained at the bottom of the tube. The pellets were subsequently washed with 70% ethanol. After centrifugation, the ethanol was removed and the plates were dried under a flow hood. Finally, pellets were re-suspended in water.

2.2.3 Molecular markers

To design new molecular markers, mutants and wild type sequences of the predicted region were compared to look for differences. If a polymorphism was present aligning these sequences, this was used to design new primers flanking the region of interest. When indels were found a primer was designed across the insertion/deletion. When SNPs were present, but not resulting in a restriction enzyme site polymorphism, dCAPS markers were designed (http://helix.wustl.edu/dcaps/dcaps.html). These markers artificially intruduce one or more point mutations in order to create a restriction enzyme site that distinguishes the mutant from the wild type allele, after digesting samples with a restriction enzyme. These molecular markers allow to discriminate mutant and wild type plants on agarose gel, creating PCR product of different sizes.

When no polymorphisms were used to design new markers, primers requiring sequencing were designed flanking the region of interest.

To verify the presence of the transposon insertion in the gene of interest, specific primers were designed on each side of the

insertion site. Both forward and reverse were used in combination with a Mu primer, which is an outward-reading primer able to prime from both ends of Mu elements. Primers design was performed using Primer3 (v.0.4.0) (Untergrasser et al., 2012) and using sequences from the online database maizegdb (http://www.maizegdb.org/) (Table 1.1).

Marker Name	Locus	Sequence (5'-3')
TP3	118.16 Chr8	Forward: TGCTTCCAGACGATCACCTGCTAC Reverse: CGTCGTCCAGGTTGTTGATGATGG
49T19	113.8 Chr8	Forward: GTCGCAGCCATGGAATGCTGGAT Reverse: GTCTTGAGCGCCTCCAAGTC
MeP	GRMZM2G038401	Forward: TGCTGGGACAAATAGACCTGACA Reverse: CTTCTCCAAACCACCGATAATCC
MeP-TaqI	GRMZM2G038401	Reverse: GTCAAGGCAGCTAGCCTTCG
38401-F1/38401-MslI-R1	GRMZM2G038401	Forward: CTGGGACAAATAGACCTGACATCCTG Reverse:CGCAGCAATTAAAGCAGCTTCATTACAAACCATGGCAA
MeP-Mu5	GRMZM2G038401	Forward: ATTAGTTGTGGACTGCGATTAGCC Reverse: TCCTTTAGGCACCTCCTTCTTACC
MuTIR6	Insertion TIR sequence	AGAGAAGCCAACGCCAWCGCCTCYATTTCGTC
SPI1-F1/SPI1-TaqI-R1	*SPI1*	Forward: ACAACAACGATGATCGTCTTTCGCTC Reverse:GGATCCGGTCCACCACCCGGTCG
Bif1-F1/R2	*BIF1*	Forward: GCCCACTATAAACTCAACCACCTC Reverse: ATGGTGAAGTGGGAGAAGAACTTG

Table 1.1: Molecular markers used for genotyping.

2.2.4 PCR

Standard Polymerase Chain Reactions (PCR), using Taq Polymerase (NewEngland BioLabs) and according to manufacturer's instructions were performed. Molecular markers indicated in Table 1.1 were used to amplify the region of interest. The PCR reaction was performed using a standard thermal cycling profile, with annealing temperature ranging from 62 to 65°C.

Touch-down PCR was also performed and the annealing temperature tested ranged from 72°C to 60°C, decreasing 1 °C degree at every set of cycles.

Each PCR was visualized using an 1.5% agarose gel using standard TAE or a 3% agarose gel using TBE buffer, depending on the expected size of the PCR product.

When using dCAPs markers, the PCR product was digested with the opportune NEB restriction enzyme (NewEngland BioLabs) (Table 1.2). The reaction was performed according to manifacturer's instructions and the conditions for the reaction varied according to the enzyme selected (Table 1.2).

After the digestion a TAE or a TBE agarose gel was run to visualized the product.

Restriction Enzyme	Digestion protocol
MslI	3 hours at 37°C
TaqαI	2 hours at 65°C

Table 1.2: Digestion enzymes used with a PCR product amplified with dCAPS markers.

2.2.5 Sequencing

When markers required sequencing were used, DNA was purified directly from PCR product using USB ExoSAP-IT PCR Product Cleanup kit (Affymetrix). PCR product was mixed with ExoSAP-IT reagent and incubate first at 37°C and then at 80°C in order to degrade remaining primers and nucleotides and then inactivate ExoSAP-IT reagent. The PCR product was ready for sequencing.

After purification, a premixed reaction for sequencing was prepared. 1.6 pmol/µl of either forward primer or reverse primer and water were added to the purified PCR product. The premixed reaction was sent for sequencing to GenScript (www.genscript.com) or Genewiz Inc. (www.genewiz.com).

2.3 RNA-seq analysis

To identify the *bif173* causative gene an approach based on RNA-seq analysis was carried out. The reason because this approach was chosen is that the *bif173* mutant was created through an EMS mutagenesis and therefore it is likely that the mutation lies in the coding region of a gene, thus it is possible to find it in the transcripts. Also, RNA-seq data will not only help to find the causative SNP in the mutant gene, but the results will provide informations on the global gene expression in the mutant.

2.3.1 Samples

Immature tassels (0.5-1 cm) from plants of an F2 segregating population were collected and dissected at the stereo microscope (Leica M205C), to identify mutant and wild type phenotypes. 236 plants from a self crossed B73/*bif173* population were screened. Tissues were frozen in liquid nitrogen and kept at -80°C. To confirm the phenotype found, leaves from the same plants were collected and genotyped

using markers TP3F/TP3R and 49T19F2/49T19R2 (Table 1.1) Homozygous *bif173* tassels, homozygous wild type tassels of the same F2 population and homozygous Oh43 tassels of the original background were bulked in order to create 3 different pools for the RNA-seq analysis.

2.3.2 RNA extraction

RNeasy Plant Mini Kit (Qiagen) was used for RNA extraction, following manufacturer's instructions. DNase treatment on column was also performed.
Agarose gel using TAE buffer was run to check the quality of the RNA samples. RNA was then quantified by Nanodrop (Nanodrop Lite Spectrophotometer, Thermo Scientific).

2.3.3 RNA-seq

RNA samples were sent for RNA sequencing to the DNA Core Illumina Sequencing Services of the University of Missouri, Columbia, USA. RNAseq libraries were prepared using the TruSeq RNA-seq library prep kit (Illumina) and sequenced on an Illumina HiSeq 2000. Obtained reads were mapped to the

maize B73 v2 genome (ZmB73_AGPv2.fa) using TopHat v2.0.8b (Trapnell et al, 2012) with the following parameters: tophat -p 1 --bowtie1 -G ZmB73_5a.59_WGS_exons.gtf. Mapped reads were visualized using the Integrative Genomics Viewer (IGV; http://www.broadinstitute.org/igv/). Reads within the 1.2 Mb *bif173* mapping window were manually inspected for SNPs and indels relative to the B73 reference genome and Oh43 and wild type sibling samples. This analysis was aided by a custom script to identify all *bif173* SNPs present on chromosome 8, where *bif173* was originally mapped by positional cloning approaches.

2.4 Transposon insertion research

UniformMU (www.maizegdb.org/documentation/uniformmu) and Mu-Illumina (teosinte.uoregon.edu/mu-illumina) resources were used to identify transposon insertions in the gene of interest (GRMZM2G038401). These resources use transposon mutagenesis as a tool for the analysis of gene function, providing knockout mutations in thousands of maize genes. Mapped and heritable insertions were searched online at MaizeGDB (www.maizegdb.org). Using this site, it was

possible to find seed stocks available at the Maize Genetics Stock Center.

Seeds were then grown in the greenhouse and plants were genotyped as described in paragraph 2.2. Primers MeP-MuF5/MeP-MuR5 and MuTIR6 were used for DNA amplification (Table 1.1). Samples were then sequenced to verify the presence of the insertion and the exact insertion site.

2.5 *in situ* hybridization

in situ hybridization was performed in order to localize the expression of the candidate gene (GRMZM2G038401) in the immature wild type tassel.

2.5.1 Tissue collection and fixation

Immature wild type tassels (0.2-0.5 cm) from plants of an F2 segregating population were collected and dissected at the stereo microscope (Leica M205C).

Samples were immediately placed into vials containing a 4% paraformaldehyde solution in PBS buffer (Amersham Biosciences) and kept on ice under vacuum. This step was performed twice and then the fixative was replaced with fresh

one and tissues in vials were placed at 4°C for 36 hours. Fixative was then removed and cold 130 mM NaCl was added. Subsequently, samples were dehydrated in graded ethanol solutions (30%, 50%, 70%, 85%), containing 130 mM NaCl. 85% ethanol was then replaced with cold 95% and 100% ethanol and samples were incubated at 4°C, replacing cold 100% ethanol for approximately 6 times.

2.5.2 Paraffin embedding

Vials were removed from the cold room and allowed to adjust to room temperature. Ethanol was replaced with room temperature 100% ethanol, incubating vials. Ethanol was then replaced with 25:75 histoclear:ethanol and tissues were incubated at room temperature. This step was repeated with 50:50 histoclear:ethanol and with 75:25 histoclear:ethanol. The last solution was then replaced with 100% histoclear. This step was repeated twice. Histoclear was then removed and replaced with fresh histoclear, adding in the vials also 20 paraplast chips and incubating at room temperature overnight. Vials were then placed at 42°C to melt the paraplast chips. New paraplast chips were added and melted until the vials were full.

Histoclear/paraplast mixture was removed and replaced with a new melted paraplast solution. Samples were incubated at 56°C, changing melted paraplast for approximately 6 times.
Tissues were then placed into small metal trays, filled with paraplast solution and covered with a plastic cassette. This step was carried out on a slides warmer and samples were then keep at room temperature before placing them at 4°C. The metal tray was later removed, leaving the tissue embedded in the solidified wax supported by the plastic cassette.

2.5.3 Sectioning and mounting tissue

Tissues embedded in wax were then ready to be sectioned using the microtome (Leica RM2255). Sections of 8 µm were cut and checked at the stereo microscope (Leica M205C). A waterbath was used to stretch out the slices and facilitate the mounting on slides. Probe on Plus Slides (Fisher Scientific) were used for tissues needed for the *in situ* hybridization. Slides were then dried overnight on the slides warmer at 37°C.

2.5.4 Probe synthesis

The open reading frame of GRMZM2G038401 was PCR amplified from cDNA of 0.6 cm B73 tassels using the Phusion DNA polymerase (New England BioLabs), according to the manifacturer's instructions. The forward primer ZM2G038401_CDS_Sfi_FWD (GAATTCGGCCGTCAAGG CCAATGACGCTCGCCTCCCTCGCCCG) and the reverse primer ZM2G038401_CDS_Sfi_REV (AGTCGACGGCCCAT GAGGCCCTACGTGGGTACAACGTCACCAA) were used for the amplification reaction at the annealing temperature of 62°C. The PCR reaction was performed using a standard thermal cycling profile required for the Phusion DNA polymerase.

PCR product was run on an agarose gel and purified using QIAquick Gel Extraction Kit (Qiagen), according to the manifacturer's instructions.

Primers used added SfiI restriction enzyme sites to the PCR amplicon and the resulting PCR product was digested using SfiI (overnight at 50°C). The digested PCR product was gel purified and directionally ligated into the SfiIA and SfiIB sites of pENTR223.1-Sfi using T4 ligase. The ligation reaction was carried out at room temperature and then transformed into

DH5alpha chemically competent cells. Transformed cells were selected on LB+agar+Spectinomycin (50 μg/ml). Colonies from the plates were inoculated in LB+Spec, grown overnight shaking, and plasmid DNA was isolated using the Qiaprep spin miniprep kit (Qiagen), according to manifacturer's instructions. Clones were confirmed by restriction enzyme digestion and end-sequenced with M13F and M13R universal primers.

The plasmid was then cut with XbaI restriction enzyme. The linearized plasmid DNA was run on an agarose gel, purified using QIAquick Gel Extraction Kit (Qiagen) and quantified using a Nanodrop (Nanodrop Lite Spectrophotometer, Thermo Scientific).

The probe was then synthesized from the linearized plasmid from the T7 RNA polymerase promoter. A labeling reaction was performed using the Riboprobe Transcription kit (Promega), according to manifacturer's instructions. Using this kit, DNA was transcribed with T7 RNA and DIG-UTPs were incorporated into the transcripts. DNase treatment was also performed and an aliquot of the reaction before and one after DNase treatment were taken and run on an agarose gel to determine the quality of the RNA after the treatment.

Probe precipitation was subsequently carried out using 3M

NaOAc and 100% EtOH. The reaction was then incubated at -20°C. After centrifuging, the pellet was washed with 70% ethanol and air dried. The probe was then resuspended in deionized water. 2X CO3 Buffer was added for the hydrolysis of probe. The reaction was then incubated at 65°C and later stopped using 10% acetic acid. 20mg/ml yeast tRNA, 3M NaOAc and 100% EtOH were added for a further precipitation. The reaction was kept at -20°C ovenight. After centrifuging, the pellet was washed with 70% ethanol and air dried. The probe was finally resuspended in 50% deionized formamide and stored at -80°C. This probe is a DIG-labeled RNA probe that is immunodetected with anti-digoxigenin conjugated to an alkaline phosphatase. The bound between digoxigenin and antibody conjugate is then visualized with the color substrates NBT/BCIP (Roche).

2.5.5 *in situ* hybridization

Pre-hybridization

Tissue sections mounted on slides (see paragraph 2.5.3) were set in a rack and placed in a jar containing histoclear. This step was repeated once. After deparaffinization, sections were

rehydrated through a graded ethanol series: 100% ethanol twice, 70% ethanol, 50% ethanol and 30% ethanol. After placing slides in water, they were transferred in 2X SSC solution and then in a solution containing 100 mM Tris pH 8, 50 mM EDTA and 1 μg/ml proteinase K. Slides were incubated at 37°C. Later slides were placed in 1X PBS containing 2 mg/ml glycine. Tissues were then washed twice in 1X PBS solution. After transferring the slides in 1X PBS and 3.7% (w/v) formaldehyde, other two washes in 1X PBS were performed. The rack with the slides was then transferred in a jar containing a solution made by 0.1 M triethanolamine pH8 and acetic anhydride. After keeping the slides in this solution, they were washed twice in 1X PBS. Tissues were then ready to be dehydrated through a graded ethanol series: 30% ethanol, 50% ethanol, 70% ethanol and twice in 100% ethanol. Slides were then dried under vacuum.

Hybridization

The probe was added to 50% deionized formamide and it was then heated at 80°C, spinned down and kept on ice. The hybridization solution was then prepared using 10X *in situ* salts (5 M NaCl, 1 M Tris-Cl, 0.5 M EDTA, $NaH_2Po_4*2H_2O$,

Na_2HPO_4), 50% deionized formamide, 50% dextran sulfate preheated at 80°C, 50X Denhardt's solution (1% Ficoll 400, 1% PVP, 1% BSA), yeast tRNA 20 µg/µl. An aliquot of this solution was added for each pair of slides to the probe/formamide solution. After mixing, the solution was applied to the slides, which were later placed into a box humidified using 2X SSC and 50% formamide. The box was kept at 55°C overnight to allow hybridization.

Post-hybridization

Pairs of slides were separated into 0.2X SSC solution prewarmed at 55°C and placed in rack. Slides were then washed twice in 0.2X SSC solution with gentle agitation at 55°C. After placing the slides in 1X PBS solution, they were transferred in block solution containing 1% Boehringer block, 100mM Tris pH 7.5 and 150 mM NaCl. This solution was later replaced with a solution containing 1% BSA, 100mM Tris pH 7.5, 150 mM NaCl and 0.3% Triton X-100. Anti-dig antibody (Roche) was then diluted 1:1250 in the previous BSA/Tris/NaCl/Triton solution and added to slides. After incubating at room temperature in a water humidified box, slides were separated into the BSA/ Tris/NaCl/Triton solution.

Using the same solution, slides were washed 4 times at room temperature and rinsed in a solution containing 100 mM Tris pH 9.5, 100 mM NaCl and 50 mM $MgCl_2$. The substrate solution, to allow the colorimetric reaction, was prepared using NBT/BCIP (Roche) and Tris pH 9.5/NaCl/$MgCl_2$ and it was added to slides. Slides were then placed in a water humidified box and kept overnight in darkness.

Slides were separated and rinsed in TE to stop the reaction and after rinsing with water, they were mounted with coverslips using few drops of Clear-Mount (Electron Microscopy Sciences) and air dried.

Slides were then visualized at the microscope (Leica DM5500B).

The marker *ZYB15* (Juarez et al., 2004) was used as positive control to verify whether the experiment was successful. *ZYB15* expression is observed in initiating suppressed bracts (Whipple et al., 2010).

3. RESULTS

3.1 *bif173* phenotype and segregation

Fig. 1.3: Phenotype of *barren inflorescence173*. a, normal tassel; b, mutant tassels.

bif173 mutants showed a *barren* phenotype, characterized by defective inflorescence development. *bif173* tassels had fewer branches and spikelets (Fig. 1.3), and *bif173* ears were smaller, with fewer kernels and more disorganized rows of kernels (Fig. 1.7). *bif173* tassels showed different degrees of severity (Fig. 1.3 b), ranging from tassels with fewer branches and spikelets to tassels where no branches and spikelets were formed, suggesting that axillary meristem initiation is impaired. Quantitative analysis of the mature tassel phenotype showed that *bif173* mutants have a reduction in branches (Fig. 1.5; Table 1.3) and spikelet pairs number (Fig. 1.6; Table 1.4),

suggesting a defect in BMs and SPMs initiation. Images of a *bif173* immature tassel under a dissecting microscope (Fig. 1.4 a) further showed that axillary meristems fail to initiate when compared to the wild type tassel (Fig. 1.4 b) where a series of SPMs and SMs was initiated.

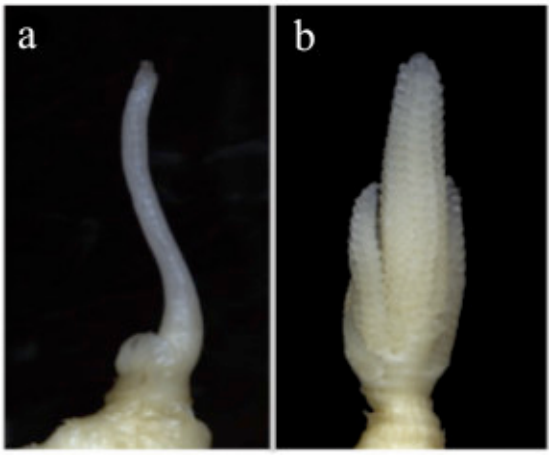

Fig. 1.4: Images of immature tassels at four weeks. a, *bif173* tassel.; b, wild type tassel. In *bif173* immature tassel, axillary meristems fail to form.

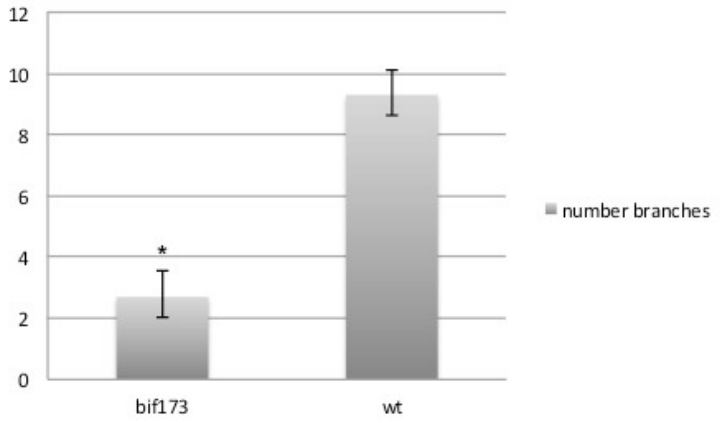

Fig. 1.5: Quantification of the number of branches of *bif173* tassels and normal tassels in the F2 population. The asterisk indicates a statistically significant difference with a p-value < 0.001.

	n. samples	**average**	**standard error**
wild type	10	9.3	±0.66
bif173	10	2.7	±0.82

Table 1.3: Quantification of the number of branches of *bif173* and wild type in the F2 population. Number of tassels used for quantification, average of the number of branches per tassel and standard error are shown. These values refer to Fig. 1.5.

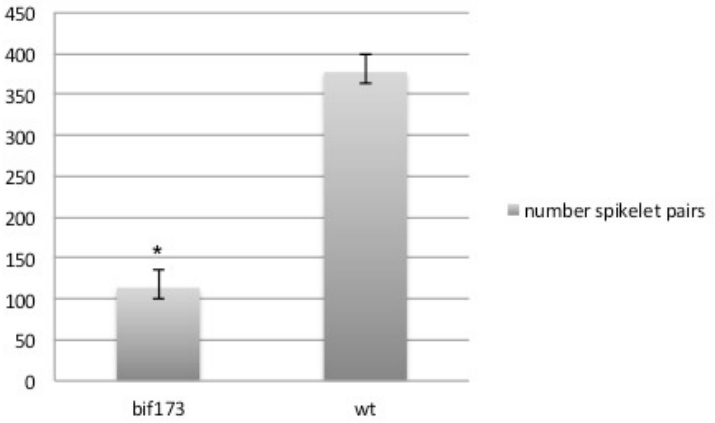

Fig. 1.6: Quantification of the number of spikelet pairs of *bif173* tassels and normal tassels in the F2 population. The asterisk indicates a statistically significant difference with a p-value < 0.001.

	n. samples	**average**	**standard error**
wild type	5	377.6	±22.23
bif173	5	114	±14.72

Table 1.4: Quantification of the number of spikelet pairs of *bif173* and wild type in the F2 population. Number of tassels used for quantification, average of the number of spikelet pairs per tassel and standard error are shown. These values refer to Fig. 1.6.

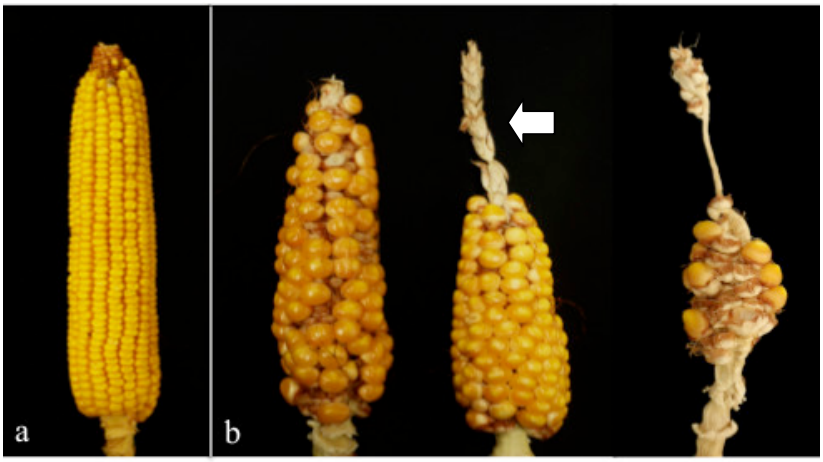

Fig. 1.7: Phenotype of *barren inflorescence173*. a, normal ear; b, mutant ears. The arrow indicates the masculinization of the ear.

Also *bif173* ears showed different degrees of severity of the phenotype, ranging from ears with fewer kernels to masculinized ears, with no kernels at the tip (Fig. 1.7 b). Quantitative analysis of the mature ear phenotype showed that *bif173* mutants display a reduction of size compared to wild type ears (Fig. 1.8; Table 1.5).

Other pleiotropic defects were observed during vegetative development as the plants appear shorter than normal (not shown).

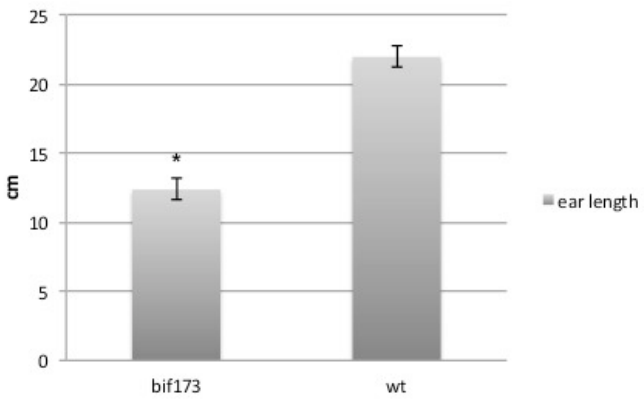

Fig 1.8: Quantification of ear length of *bif173* mutant ears and normal ears in the F2 population. The asterisk indicates a statistically significant difference with a p-value < 0.001.

	n. samples	**average**	**standard error**
wild type	10	21.95	±0.99
bif173	18	12.36	±2.24

Table 1.5: Quantification of ear length of *bif173* mutant ears and normal ears in the F2 population. Number of ears measured, average ear length and standard error are shown. These values refer to Fig. 1.8.

The *bif173* phenotype appears to be incompletely penetrant. In fact, even though *bif173* is a recessive mutation, the percentage of mutants found in different segregating populations was always less than 25% (Table 1.6 and Table 1.7). Also, the percentage of severe mutants appears to vary with the season,

with an higher percentage (10-12%) during the summer and a lower percentage (2-9%) during the winter (Table 1.7), suggesting that the severity of the phenotype might be affected by either temperature, light or general growth conditions (field vs. greenhouse).

F2 B73x*bif173* populations	**# severe mutants**	**# weak and severe mutants**	**Tot # plants**	**% severe mutants**	**% weak and severe mutants**
1	36	43	365	10	12
2	28	39	222	12	17
3	18	30	183	10	16
4	12	19	82	15	23
5	7	19	96	7	20
6	4	9	54	7	17
7	1	3	41	2	7
8	0	2	14	0	14
9	0	5	60	0	8
10	2	6	65	3	9

Table 1.6: Segregation of 10 different F2 B73x*bif173* populations, grown in the field during the summer. Total number of severe mutants, total number of weak and severe mutants, total number of plants, percentage of severe mutants and percentage of weak and severe mutants are indicated.

F2 B73x*bif173* populations		# severe mutants	Tot # plants	% severe mutants
1	Summer	36	365	10
	Winter	6	121	5
2	Summer	28	222	12
	Winter	10	115	9
3	Summer	18	183	10
	Winter	1	60	2

Table 1.7: Percentage of severe *bif173* mutants in three different F2 B73x*bif173* populations, grown in summer and winter.

3.2 Interaction of *bif173* with genes involved in auxin pathway

Several *barren* mutants have been implicated in the biosynthesis, transport or signaling of the plant hormone auxin. Since several *barren* mutants are affected in the auxin pathway, to investigate if this is also the case of *bif173*, *bif173*;*Bif1* and *bif173*;*spi1* double mutants were created.

Bif1 and *spi1* mutants also have a *barren* phenotype with a reduced number of tassel branches, spikelets and florets in both tassels and ears (Barazesh and McSteen, 2008; Gallavotti et al., 2008). These mutants are affected in the signaling and biosynthesis of the plant hormone auxin, respectively (unpublished results; Gallavotti et al., 2008).

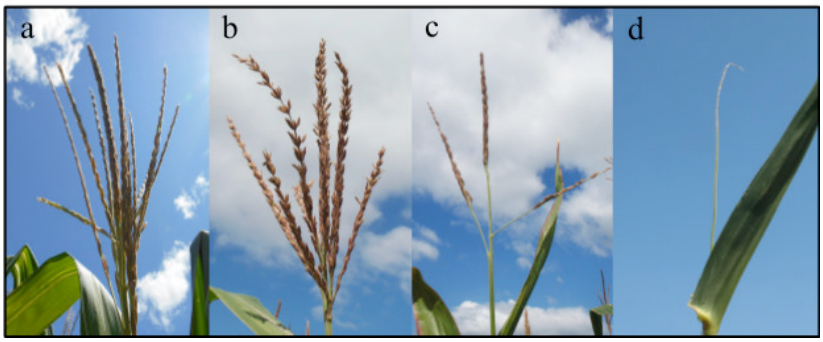

Fig. 1.9: Phenotype of *barren inflorescence173* (*bif173*) and *Barren inflorescence1* (*Bif1*). a, normal tassel; b, mutant *bif173* tassel; c, mutant *Bif1* tassel; d, double mutant *bif173*;*Bif1* tassel.

bif173;*Bif1* double mutants displayed a synergistic phenotype, *bif173/bif173*;*Bif1*/+ mutants produced a completely *barren* tassel, with no branches or spikelets (Fig. 1.9 d). This suggests that axillary meristem initiation is severely affected. Although *bif173* showed a mild phenotype in this F2 population (Fig. 1.9 b), both *bif173* and *Bif1* single mutants had fewer branches and spikelets (Fig. 1.9 b, c), but not nearly as severe as in the double mutants. Quantitative analysis of the mature tassels phenotype confirmed that double mutant plants have a significant reduction in branches (Fig. 1.10; Table 1.8) and spikelet-pair number (Fig. 1.11; Table 1.9).

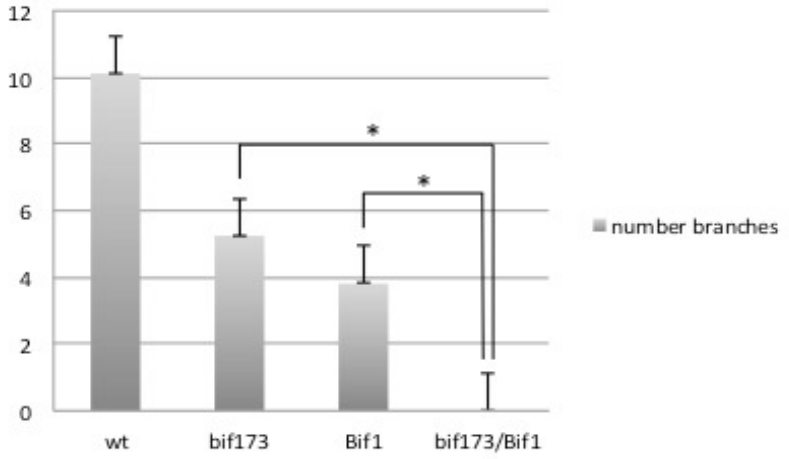

Fig. 1.10: Quantification of the number of branches of wild type tassels, *bif173* tassels, *Bif1* tassels and *bif173*;*Bif1* tassels. The asterisk indicates a statistically significant difference with a p-value < 0.001.

	n. samples	**average**	**standard error**
wild type	8	10.12	±0.93
bif173	4	5.25	±1.10
Bif1	17	3.82	±0.33
bif173*;*Bif1	7	0	0

Table 1.8: Quantification of the number of branches of wild type tassels, *bif173* tassels, *Bif1* tassels and *bif173*;*Bif1* tassels. Number of tassels used for quantification, average of the number of branches per tassel and standard error are shown. These values refer to Fig. 1.10.

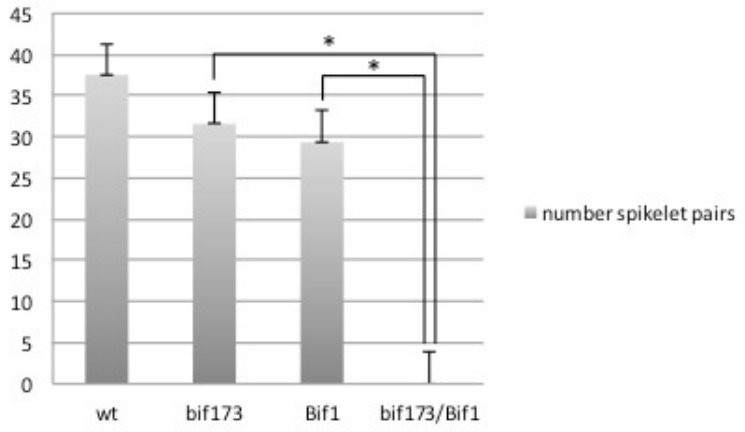

Fig. 1.11: Quantification of the number of spikelet pairs of wild type tassels, *bif173* tassels, *Bif1* tassels and *bif173*;*Bif1* tassels. The asterisk indicates a statistically significant difference with a p-value < 0.001.

	n. samples	**average**	**standard error**
wild type	8	37.53	±3.80
bif173	4	31.58	±2.90
Bif1	17	29.35	±2.86
bif173*;*Bif1	7	0	0

Table 1.9: Quantification of the number of spikelet pairs of wild type tassels, *bif173* tassels, *Bif1* tassels and *bif173*;*Bif1* tassels. Number of tassels used for quantification, average of the number spikelet pairs per tassel and standard error are shown. These values refer to Fig. 1.11.

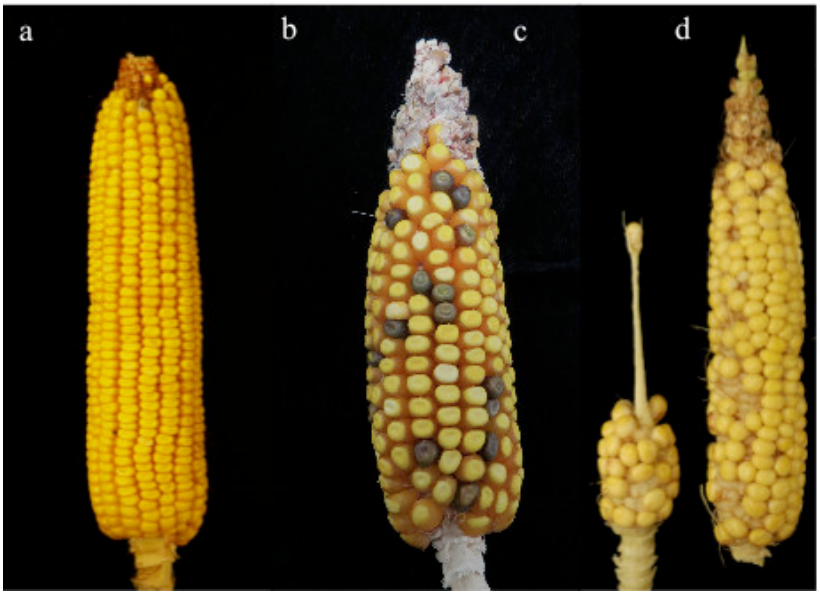

Fig. 1.12: Phenotype of *barren inflorescence173* (*bif173*) and *Barren inflorescence1* (*Bif1*). a, normal ear; b, mutant *bif173* ear; c, double mutant *bif173*;*Bif1* ear; d, mutant *Bif1* ear.

Also *bif173*;*Bif1* ears showed a severe phenotype with a considerable reduction in size and in the number of kernels (Fig. 1.12 c) when compared to wild type and both single mutants (Fig. 1.12 a, b, d). *bif173* and *Bif1* ears showed a mild phenotype (Fig. 1.12 b, d).

Thus, *bif173*;*Bif1* double mutants phenotype is more severe than both single mutants, suggesting that *BIF173* might be involved in auxin signaling.

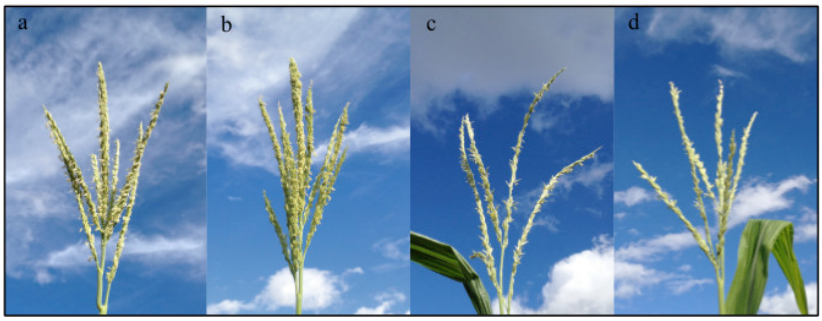

Fig. 1.13: Phenotype of *barren inflorescence173* (*bif173*) and *sparse inflorescence1* (*spi1*). a, normal tassel; b, mutant *bif173* tassel; c, mutant *spi1* tassel; d, double mutant *bif173*;*spi1* tassel.

bif173;*spi1* double mutants were also created (Fig. 1.13). These mutants produced a tassel with a reduced number of branches and spikelets (Fig. 1.13 d), which is very similar to *spi1* tassel (Fig. 1.13 c). *bif173* tassel in this population showed a very mild phenotype (Fig. 1.13 b). Double mutant ears also did not show a synergistic interaction between *BIF173* and *SPI1*. The lack of an enhancement of the single *spi1* mutant phenotype in the double *bif173;spi1* mutants may be interpreted as an epistatic interaction, where both genes work in the same pathway, or more likely, could suggest that *BIF173* is not involved in auxin biosynthesis.

3.3 Identification of the causative gene

The *bif173* mutant was first identified in an ethyl methanesulfonate (EMS) mutagenesis screen targeting mutants affected in the formation of axillary meristems. The mutagenized population of interest was created using EMS treated pollen from the maize inbred line Oh43 to fertilize wild type ears of the maize inbred line A632, as part of the Maize Inflorescence Project.

The *bif173* mutant was initially identified in a M2 population consisting of only 30 plants. Based on the segregation observed in this M2 population and the absence of a mutant phenotype in the M1, the mutation appeared recessive. *bif173* was identified due to the typical *barren* phenotype of the mutant inflorescences (Fig. 1.3). Heterozygous normal looking plants from the M2 were self-crossed and the resulting M3 population was used for the preliminary mapping, in order to identify the gene responsible for *bif173* mutation. An initial Bulk Segregant Analysis (BSA), using the MASSarray system developed by Sequenom was carried out at Iowa State University (Liu et al., 2010). The analysis compared approximately 1000 single nucleotide polymorphisms (SNPs) between the mutant and wild type genomes and it showed that the *BIF173* locus was

linked to chromosome 8 between 8.04 and 8.05. This analysis confirmed that *bif173* represents a novel maize *barren* mutant.

From the M3 population, several plants heterozygous for the *BIF173* locus plants were self-crossed to generate an M4 population for map based cloning. However, in the M4 population the severity of the mutant phenotype was reduced and the entire population was weaker and smaller, as consequence of fixation of deleterious alleles and inbreeding. Thus, *bif173* was crossed into the B73 inbred line in order to continue the fine mapping. Pollen from two homozygous *bif173* plants from the M4 population was used to fertilize B73 ears. The resulting F1 population was subsequently self-crossed to generate a new F2 population to facilitate the map-based cloning approach. The new mapping population consisted of 2,987 F2 plants and the *bif173* phenotype reappeared, with a much stronger phenotype. On this population, a fine mapping approach using several PCR-based molecular markers was carried out and it succeeded in restricting the *BIF173* locus to a small 1.2 Mb window on chromosome 8 (Fig. 1.14), but further analysis was needed to identify the causative gene among the 27 genes included in the predicted region (Table 1.10).

In order to achieve that, a different approach was carried out. Leveraging on the above-mentioned results, RNA-seq analysis (Liu et al., 2012) was performed to closely examine the mapping window (Fig. 1.14).

Three pools of samples were created and subjected to RNA-seq analysis: *bif173* mutant, the wild type sibling and wild type original background Oh43.

Immature tassels of 0.5-1 cm from a *bif173*/B73 F2 population were dissected and mutants and wild type samples were identified (Fig. 1.4). Since *bif173* phenotype is not fully penetrant, samples were also genotyped with flanking markers to confirm the phenotype. For the same reason only severe mutants and only homozygous wild type siblings were considered. These samples together with immature tassels from the original EMS-mutagenized background Oh43 were used for a bulk RNA extraction of each genotype and later for RNA-seq analysis. 28 million, 45 million, and 28 million 100bp single-end reads were obtained for the *bif173* mutant, the wild type sibling, and the Oh43 background samples, respectively. The goal was to analyze all the transcripts from all the genes contained within the mapping window to identify SNPs that could serve as candidates for the *bif173* mutation. Due to our

experimental design where only homozygous mutant and wild type samples were bulked, a causative SNP should be present only in the mutant reads and not in the wild type pool or the Oh43 pool. If present also in the Oh43 sample, a SNP instead represents a naturally occurring polymorphism between the different background used in the crosses. By manually scanning in a genome browser all the reads within the mapping window from the three different pools, we identified one SNP present only in the *bif173* mutant transcripts. This SNP was found in all the mutant reads and caused a missense mutation, in the coding sequence of gene GRMZM2G038401 (Fig. 1.15). This substitution represents a non-synonymous mutation, resulting in a codon that codes for a different amino acid, where an Isoleucine (I) is replaced by a Phenylalanine (F).

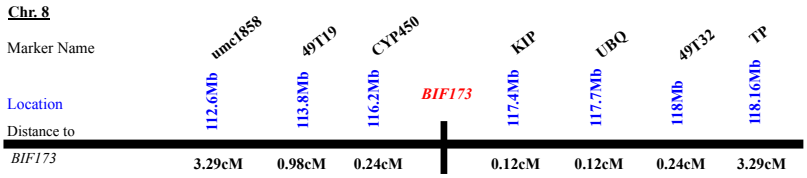

Fig. 1.14: Map location of *BIF173* locus. The markers used in the fine mapping, the physical map locations and the genetic distance between *BIF173* and the markers are indicated.

Locus on Chr.8	**Gene Name**	**Predicted Protein**
116.25	GRMZM2G038401	Peptidase family
116.3	GRMZM2G055489	Sucrose-6F-phosphate phosphohydrolase
116.31	GRMZM2G055462	unknown function
116.4	GRMZM2G082384	Kinase motor domain
116.42	GRMZM2G382792	GDP-futose protein
116.48	GRMZM2G421415	Fasciclin domain
116.488	GRMZM2G583274	Unknown
116.53	GRMZM2G009936	Ribosomal Protein
116.16	GRMZM5G802801	heat shock protein
116.2	GRMZM5G874500	tRNA synthetase classe
116.67	GRMZM2G008032	Unknown
116.678	GRMZM2G700614	Unknown
116.77	GRMZM2G007276	ubiquitin conjugating enzyme
116.849	GRMZM2G336908	GTP cyclohydrase
116.85	GRMZM2G035202	PTPLA
116.86	GRMZM5G883149	Clathrin adaptor complex
116.865	GRMZM5G886109	Unknown
116.98	GRMZM5G879851	Unknown
117.072	GRMZM2G178815	Unknown
117.078	GRMZM2G178803	late embryogenesis abundant protein
117.14	GRMZM2G090563	Transmembrance protein
117.15	GRMZM2G390400	SAC3/GANP/Nin1/mts3/eIF-3 p25 family
117.19	GRMZM2G090732	protein kinase domain
117.27	GRMZM2G175349	zinc finger C3HC4 type
117.28	GRMZM2G538922	Unknown
117.29	GRMZM2G095905	PWWP protein
117.3	GRMZM2G095921	Unknown

Table 1.10: List of candidate genes for *bif173* in the 1.2 Mb mapping window.

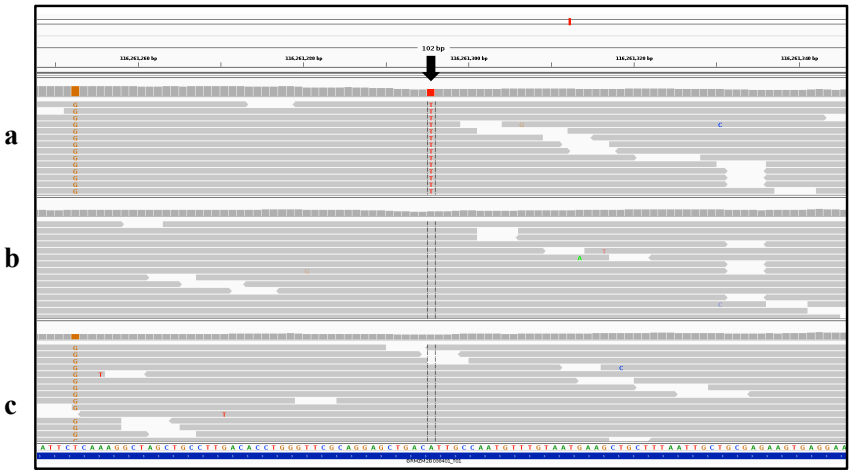

Fig. 1.15: RNA-seq data. a, *bif173* reads; b, wild type sibling reads; c, Oh43 reads. Arrow indicates the missense mutation found in the coding region of gene GRMZM2G038401.

Fig. 1.16: Schematic representation of the candidate gene GRMZM2G038401. Positions of missense mutation (blue bar) and transposon insertion (red arrowhead) are indicated.

Based on the amount of reads obtained from the 3 pools, this gene was not differentially expressed between mutant and wild type samples. No other SNPs that matched our criteria was identified, making GRMZM2G038401 a likely candidate gene for the *bif173* mutation.

The GRMZM2G038401 gene consists of 8 exons (Fig. 1.16) and it encodes a protein of 815 amino acids, sharing features characteristic to an FtsH ATP-dependent metalloprotease.

FtsHs (filamentation temperature sensitive) are a family of membrane bound proteases involved in housekeeping proteolysis of membrane proteins. They are found in all prokaryotes except Archaebacteria and in eukaryotes are restricted to organelles derived by endosymbiosis (mitochondria and chloroplasts) (Wagner et al., 2011). These proteases are known to have a crucial role in thermotolerance (Thorness et al., 1993; Duerling et al., 1995; Duwat et al., 1995; Herman et al., 1995; Fischer et al., 2002; Chen et al., 2006) and in response to light stress (Ostersetzer and Adam, 1997; Chen et al., 2000; Lindahl et al., 2000; Bailey et al., 2002; Sakamoto et al., 2002; Silva et al., 2003; Yu et al., 2005, Zaltsman et al., 2005). In *A. thaliana* 12 FtsH members are present, 8 are exclusively targeted to chloroplasts (Ferro et al.,

2010), 3 are located in the mitochondria (Janska, 2005) and one is dually targeted to both organelles (Urantowka et al., 2005).

Sequence analysis of the protein encoded by the GRMZM2G038401 gene showed its homology with FtsH proteins in various organisms.

The predicted amino acid sequence of the maize FtsH-like protease compared with the GenBank database by BLASTP program showed the highest identity with the *A. thaliana* FtsH10 (71%), and FtsH3 (71%), both proteases localized in the mitochondria (Janska, 2005). Maize FtsH protease also exhibited considerable identity to the *S. cerevisiae* Yta12 (52%) as well as to the bacterial ancestor *E.coli* FtsH (41%). These amino acid sequences were used to generate an alignment which reveals several well-conserved regions of these proteases (Fig. 1.17).

Maize FtsH-like contains an AAA ATP-ase domain characterized by a highly conserved AAA cassette containing the Walker A (position 369-378) and B (position 426-433) motifs necessary for nucleotide binding and hydrolysis as well as the “second region of homology” (SRH) (position 470-489) important for oligomerization and nucleotide hydrolysis (Tomoyasu et al., 1993; Ogura and Wilkinson, 2001;

Bieniossek et al., 2009). It also contains a protease domain, located C-terminal to the AAA domain, which carries a zinc-binding sequence (position 594-598) (Fig. 1.17).

The amino acid sequences of these regions which are required for ATPase activity are highly conserved, not only among FtsHs found in *A. thaliana*, but also among other FtsH proteins in other eukaryotes (*S. cerevisiae*) and prokaryotes (*E. coli*) (Fig. 1.17).

The missense mutation is found in the exon 6 of the gene GRMZM2G038401 (116,261,295) (Fig. 1.16) and the resulting amino acid substitution occurs in a region between SHR and zinc-binding domains (Fig. 1.17).

As shown in Fig. 1.17 the homology among FtsH proteases is not restricted to the conserved motifs but spans almost the entire protein. In fact, although the mutation is in an interdomain region, it interests an amino acid which is very conserved from prokaryotes to eukaryotes. The mutated amino acid is an aliphatic amino acid which can be either a Leucine (L) (*E. coli*) or a Isolecucine (I) (*S. cerevisiae*, *Z. mays* and *A. thaliana*) (Fig. 1.17) and in the mutants it is changed to a Phenylalanine (F), which has different properties due to the aromatic ring.

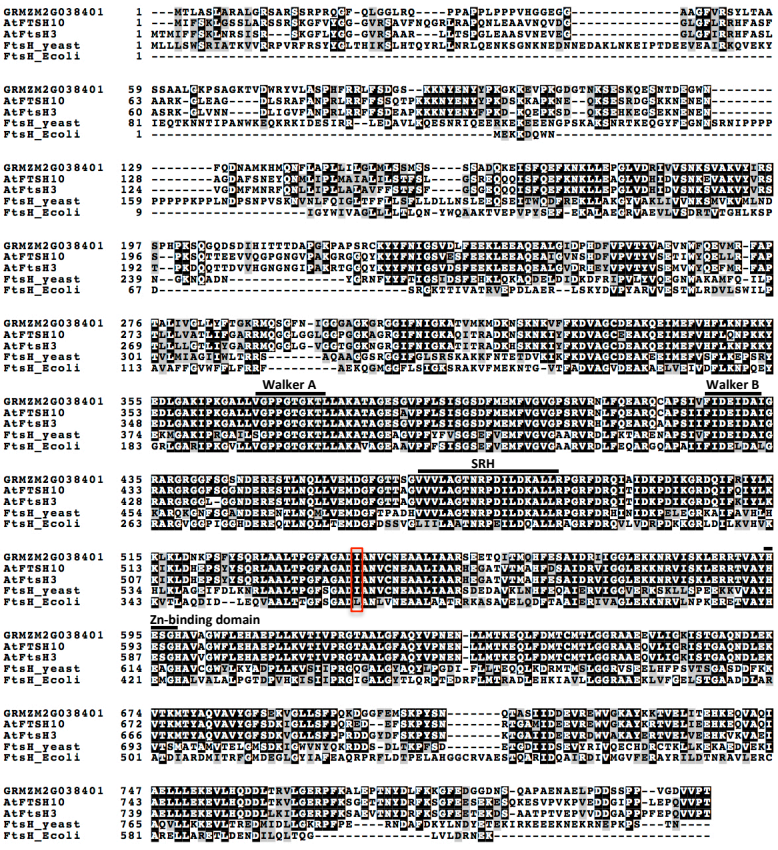

Fig. 1.17: Multiple alignment of the predicted amino acid sequences of the maize FtsH-like protease encoded by GRMZM2G038401 and the related FtsH proteases. Sequences have been aligned using ClustalW program (NCBI accession numbers in parentheses): FtsH-like protease from *Z. mays* (AFW82207.1), FtsH10 protease from *A. thaliana* (NP_172231.2), FtsH3 protease from *A. thaliana* (NP_850129.1), Yta 12p from *S. cerevisiae* (yeast, NP_013807.1), FtsH from *E. coli* (EQY54653.1). Structural motifs Walker A, Walker B, SRH and zinc binding domain are indicated. Red box indicates the position of the mutated amino acid. Residues that are identical or similar in at least three proteins are colored in black and gray, respectively.

To further confirm that the SNP linked to the causative gene is a mutation and not a polymorphism, 29 different maize inbred lines were sequenced. Table 1.11 shows that the codon containing the mutated nucleotide (A to T) is present only in *bif173* sequences. This nucleotide triplet in all the other inbred lines is the same as in the B73 wild type sequence. The wild type codon is also found in teosinte sequence, the closest wild relative of maize, as a further confirmation of the high conservation. The presence of the SNP only in *bif173* sequence suggests that it represents a mutation and not a polymorphism due to the genetic variability among maize inbred lines.

To prove that GRMZM2G038401 is the gene responsible for the *bif173* mutation, additional mutant alleles are needed. Using the UniformMu database, a transposon insertion in the 5' UTR of the gene was found (Fig. 1.16) and seed stocks were ordered from the Maize Genetics Cooperation Stock Center. Plants were genotyped to verify the presence of the insertion. Three plants resulted heterozygous for the insertion, the others were all wild type. The presence of the insertion was also checked through sequencing. These three plants were self-crossed in order to obtain a homozygous mutant and observe the phenotype. This F2 population is growing in our winter

nursery in Hawaii. If plants homozygous for the transposon insertion show a phenotype resembling the original *bif173* mutant, we will confirm that the gene GRMZM2G038401 represents the *BIF173* locus.

The gene is broadly expressed in vegetative and reproductive tissues and it is highly expressed in SAM and tassel and ear primordia, according to the data of Bolduc et al., 2012, published on qTeller database (qteller.com). To investigate the localization of GRMZM2G038401 expression during inflorescence development, a preliminary RNA *in situ* hybridization was performed on wild type immature tassels of 0.2 mm length. The results (Fig. 1.18) showed a ubiquitous signal, with stronger expression in meristematic tissues, such as inflorescence, branch and spikelet-pair meristems (Fig. 1.18 a, b). This contrasts with the localized signal observed in our control samples, hybridized with a probe for the *ZYB15* gene, a marker for bract primordia (Fig. 1.18 c, d) (Juarez et al., 2004).

Inbred lines	**Codon containing the SNP**	**Inbred lines**	**Codon containing the SNP**
B73	**A**TT	W22	**A**TT
A619	**A**TT	Mo17	**A**TT
CML247	**A**TT	CML228	**A**TT
KY21	**A**TT	CML52	**A**TT
CML69	**A**TT	Ki3	**A**TT
M162W	**A**TT	Tx303	**A**TT
M37W	**A**TT	Tzi8	**A**TT
CML103	**A**TT	Mo18w	**A**TT
B97	**A**TT	CML277	**A**TT
P39	**A**TT	LI14H	**A**TT
MS71	**A**TT	Nc350	**A**TT
CML333	**A**TT	HP301	**A**TT
Oh7B	**A**TT	Oh43	**A**TT
Nc358	**A**TT	teosinte	**A**TT
Ki11	**A**TT	***bif173***	**T**TT
CML322	**A**TT		

Table 1.11: Codon containing the SNP in *bif173* mutant, 29 different maize inbred lines and teosinte. The mutated nucleotide (A to T) is indicated in bold.

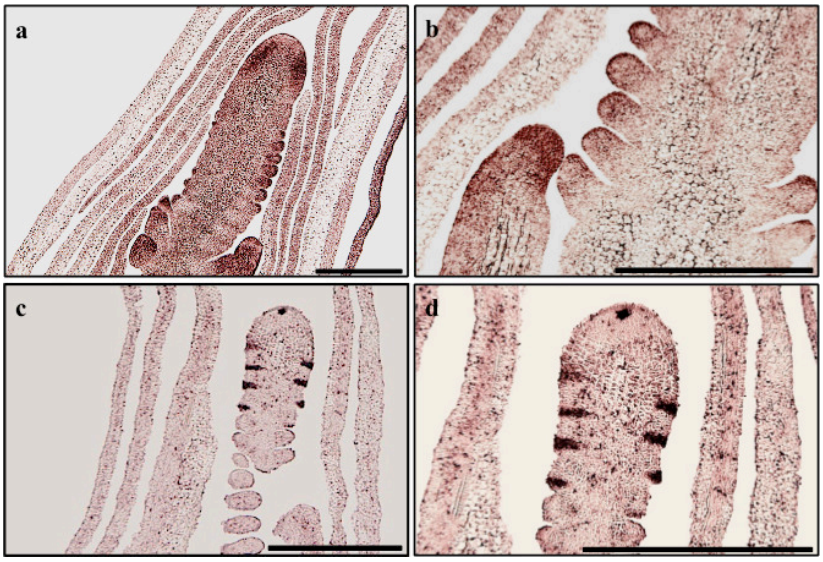

Fig. 1.18: *in situ* hybridization performed on wild type immature tassels of 0.2 mm length. a, b show the localization of GRMZM2G038401 expression, with a stronger signal in in meristematic tissues. c, d show the localization of *ZYB15* expression in bract primordia. Scale bars: 500 µm.

4. DISCUSSION

Plant development relies on the activity of meristems, highly organized and regulated groups of stem cells responsible for the formation of all post-embryonic organs. Whereas the shoot and the root apical meristems, formed during embryogenesis, establish the main axis of plant growth (apical to basal), axillary meristems are responsible for the formation of secondary axes of growth, such as branches and flowers. In maize, axillary meristems activity determines the development and architecture of male and female inflorescences, the tassel and the ear, respectively. The complex structure of maize inflorescences is the result of a hierarchical process where four different types of axillary meristems (BMs, SPMs, SMs, FMs) are involved. A proper regulation of these meristems is essential for a normal development of the inflorescence and mutants affected in the formation of axillary meristems are generally referred to as *barren*.

In this work, a new *barren* mutant, *barren inflorescence173* (*bif173*), has been characterized. *bif173* mutants show defects in inflorescence development and in particular in BMs and

SPMs initiation. The phenotype shows different degrees of severity and it is characterized by a reduction in the number of spikelet pairs and branches in the tassel and smaller and more disorganized ears.

bif173 phenotype is not fully penetrant, in fact, although it is a recessive mutant, the percentage of mutants found in a F2 segregating population was lower than expected. This is likely due to the fact that this mutant is influenced by environmental factors. By comparing *bif173* segregation between summer and winter we observed that during the summer the percentage of severe mutants is higher, suggesting that the severity of the mutant phenotype might be related to temperature or light changes.

The *bif173* phenotype is reminiscent of mutations affecting auxin pathway. Several *barren* mutants are affected in the biosynthesis, transport or signaling of the plant hormone auxin, like *Barren inflorescence1* (*Bif1*) and *sparse inflorescence1* (*spi1*), affected in signaling and biosynthesis, respectively (Barazesh and McSteen, 2008, Gallavotti et al., 2008). *bif173*;*Bif1* and *bif173*;*spi1* double mutants were studied to investigate if *BIF173* plays any role in auxin biology. *bif173*;*Bif1* double mutants display a synergistic phenotype,

with severe defects in axillary meristems initiation in both the tassel and the ear, whereas *bif173*;*spi1* double mutants phenotype is similar to *spi1* single mutant and no synergistic effect is detected. These results led us to conclude that *BIF173* is involved in auxin biology and may play a role in auxin signaling.

To shed light on the genetic regulation of axillary meristems in this mutant and increase the understanding of the molecular mechanisms involved in maize inflorescence development, the identification of gene responsible of *bif173* mutation is crucial. Previous Bulk Segregant Analysis and positional cloning approaches were able to link *BIF173* locus on chromosome 8, assigning this locus to a small 1.2 Mb window. To identify the causative gene a RNA-seq Analysis was carried out, in order to analyze all the transcripts within the mapping window. Scanning all the reads from three different pools of samples (*bif173* mutants, wild type siblings and wild type OH43), one SNP that was only present in all the mutant transcripts was detected.

This SNP represents a non-synonymous mutation occurring in the coding region of the gene GRMZM2G038401 which

encodes a metalloprotease, homologous to the FtsH ATP-dependent metalloproteases.

FtsHs (**f**ilamentation **t**emperature **s**ensitive) are a family of membrane bound proteases involved in several fundamental biological processes (Wagner et al., 2011). The name is deduced from the growth behaviour of the *Escherichia coli ftsH* mutant, which has a filamentous temperature-sensitive growth phenotype (Santos and De Almeida, 1975; Begg et al., 1992). In *E. coli*, FtsH is involved in the regulation of the heat-shock transcription factor σ^{32} (Herman et al., 1995; Tomoyasu et al., 1995) and it is essential for survival at high temperature (Langer et al., 2000). FtsHs seem to be present in all prokaryotes, except Archaebacteria, and in eukaryotes where are restricted to organelles derived by endosymbiosis (mitochondria and chloroplasts) (Wagner et al., 2011). *S. cerevisiae* genome contains three FtsH genes, all producing proteins targeted to the mitochondria (Schnall et al., 1994). They act as molecular chaperones (Rep et al., 1996) degrading unassembled cytochrome oxidase subunit II and other denatured proteins (Weber et al., 1996) and they play an essential role in thermotolerance (Thorsness et al., 1993).

The protein encoded by the GRMZM2G038401 gene shares features with FtsH proteins in various organisms, including *E. coli* and *S. cerevisiae*, and it shows the highest homology with FtsH10 and FtsH3 in *Arabidopsis thaliana.*

FtsH10 and FtsH3 proteases are two of the 12 members of the FtsH family present in *A. thaliana* (Sokolenko et al., 2002). These two proteases are located in the inner membrane of mitochondria where they form hetero- and homo-oligomeric complexes (Janska et al., 2010; Piechota et al., 2010) and like their yeast counterparts, assemble with prohibitins (Piechota et al., 2008, 2010). FtsH3 and FtsH10 proteases show a chaperone-like activity in the assembly/stability of the oxidative phosphorylation system, and in *ftsh3* and *ftsh10* mutants, the activity of the complex I and V of oxidative system is strongly decreased (Kolodziejczak et al., 2007). Both FtsH3 and FtsH10 are able to complement the respiratory deficiency of yeast mutants lacking FtsH proteases, indicating that they may compensate for at least some functions of yeast proteases and play the same role in *A. thaliana* mitochondria (Piechota et al., 2010).

Also, *A. thaliana ftsh3* and *ftsh10* mutants exhibit morphological aberrations when placed in the field as young

plants, showing a decrease in plant size and in the number of seeds produced. No phenotypic differences with wild type are observed when older *ftsh3* and *ftsh10* plants, pre-grown under laboratory growth conditions, are placed outdoors (Wagner et al., 2011).

These findings suggest that FtsH3 and FtsH10 might play a role in thermotolerance and/or response to other stress factors and that their function is necessary for normal plant development.

Other studies in *A. thaliana* reveal the importance of FtsHs as proteases responsive to stress, by repairing and protecting membrane systems in chloroplast and mitochondria.

FtsH4 is also located in the mitochondria where it prevents accumulation of oxidatevely damaged proteins (Janska, 2005; Gibala et al., 2009). *ftsh4* mutants show a severe phenotype when grown in short day conditions, revealing defects in leaf morphology and in the ultrastructure of chloroplast and mitochondria (Gibala et al., 2009). In the chloroplast, FtsH11 protects the photosynthetic apparatus from damage caused by elevated temperatures, contributing to *A. thaliana* thermotolerance at all stages of development, consistent with

the original role played by *E. coli* and *S. cerevisiae* FtsH proteases (Chen et al., 2006).

Furthermore, other *A. thaliana* FtsH proteases located in the chloroplasts are shown to be involved in the repair of photosynthesis systems damaged by oxidative stress under high light levels (Ostersetzer and Adam, 1997; Lindahl et al., 2000; Bailey et al., 2002; Yu et al., 2005; Zaltsman et al., 2005; Zelisko et al., 2005). Mutations in these genes result typically in sensitivity to high light levels (Bailey et al., 2002, Sakamoto et al., 2002) and in a phenotype of leaves showing variegated green and white sectors (Sakamoto et al., 2003).

In maize, the protein encoded by GRMZM2G038401 has not been characterized yet. However, the highly conserved amino acid sequence of these proteins from prokaryotes to eukariotes and the roles of FtsHs in *A. thaliana* and other organisms (*E. coli* and *S. cerevisiae*), strongly suggest that also FtsH in maize might be involved in similar mechanisms. This explains the not fully penetrant *bif173* phenotype and the higher percentage of *bif173* severe mutants in the summer, leading to the hypothesis that also in maize this metalloprotease might be involved in thermotolerance and/or in response to light stress.

Furthermore, the localization of GRMZM2G038401 gene expression appears to be consistent with the numerous functions of the FtsH metalloproteases and their localization in the membranes of mitochondria and chloroplasts. In fact, the results of the *in situ* hybridization performed on immature wild type tassels show a ubiquitous signal using a specific probe for the causative gene.

Although we have not proved it yet, as evidence that the GRMZM2G038401 gene is a good candidate to be responsible for the *bif173* mutation is the fact that the SNP found in the RNA-seq reads is not present in teosinte and in any of the 29 maize inbred lines used in this work. This confirms that the SNP does not represent a naturally occurring polymorphism due to the genetic variability among maize backgrounds.

To confirm that GRMZM2G038401 gene is the *bif173* causative gene, plants homozygous for a transposon insertion are currently growing in our winter nursery in Hawaii. If the phenotype resembles the *bif173* mutant phenotype, this gene will be confirmed as the gene responsible for *bif173* mutation. Also, in the case the plants homozygous for the insertion have the same *bif173* phenotype, they can be crossed to a *bif173* mutant to run a complementation test. If the mutant phenotype

persists in the F1 population then there has not been complementation and this gene is confirmed as the causative gene. Alternative approaches we are pursuing to verify are: i) rescue of the *bif173* phenotype with a transgenic construct using the entire wild type genomic region *pBIF173::HA3-YFP-BIF173* ; ii) using targeted EMS mutagenesis (EMS-treated wild type pollen used on *bif173* homozygous ears; the resulting F1 should all be wild type; if mutant a new allele is generated – confirmation by sequencing).

If the phenotype will reveal that the GRMZM2G038401 gene is the gene responsible for the *bif173* mutation, this will be the first reported case where a gene encoding a metalloprotease is involved in the axillary meristems formation during inflorescence development. This finding will also contribute to increase our understanding of auxin biology, investigating the role of a metalloprotease as new player in auxin pathways.

REFERENCES

Ambrose BA, Lerner DR, Cicen P, Padilla CM, Yanofsky MF, Schmidt RJ. 2000. molecular and genetic analyses of the *silky1* gene reveal conservation in floral organ specification between eudicots and monocots. *Molecular cell* **5**(3)**,** 569-579.

Bailey S, Thompson E, Nixon PJ, Horton P, Mullineaux CW, Robinson C,Mann NH. 2002. A critical role for the Var2 FtsH homologue of *Arabidopsis thaliana* in the photosystem II repair cycle in vivo. *Journal of Biological Chemistry* **277**, 2006-2011.

Barazesh S, McSteen P. 2008. *Barren inflorescence1* functions in organogenesis during vegetative and inflorescence development in maize. *Genetics* **179**, 389-401.

Begg KJ, Tomoyasu T, Donachie WD, Khattar M, Niki H, Yamanaka K, Hiraga S, Ogura T. 1992. *Escherichia coli* mutant Y16 is a double mutant carrying thermosensitive ftsH and ftsl mutations. *Journal Bacteriology* **174**, 2416-2417.

Benjamins R, Scheres B. 2008. Auxin: The looping Star in plant development. *The annual Review of Plant Biology* **59**, 443-65.

Bennett T, Leyser O. 2006. Something on the side: axillary meristems and plant development. *Plant Molecular Biology* **60**, 843-54.

Bieniossek C, NiederHauser B, Baumann UM. 2009. The crystal structure of apo-FtsH reveals domain movements necessary for substrate unfolding and traslocation. *Proceedings of the National Academy of Sciences USA* **106**, 21579-21584.

Bolduc N, Yilmaz A, Mejia-Guerra M, Morohashi K, O'Connor D, Grotewold E and Hake S. 2012. Unraveling the KNOTTED1 regulatory network in maize meristems. *Genes & Development* **26**,

1685-690.

Bommert P, Lunde C, Nardmann J, Vollbrecht E, Running M, Jackson D, Hake S, Werr W. 2005. *thick tassel dwarf1* encodes a putative maize ortholog of the Arabidopsis CLAVATA1 leucine-rich repeat receptor-like kinase. *Development* **132**, 1235-1245.

Bonnett O T. 1954. The Inflorescences of maize. *Science* **120**(3107)**,** 77-87.

Bortiri E, Chuck G, Vollbrecht E, Rocheford T, Martienssen R and Hake S. 2006. *ramosa2* encodes a LATERAL ORGAN BOUNDARY domain protein that determines the fate of stem cells in branch meristems of maize. *Plant Cell* **18**, 574-585.

Bortiri E, Hake S. 2007. Flowering and determinacy in maize. *Journal of Experimental Botany* **58**(5), 909-916.

Bowman JL, Smyth DR, Meyerowitz EM. 1991. Genetic interactions among floral homeotic genes of *Arabidopsis. Development* **112**, 1–20.

Chen J, Burke JJ, VeltenJ, Xin Z. 2006. Ftsh11 protease plays a critical role in *Arabidopsis* thermotolerance. *Plant Journal* **48**, 73-84.

Chen M, Choi Y, Voytas DF, Rodermel S. 2000. Mutations in the *Arabidopsis* VAR2 locus cause leaf variegation due to the loss of chloroplast FtsH protease. *Plant Journal* **22**, 303-313.

Cheng PC, Greyson RI and Walden DB. 1983. Organ initiation and the development of unisexual flowers in the tassel and ear of *Zea mays. American Journal of Botany* **70**, 450-462.

Cheng YF, Dai XH, Zhao YD. 2006. Auxin biosynthesis by the YUCCA flavin monooxygenases controls the formation of floral

organs and vascular tissues in *Arabidopsis*. *Genes and Development* **20,** 1790-1799.

Chuck G, Muszynski M, Kellog E, Hake S, Schmidt R. 2002. The Control of spikelet meristem identity by the *branched silkless1* gene in maize. *Science* **298**(5596)**,** 1238-1241.

Chuck G, Meeley RB, Hake S. 1998. The control of maize spikelet meristem fate by the *APETALA2*-like gene *indeterminate spikelet1*. *Genes & Development* **12**(8)**,** 1145-1154.

Chuck G, Meeley RB, Irish E, Sakai H and Hake S. 2007. The maize *tasselseed4* microRNA controls sex determination and meristem cell fate by targeting *Tasselseed6/indeterminate spikelet1*. *Nature Genetics* **39**, 1517-1521.

Chuck G, Whipple C, Jackson D, Hake S. 2010. The maize SBP-box transcription factor encoded by *tasselsheath4* regulates bract development and the establishment of meristem boundaries. *Development* **137**(8)**,** 1243-1250.

Coen ES, Meyerowitz EM. 1991. The war of the whorls: genetic interactions controlling flower development. *Nature* **353**, 31–37.

Colombo L, Marziani G, Masiero S, Wittich PE, Schmidt R, Gorla MS, Pe' ME. 1998. BRANCHED SILKLESS mediates the transition from spikelet to floral meristem during *Zea mays* ear development. *Plant Journal* **16**, 355–363.

Dellaporta SL, Calderon-Urrea A. 1994. The sex determination process in maize. *Science* **266**, 1501–1505.

Deuerling E, Paeslack B, Schumann W. 1995. The FtsH gene *of Bacillus subtilis* is transiently induced after osmotic and temperature upshift. *Journal Bacteriology* **177**, 4105-4112.

Duwat P, Ehrlich SD, Gruss A. 1995. The recA gene of *Lactococcus lactis*: characterization and involvement in oxidative and thermal stress. *Molecular Microbiology* **17**, 1121-1131.

Ferro M, Brugiere S, Salvi D, Seigneurin-Berny D, Court M, Moyet L, Ramus C, Miras S, Mellal M, Le Gall S, Kieffer-Jaquinod S, Bruley C, Garin J, Joyard J, Masselon C, Rolland N. 2010. AT_CHLORO, a comprehensive chloroplast proteome database with subplastidial localization and curated information on envelope proteins. *Molecular & Cellular Proteomics* **9**, 1063-1084.

Fischer B, Rummel G, Aldridge P, Jenal U. 2002. The FtsH protease is involved in development, stress response and heat shock control in *Caulobacter crescentus*. *Molecular Microbiology* **44**, 461-478.

Friml J, Yang X, Michniewicz M, Weijers D, Quint A, Tietz O, Benjamins R, Ouwerkerk PB, Ljung K, Sandberg G, Hooykaas PJ, Palme K and Offringa R. 2004. A PINOID-dependent binary switch in apical-basal PIN polar targeting directs auxin efflux. *Science* **306**, 862-865.

Gallavotti A, Barazesh S, Malcomber S, Hall D, Jackson D, Schmidt RJ, McSteen P. 2008. *Sparse inflorescence1* encodes a monocot-specific YUCCA-like gene required for vegetative and reproductive development in maize. *Proceedings of National Academy of Sciences, USA* **105**, 15196-15201.

Gallavotti A, Long J, Stanfield S, Yang X, Jackson D, Vollbrecht E, Schmidt R. 2010. The control of axillary meristem fate in maize *ramosa* pathway. *Development* **137**, 2849-856.

Gallavotti A, Malcomber S, Gaines C, Stanfield S, Whipple C, Kellog E, Schmidt RJ. 2011. BARREN STALK FASTIGIATE1 is an AT-hook protein required for the formation of maize ears. *The plant Cell* **23**, 1756-1771.

Gallavotti A, Zhao Q, Kyozuka J, Meeley RB, Ritter M, Doebley JF, Pe ME, Schmidt RJ. 2004. The role of *barren stalk1* in the architecture of maize. *Nature* **432**, 630–635.

Gallavotti A. 2013. The role of auxin in shaping shoot architecture. *Journal of Experimental Botany* **64** (9), 2593-2608.

Galweiler L, Guan CH, Muller A, Wisman E, Mendgen K, Yephremov A, Palme K. 1998. Regulation of polar auxin transport by AtPIN1 in *Arabidopsis* vascular tissue. *Science* **282**, 2226-2230.

Gibala M, Kicia M, Sakamoto W, Gola EM, Kubrakiewicz J, Smakowska E, Janska H. 2009. The lack of mitochondrial AtFtsH4 protease alters *Arabidopsis* leaf morphology at the late stage of rosette development under shot-day photoperiod. *Plant Journal* **59**, 685-699.

Goldsmith M H.1993. Cellular signaling: New insights into the action of the plant growth hormone auxin. *Proceedings of the National Academy of Sciences USA* **90**, 11442-11445.

Greb T, Clarenz O, Schäfer E, Müller D, Herrero R, Smitz G, Theres K. 2003. Molecular analysis of the LATERAL SOPPRESSOR gene in *Arabidopsis* reveals a conserved control mechanism for axillari meristem formation. *Genes Development* **17**, 1175-1187.

Herman C, Thevenet D, D'Ari R, Bouloc P. 1995. Degradation of σ^{32}, the heat shock regulator in *Escherichia coli*, is governed by HfiB. *Proceedings of the National Academy of Sciences USA* **92**, 3516-3520.

Irish EE. 1996. Regulation of sex determination in maize. *BioEssays* **18**, 363–369.

Irish EE. 1997. Experimental analysis of tassel development in the maize mutant *Tassel Seed 6. Plant Physiology* **114**, 817-825.

Janska H, Piechota J, Kwasniak M. 2010. ATP-dependent proteases in biogenesis and maintenance of plant mitochondria. *Biochimica et Biophysica Acta* **1797**, 1071-1075.

Janska H. 2005. ATP dependent proteases in plant mitochondria: what do we know about them today? *Physiologia Plantarum* **123**, 399-405.

Juarez MT, Twigg RW, Timmermans MC. 2004. Specification of adaxial cell fate during maize leaf development. *Development* **131**: 4533-4544.

Kiesselbach TA. 1949. The structure and reproduction of corn. Univ. Nebraska Coll. Agric., *Agricultural Experiment Station Research Bullettin* **161,** 1-96.

Kolodziejczak M, Gibala M, Urantowka A, Janska H. 2007. The significance of *Arabidopsis* AAA proteases for activity and assembly/stability of mitochondrial oxphos complexes. *Physiologia Plantarum* **129**, 135-142.

Langer T. 2000. AAA proteases: cellular machines for degrading membrane proteins. *Trends in Biochemical Sci*ences **25**, 247-251.

Laudencia-Chingcuanco D, Hake S. 2002. The *indeterminate floral apex1* gene regulates meristem determinacy and identity in the maize inflorescence. *Development* **129**(11)**,** 2629-2638.

Leyser O. 2003. Regulation of shoot branching by auxine. *Trends in Plant Sci*ences **8**, 541-545.

Lindahl M, Spetea C, Hundal T, Oppenheim AB, Adam Z, Andersson B. 2000. The thylakoid FtsH protease plays a role in the light-induced turnover of the photosystem II D1 protein. *Plant Cell* **12**, 419-431.

Liu S, Chen HD, Makarevitch I, Shirmer R, Emrich SJ, Dietrich CR, Barbazuk WB, Springer NM and Schnable PS. 2010. High-throughput genetic mapping of mutants via quantitative single nucleotide polymorphism typing. *Genetics* **184**, 19-U51.

Liu S, Yeh C, Tang HM, Nettleton D, Schnable PS. 2012. Gene mapping via Bulked Segregant RNA-seq (BSR-Seq). *PlosOne* **7**(5), DOI: 10.1371/journal.pone.0036406

Long JA, Barton MK. 2000. Initiation of axillary and floral meristems in *Arabidopsis*. *Developmental Biology* **218**, 341-353.

Lunde CF, S. Hake S. 2005. Florets & rosettes meristem genes in maize and *Arabidopsis*. *Maydica* **50** , 451-458.

McSteen P, Hake S. 2001. *Barren inflorescence2* regulates axillary meristem development in the maize inflorescence. *Development* **128**, 2881–2891.

McSteen P, Laudencia-Chingcuanco D, Colasanti J. 2000. A floret by any other name: control of meristem identity in maize. *Trends in Plant Science* **5**(2)**,** 61-66.

McSteen P, Malcomber S, Skirpan A, Lunde C, Wu X, Kellogg E, Hake S. 2007. *Barren inflorescence2* encodes a co-ortholog of the *PINOID* serine/threonine kinase and is required for organogenesis during inflorescence and vegetative development in maize. *Plant Physiology* **144**, 1000–1011.

Mena M, Ambrose BA, Meeley RB, Briggs SP, Yanofsky MF, Schmidt RJ. 1996. Diversification of C-function activity in maize flower development. *Science* **274**, 1537–1540.

Michniewicz M, Zago MK, Abas L, Weijers D, Schweighofer A, Meskiene I, Heisler MG, Ohno C, Zhang J, Huang F, Schwab R,

Weigel D, Meyerowitz EM, Luschnig C, Offringa R and Friml J. 2007. Antagonistic regulation of PIN phosphorylation by PP2A and PINOID directs auxin flux. *Cell* **130**, 1044-1056.

Neuffer M, Coe E, Wessler S. 1997. Mutants of maize (Plainview: Cold Spring Harbor Laboratory Press).

Ogura T, Wilkinson AJ. 2001. AAA(+) superfamily ATPases: common structure-diverse function. *Genes Cells* **6**, 575-597.

Okada K, Ueda J, Komaki MK, Bell CJ, Shimura Y. 1991. Requirement of the auxin polar transport-system in early stages of *Arabidopsis* floral bud formation. *The Plant Cell* **3**, 677-684.

Ostersetzer O, Adam Z. 1997. Light-stimulated degradation of an unassembled Rieske FeS protein by a thylakoid-bound protease: the possible role of the FtsH protease. *Plant Cell* **9**, 957-965.

Parkinson SE, Gross SM, Hollick JB. 2007. Maize sex determination and abaxial leaf fates are canalized by a factor that maintains repressed epigenetic states. *Developmental Biology* **308**, 462-473.

Phillips KA, Skirpan AL, Liu X, Christensen A, Slewinski TL, Hudson C, Barazesh S, Cohen JD, Malcomber S, McSteen P. 2011. *Vanishing tassel2* encodes a grass-specific tryptophan aminotransferase required for vegetative and reproductive development in maize. *The Plant Cell* **23**, 550-566.

Piechota J, Kolodziejczak H, Janska H. 2008. Prohibitins and m-AAA proteases form a 2 MDa supercomplex in plant mitochondria. *FEBS Journal* **227**, 3-64.

Piechota, J, Kolodziejczak M, Juszczak I, Sakamoto W, Janska H. 2010: Identification and characterization of high molecular weight complexes formed by matrix AAA proteases and prohibitins in

mitochondria of *Arabidopsis thaliana*. 2010. *The Journal of Biological Chemistry* **285**, 12512-1252.

Rep M, van Dijl JM, Suda K, Schatz G, Grivell LA, Suzuki CK. 1996. Promotion of mitochondrial membrane complex assembly by a proteolytically inactine yeast Lon. *Science* **274**, 103-106.

Ritter MK, Padilla CM, Schmidt RJ. 2002. The maize mutant *barren stalk1* is defective in axillary meristem development. *American Journal of Botany* **89**, 203–210 .

Sakamoto W, Tamura T, Hanba-Tomita Y, Murata M. 2002. The *VAR1* locus of *Arabidopsis* encodes a chloroplastic ftsh and is responsible for leaf variegation in the mutant alleles. *Genes Cells* **7**, 769-780.

Sakamoto W, Zaltsman A, Adam Z, Talkahashi Y. 2003. Coordinated regulation and complex formation of YELLOW VARIEGATED1 and YELLOW VARIEGATED2, chloroplastic FtsH metalloproteases involved in the repair cycle of photosystem II in *Arabidopsis* thylakoid membranes. *Plant Cell* **15**, 2843-2855.

Santos D, De Almeida DF. 1975. Isolation and characterization of a new temperature-sensitive cell division mutant of *Escherichia coli* K-12. *Journal of Bacteriology* **124**, 1502-1507.

Satoh-Nagasawa N, Nagasawa N, Malcomber S, Sakai H, Jackson D. 2006. A trehalose metabolic enzyme controls inflorescence architecture in maize. *Nature* **441**, 227-230.

Schmidt RJ, Veit B, Mandel MA, Mena M, Hake S, Yanofsky MF. 1993. Identification and molecular characterization of *ZAG1* the maize homolog of the *Arabidopsis* floral homeotic gene *AGAMOUS. Plant Cell* **5**, 729–737.

Schnall R, Mannhaupt G, Stucka R, Tauer R, Ehnle S, Schwarzlose C, Vetter I, Feldmann H. 1994. Identification of a set of yeast genes coding for a novel family of putative ATPases with high similarity to constituens of the 26S protease complex. *Yeast* **10**, 1141-1155.

Silva P, Thompson E, Bailey S, Kruse O, Mullineaux CW, Robinson C, Mann NH, Nixon PJ. 2003. FtsH is involved in the early stages of repair of photosystem II in *Synechocystis* sp PCC 6803. *Plant Cell* **15**, 2152-2164.

Skirpan A, Wu X, McSteen P. 2008. Genetic and physical interaction suggest that BARREN STALK1 is a target of BARREN INFLORESCENCE2 in maize inflorescence development. *The Plant Journal* **55,** 787-797.

Socolenko A, Poijdaeva E, Zinchenko V, Panichkin V, Glaser VM, Hermann RG, Shestakov SV. 2002. The gene complement for proteolysis in the cyanobacterium *Synechocystis* sp.PCC 6803 and *Arabidopsis thaliana* chloroplasts. *Current Genet*ics **41**, 291-310.

Steeves TA, Sussex IM. 1989. Patterns in Plant Development. *Cambridge: Cambridge University Press.*

Taguchi-Shiobara F, Yuan Z, Hake S, Jackson D. 2001. The *fasciated ear2* gene encodes a leucine-rich repeat receptor-like protein that regulates shoot meristem proliferation in maize. *Genes & Development* **15**, 2755–2766.

Theissen G, Strater T, Fischer A, Saedler H. 1995. Structural characterization, chromosomal localization and phylogenetic evaluation of two pairs of *AGAMOUS-like* MADS-box genes from maize. *Gene* **156**, 155–166.

Thorness PE, White KH, Fox TD. 1993. Inactivation of YME1, a member of the ftsH-SEC18-PAS1-CDC48 family of putative ATPase-encoding genes, causes increased escape of DNA from

mitochondria in *Saccharomyces cerevisiae. Molecular and Cellular Biology* **13**, 5418-5426.

Tobena-Santamaria R, Bliek M, Ljung K, Sandberg G, Mol JNM, Souer E, Koes R. 2002. FLOOZY of petunia is a flavin mono-oxygenase-like protein required for the specification of leaf and flower architecture. *Genes and Development* **16**, 753-763.

Tomoyasu T, Gamer J, Bukau B, Kanemori M, Mori H, Rutman AJ, Oppenheim AB, Yura T, Yamanaka K, Niki H, Hiraga S, Ogura T. 1995. *Escherichia coli* FtsH is a membrane-bound, ATP-dependent protease witch degrades the heat-shock transcription factor sigma 32. *EMBO Journal* **14**, 2551-2560.

Tomoyasu T, Yuki T, Morimura S, Mori H, Yamanaka K, Niki H, Hiraga S, Ogura T. 1993. The *Escherichia coli* FtsH protein is a prokaryotic member of a protein family of putative ATPases involved in membrane functions, cell-cycle control, and gene expression. *Journal of Bacteriology* **175**, 1344-1351.

Trapnell C, Roberts A, Goff L, Pertea G, Kim D, Kelley DR, Pimentel H, Salzberg SL, Rinn JL, Pachter L. 2012. Differential gene and transcript expression analysis of RNA-seq experiments with TopHat and Cufflinks. *Nature Protocols* **7**, 562-578.

Untergrasser A, Cutcutache I, Koressaar T, Ye J, Faircloth BC, Remm M, Rozen SG. 2012 Primer3 - new capabilities and interfaces. *Nucleic Acids Research* **40**(15), e115.

Urantowka A, Knorpp C, Olczak T, Kolodziejczak M, Janska H. 2005. Plant mitochondria contain at least two i-AAA-like complexes. *Plant Molecular Biology* **59**, 239-252.

Vanneste S, Friml J. 2009. Auxin: A trigger for change in plant development, *Cell* **6**, 1005-1016.

Vert G, Chory J. 2011. Crosstalk in cellular signaling: background noise or the real thing?. *Developmental Cell* **21,** 985-991.

Vollbrecht E, Schmidt RJ. 2009. Development of the inflorescences. Handbook of maize: Its Biology. Bennetzen JL, Hake SC. *Springer New York*. 13-40.

Vollbrecht E, Springer P, Goh L, Buckler E and Martienssen R. 2005. Architecture of floral branch systems in maize and related grasses. *Nature* **436**, 1119-126

Wagner R, Aigner H, Pruzinska A, Jankanpaa HJ, Jansson S, Funk C. 2011. Fitness analyses of *Arabidopsis thaliana* mutants depleted of FtsH metalloproteases and characterization of three *ftsh6* deletion mutants exposed to high light stress, senescence and chilling. *New Phytologist* **191**, 449-458.

Walsh J, Freeling M. 1999. The *liguleless2* gene of maize functions during the transition from the vegetative to the reproductive shoot apex. *The Plant Journal* **19**(4)**,** 489-495.

Weber ER, Hanekamp T, Thorsness PE. 1996. Biochemical and functional analysis of the YME1 gene product, an ATP and zinc-dependent mitochondrial protease from S. cerevisiae. *Molecular and Cellular Biology* **7**, 307-317.

Weigel D, Jurgens G. 2002. Stem cells that make stems. *Nature* **415**, 751–754.

Whipple CJ, Hall DH, DeBlasio S, Taguchi-Shiobara F, Schmidt RJ, Jackson DP. 2010. A conserved mechanism of bract suppression in the grass family. *The Plant Cell* **22** (3), 365-578.

Woo YM, Park HJ, Su'udi M, Yang Jl, Park JJ, Back K, Park YM, An G. 2007. Constitutively wilted 1, a member of the rice YUCCA

gene family, is required for maintaining water homeostasis and an appropriate root to shoot ratio. *Plant Molecular Biology* **65**, 125-136.

Wu X, Skirpan A, McSteen P. 2009. *Suppressor of sessile spikelets1* functions in the *ramosa* pathway controlling meristem determinacy in maize. *Plant Physiology* **149**(1), 205-219.

Wu XT, McSteen P. 2007. The role of auxin transport during inflorescence development in maize (Zea mays, Poaceae). *American Journal of Botany* **94**, 1745-1755.

Yamamoto Y, Kamiya N, Morinaka Y, Matsuoka M, Sazuka T. 2007. Auxin biosynthesis by the YUCCA genes in rice. *Plant Physiology* **143**, 1362-1371.

Yu F, Park S, Rodermel SR. 2005. Functional redundancy of AtFtsH metalloproteases in thylakoid membrane complexes. *Plant Physiology* **138**, 1957-1966.

Zaltsman A, Ori N, Adam Z. 2005. Two types of FtsH protease subunits are required for chloroplast biogenesis and photosystem II repair in *Arabidopsis.Plant Cell* **17**, 2782-2790.

Zelisko A, Garcia-Lorenzo M, Jackowski G, Jansson S, Funk C. 2005. AtFtsH6 is involved in the degradation of the light-harvesting complex II during high-light acclimation and senescence. *Proceedings of the National Academy of Sciences USA* **102**, 13699-13704.

Zhao YD, Christensen SK, Fankhauser C, Cashman JR, Cohen JD, Weigel D, Chory J. 2001. A role for flavin monooxygenase-like enzymes in auxin biosynthesis. *Science* **291**, 306–309.

CHAPTER II

GENETIC REGULATION OF MAIZE MEGAGAMETOPHYTE AND EMBRYO DEVELOPMENT

1. INTRODUCTION

1.1 Plant life cycle

The plant life cycle is characterized by the alternation of generations between a diploid sporophyte and a haploid gametophyte. The mature sporophyte produces haploid spores by meiosis, which then grow, dividing by mitosis, into gametophytes. The differentiated gametophytes in turn produce either the male gametes (sperm) or female gametes (egg cells) (Reiser and Fisher, 1993).

In contrast to lower plant species, in which the gametophyte is the dominant, free-living generation (Cove and Knight, 1993), gametophytes of angiosperms are smaller and less complex than the sporophyte and are formed within specialized organs

of the flower (Reiser and Fisher, 1993). The sexually dimorphic, multicellular gametophytes produce the gametes and are, thus, at the center of plant reproductive biology. Male and female gametophytes develop in the sexual organs of the flower. The male gametophyte (pollen or microgametophyte) develops within the stamen's anther, whereas the female gametophyte (embryo sac or megagametophyte) is a product of the ovule within the carpel's ovary. In the anthers, each spore mother cell (microsporocyte) divides by meiosis, forming four spores. In each spore the nucleus divides, forming a vegetative nucleus and a generative nucleus (Reiser and Fisher, 1993). The latter then divides forming two sperm cells. Thus, the mature pollen grain contains a male gametophyte consisting of three haploid cells (Kiesselbach, 1949). In the ovule, the single spore mother cell (megasporocyte) also forms four spores by meiosis, three of which degenerate. The remaining spore undergoes three successive nuclear divisions without cellularization to produce an eigth-nucleate embryo sac (megagametophyte) (Russell, 1979). Cellularization results in a seven-celled gametophyte containing three antipodal cells at the chalazal pole, one egg cell and two synergid cells at the micropylar pole and a central cell in the center, which inherits

two nuclei referred to as polar nuclei (Willemse and van Went, 1984; Huang and Russell, 1992; Yadegari and Drews, 2004).

This stage of the embryo sac represents the mature gametophyte, ready for the fertilization. Sexual reproduction in angiosperms is initiated when pollen is transferred from anther to stigma of the pistil (Drews et al., 1998). Shortly thereafter, the male gametophyte germinates a pollen tube and delivers its two sperm cells to the female gametophyte to effect "double" fertilization, in which haploid egg cell and diploid central cell both become fertilized. After fertilization, the egg cell and central cell give rise to the seed's diploid embryo and triploid endosperm, respectively (Maheshwari, 1950; Russell, 1993). At this point a new diploid sporophyte is formed (Dumas and Mogensen, 1993).

1.2 Maize megagametophyte: formation and development

The process of embryo sac development can be divided into two stages: megasporogenesis and megagametogenesis. In general, during megasporogenesis, the megasporocyte (megaspore mother cell) undergoes meiosis and four

megaspore nuclei are produced. Subsequent mitotic divisions, nuclear migration, and cytokinesis during megagametogenesis produce the mature embryo sac (Reiser and Fisher, 1993). Considerable diversity in the pattern of embryo sac development is found among plant species. Maize embryo sac development can be explained through the most common *Polygonum*-type pattern (Russell, 1979; Mansfield et al., 1990; Webb and Gunning, 1990).

Specification of the megasporocyte, production of a functional megaspore (megasporogenesis), formation of the embryo sac (megagametogenesis), and embryogenesis all occur within the ovule. The ovule is a specialized structure derived from the placenta of the ovary wall and it is the source of the megagametophyte and the progenitor of the seed (Reiser and Fisher, 1993) (Fig. 2.1).

In maize only one single sessile ovule is produced within the carpels and is derived at the part above the attachment of the carpels. Three undiverged carpels develop from a ring-like outgrowth at the base of the functional pistil in the upper floret in each spikelet of the ear. The united carpels, which will form the ovary wall or pericarp of the mature kernel, grow upward until they completely enclose the ovule (Kiesselbach, 1949).

Where they meet, the functionless so-called stylar canal is formed (Guignard, 1901; True, 1893). While the carpels are growing, the two anterior ones, which face the ear tip, form outgrowths which develop into a style or silk (Kiesselbach, 1949) (Fig. 2.1).

The ovule consists of a nucellus with two integuments or rudimentary seed coats. The nucellus represents the megasporangium and it is where the megaspore is produced and where the embryo sac develops (Reiser and Fisher, 1993). In maize, there is no defined funiculus or ovule stalk and any rudiment of such a structure is merged with the plancental tissue at the broad, circular seat of ovule attachment. This region is co-extensive with the chalaza which is the location where the nucellus and integuments of the ovule are united. The growth of both nucellus and integuments is more rapid on the posterior side of the ovule, which thereby becomes approximately inverted and curved. The inner integument grows until it forms a thin membrane covering the entire nucellus except for a small opening, the micropyle. The outer integument growing up from the posterior side does not extend as far, reaching only a little beyond the stylar canal (Kiesselbach, 1949) (Fig. 2.1).

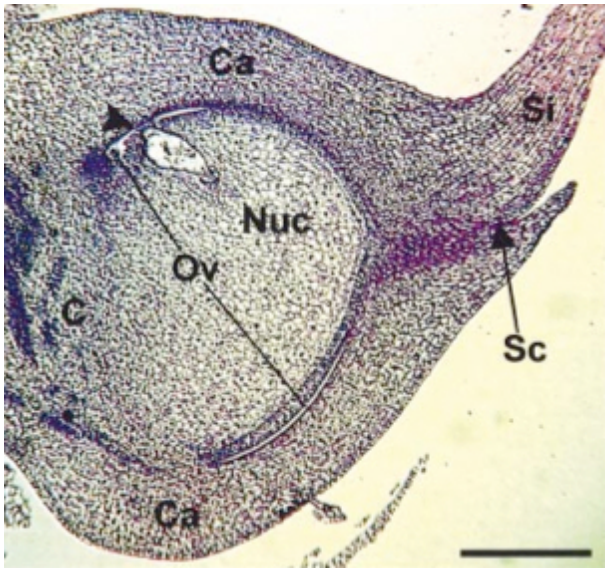

Fig. 2.1: Longitudinal section of a kernel shortly before fertilization. The ovule consists of the integuments, nucellus and embryo sac. The arrowhead indicates the micropylar region of the embryo sac. Ca, carpel; C, chalaza; Nuc, nucellus tissue; Ov, ovule; Sc, stylar canal; Si, silk. Scale bars: 300 μm (Cordts et al., 2001).

It is in the young nucellus of the ovule that the megasporogenesis starts. An axial row of cells is often noticed which terminates in a cell larger than the other ones and with a more prominent nucleus. This terminal cell, called archesporial cell, directly differentiates into the megasporocyte, or

megaspore mother cell, and elongates perpendicular to the ovule surface along the mycropylar-calazal axis before meiosis. Through meiosis, the megaspore mother cell forms a group of four megaspores and three of them soon degenerate, while the largest and chalazal-most megaspore persists to be the only functional megaspore and to function as the first cell of the embryo sac. The subsequent development of the megagametophyte is under the control of the haploid genome (Kiesselbach, 1949; Evans and Grossniklaus, 2008).

After meiosis, a central vacuole forms in the functional megaspore, and the megagametophyte enlarges throughout megagametogenesis primarily through enlargement of this vacuole (Evans and Grossniklaus, 2008). The surrounding nucellar cells degenerate and collapse, leaving a halo of appressed nucellar cell walls around the embryo sac (Russell, 1979). This vacuole forms chalazal to the single nucleus (Russell, 1979; Vollbrecht and Hake, 1995; Barrell and Grossniklaus, 2005). During megagametogenesis the functional megaspore undergoes three rounds of nuclear divisions and after the last round of mitosis a group of four nuclei at each end of the embryo sac is formed (Fig. 2.2). One nucleus from each group, called polar nucleus, moves toward the center of the

embryo sac until they meet and remain in contact. These two polar nuclei together form the central cell and in maize they remain in contact but they do not fuse until after fertilization (Kiesselbach, 1949; Evans and Grossniklaus, 2008). In many other species, including *A. thaliana*, the polar nuclei fuse to form a diploid central cell nucleus before fertilization (Portereiko et al., 2006). The three nuclei at the chalazal end, farthest from the micropyle, are the antipodal cells. These cells start to divide until a group of about 20 to 40 antipodal cells is formed (Fig. 2.2). This division of the antipodal cells is characteristic of the grass family (Kiesselbach, 1949; Evans and Grossniklaus, 2008). One of the nuclei at the micropylar end enlarges and becomes the nucleus of the egg cell, while the others become nuclei of the synergids. This group of three cells at the micropylar pole is often called the egg apparatus (Kiesselbach, 1949; Evans and Grossniklaus, 2008) (Fig. 2.2).

Thus, the mature embryo sac, located at the midline of the ovule towards the tip of the ear, is composed by eight nuclei and seven cells (Kiesselbach, 1949; Evans and Grossniklaus, 2008). These cells are striclty connected to each other through plasmodesmata, but no connections are found between megagametophyte cells and nucellar cells, in order to establish

a peculiar non-sporophytic environment for gametophyte development (Diboll and Larson ,1966).

The seven cells composing the embryo sac are, from the micropyle to the chalaza, the two synergids, which have an important role in pollen tube attraction, the egg cell, the binucleate central cell, and the three antipodals, which are believed to function as transfer cells for the embryo sac (Kiesselbach, 1949; Evans and Grossniklaus, 2008) (Fig. 2.2).

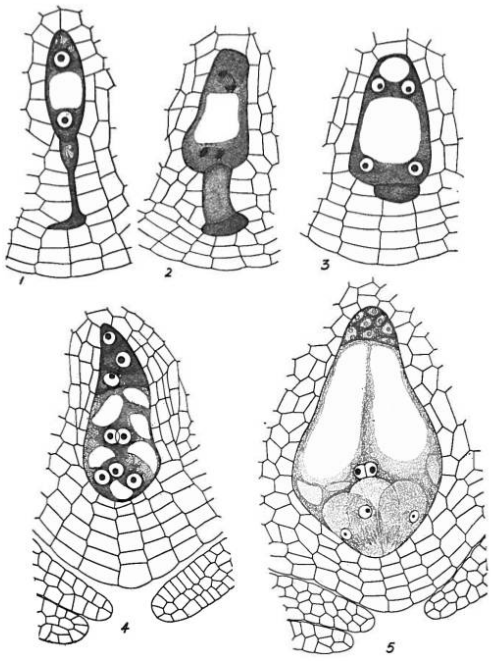

Fig. 2.2: Successive stages in the development of the embryo sac in maize. 1, two-nucleate stage (X 500); 2, two nuclei dividing to form four (X 500); 3, four-nucleate stage (X 500); 4, eight-nucleate stage where antipodal cells are formed above, polar nuclei have approached each other near the center, egg and synegids are below (X 400); 5, mature embryo sac where antipodal cells have divided to form a group of cells (X250). (Kiesselbach, 1949).

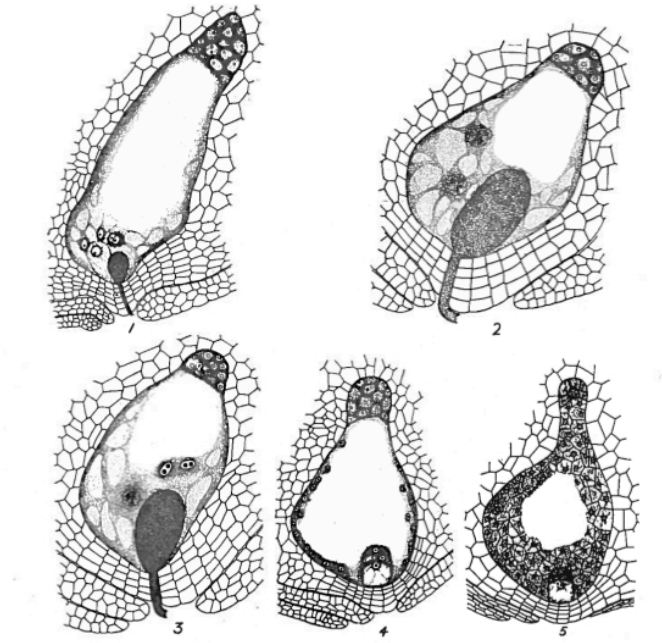

Fig. 2.3: Double fertilization and young embryo and endosperm stages. 1, pollen tube just entered into embryo sac and contents discharged (X 120); 2, after fertilization, showing one male nucleus fusing with the egg nucleus to form the zygote and the other fusing with one of the two polar nuclei preliminary to the triple fusion to form the primary endosperm nucleus (X 160); 3, endosperm nucleus divided (X 160); 4, three-cell stage of embryo and free-nuclear stage of endosperm (X 80); 5, older stage of embryo and endosperm becomes cellular (X 60). (Kiesselbach, 1949).

1.3 Maize embryo: formation and development

The embryo (and seed) development in maize starts with a double fertilization event (Fig. 2.3), producing a diploid fertilized egg and a triploid primary endosperm.

The primary endosperm nucleus divides mitotically within 3 to 5 hours after fertilization, and repeated divisions continue until a number of free nuclei are formed. The embryo sac enlarges and a central vacuole is formed. Each free nucleus divides until the cavity becomes filled with cellular tissue (Fig. 2.3). These cells forms the starchy endosperm, which occupies most of the endosperm and is composed by cells filled with nutrient reserves, mainly starch granules, but also protein bodies (Kiesselbach, 1949).

At the base of the endosperm, cells become differentiated and function as a conducting tissue called the basal endosperm transfer layer (BETL), that serves for conducting food from the mother plant to the growing endosperm and indirectly to the embryo (Weatherwax, 1930; Thompson et al., 2001). Other cells, of the outer cell layer, differentiate to form the aleurone layer, the cells of which contain aleurone grains and oil but no starch (Kiesselbach, 1949) (Fig. 2.4). This is a digestive tissue which plays an important role during germination. Also, a

specialized group of other cells adjacent to the embryo, embryo surrounding region (ESR), may be involved in the exchange of resources and signals (Opsahl-Ferstad et al., 1997). Immediately outside the aleurone layer, a very thin membranous tissue derived from the outer epidermal wall of the nucellus persists as a continuous covering between the aleurone and the pericarp, which is the transformed ovary wall and the tough outer covering of the seed, furnishing protection for the interior parts (Kiesselbach, 1949).

The fertilized egg does not begin to divide as soon as after fertilization as does the primary endosperm nucleus (Fig. 2.3). The fertilization process occurs between 16 and 24 hours after pollination, depending on the maize genetic background and environmental conditions (Kiesselbach, 1949). The two fusion events appear to occur simultaneously or nearly so, but the timing of the first division of the two fertilization products differs greatly (Randolph, 1936). The young embryo or proembryo develops much slower than the endosperm in its early stages, starting dividing about 40 hours after pollination (Kiesselbach, 1949).

The zygote is asymmetric, generating a small apical and a large basal cells. The basal cell forms the suspensor whose growth

serves to orient the embryo properly with respect to the endosperm (Fig. 2.3). The suspensor soon ceases to enlarge and degenerates. The small apical cell starts enlarging through cell divisions and it forms the proembryo, an ovoid structure of indifferentiated cells.

The first further differentiation of the embryo is the appearence of a region of small cells, more densely filled with protoplasm, on the anterior side of the embryo, below its tip. This is the region where the stem tip or shoot apical meristem (SAM) develops. Cells opposite to the developing endosperm remain small and dense and cells next to the endosperm start to enlarge. The smaller cells will produce the embryo axis whereas the enlarged cells will produce the scutellum, which is the first leaf and it is attached to the scutellar node. This differentiation determines that the embryo shifts to a bilateral symmetry (Kiesselbach, 1949) (Fig. 2.4). The scutellum is supposed to be the single cotyledon in the monocotyledoneus embryos, it never functions as a true foliage leaf but it is modified as a food storage organ and serves to digest and absorb the endosperm nutrients during growth of the embryo and seedling (Harz, 1885; Rowlee and Doherty, 1898; Gager, 1907). A ring of tissue forms around the SAM which develops

into the coleoptile, which is the second leaf, modified to act as a protective covering for the plumule or first bud of the plant which grows throughout the soil during germination. The growing point of the stem next begins to form leaves initials (usually five or six), the first of which is at the base of the SAM, next to the coleoptilar ring (Fig. 2.4). These leaves remain all rolled up inside of the coleoptile until emergence during germination. At about the same time the tissues in the lower part of the embryo begin differentiating to form the initial of the primary root. Cells surrounding the root meristem form the coleorhiza, which protects the meristem during root emergence. A number of lateral root initials form just above the scutellar node (Kiesselbach, 1949) (Fig. 2.4).

During maturation the embryo increases in size and accumulates storage products, mainly lipids and proteins. This takes place especially in the scutellum, which greatly increases in size. About 45-50 days after pollination the embryo is fully differentiated with a central axis terminating at the basal end by the primary root, protected by the choleoriza, and at the other hand by the stem tip, with five or six short internodes and leaf primordia surrounded by the coleoptile. The mature seed consists of embryo, endosperm and remnants of the seed coats

and nucellus. This seed is permanently enclosed in the adhering pericarp to form a one-seeded fruit botanically called caryopsis but commonly known as kernel (Kiesselbach, 1949) (Fig. 2.4).

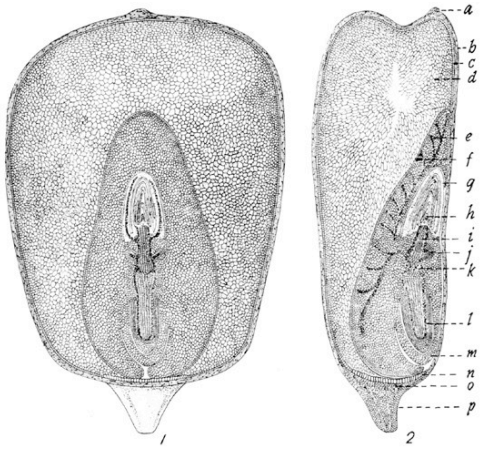

Fig. 2.4: Mature kernel. 1 and 2 vertical sections of a mature kernel, showing arrangement of organs and tissues. a, silk scar; b, pericarp; c, aleurone; d, endosperm; e, scutellum; f, glandular layer of scutellum; g, coleoptile; h, plumule with stem and leaves; i, first internode; j, lateral root; k, scutellar node; l, primary root; m, coleorhiza; n, basal conducting cells of endosperm; o, brown abscission layer; p, pedicel or flower stalk (X 7) (Coe, 2001).

1.4 Genetic and epigenetic regulation in plant development

Proteins involved in the female gametophyte development and function could be encoded by genes expressed either within the female gametophyte or in the surrounding sporophytic cells of the ovule. Female gametophyte-expressed genes regulating specific steps of the female gametophyte development have

been identified. Mutations in these genes can be identified as lethals in which female gametophytes harboring the mutation either abort development or are nonfunctional. They may affect female gametophyte–specific processes, such as the establishment of female gametophyte polarity, specification and differentiation of the female gametophyte cells, polar nuclei migration and fusion, antipodal cell death, pollen tube guidance, fertilization, and the induction of seed development (Drews et al., 2008).

Many genes required for female gametophyte development have been identified in *A. thaliana* including *FERTILIZATION-INDEPENDENT ENDOSPERM* (*FIE*) (Ohad et al., 1996, 1999), *MEDEA* (*MEA*) (Chaudhury et al., 1997; Grossniklaus et al., 1998; Kiyosue et al., 1999), *FERTILIZATION-INDEPENDENT SEED2* (*FIS2*) (Chaudhury et al., 1997; Luo et al., 1999), *MULTICOPY SUPPRESSOR OF IRA* (*MSI1*) (Köhler et al., 2003a; Guitton et al., 2004), *DEMETER* (*DME*) (Choi et al., 2002), *FIE, FIS2, MEA, MSI1,* and *DME* are known to function in the central cell specifically. Loss-of-function mutations in the *FIE, FIS2, MEA,* and *MSI1* genes result in autonomous endosperm development in the absence of fertilization. DME is a regulatory molecule required for *MEA*

expression in the central cell and endosperm (Choi et al., 2002; Gehring et al., 2006). Some gametophyte expressed genes have been identified also in maize and their mutations reduce fertility and seed set (Evans and Grossniklaus, 2008).

In summary, it is evident the importance of megagametophyte expressed genes in regulating embryo sac development and also in controlling embryogenesis and seed development.

Many genes also involved in plant embryo development have been characterized (José-Estanyol et al., 2009). A number of large screenings for embryo mutants have provided a collection of nearly 750 DNA loci essential for embryogenesis (Tzafrir et al., 2003) and have led to the idea that correct embryo development requires the sequential and coordinated action of specific genes (José-Estanyol et al., 2009). Systematic analyses of seed defective mutants in *A. thaliana* showed that many genes are essential to seed development and they are collectively termed *EMB* genes (Shen et al., 2013). The *EMB* genes possess several functions in many processes such as transcription and regulation (Vroemen et al., 2003; Ding et al., 2006), DNA replication (Springer et al., 1995), protein translation (Uwer et al., 1998; Apuya et al., 2002), protein degradation (Doelling et al., 2001) and metabolism (Eastmond

et al., 2002). Genes regulating seed development have been identified also in maize and mutations in these genes result mainly in defects in embryo and/or endosperm development (Neuffer and Sheridan, 1980; Sheridan and Neuffer, 1980; Clark and Sheridan, 1991; Fu et al., 2002; Fu and Scanlon, 2004).

Morphological, cytological analysis, together with the use of gene markers have provided valuable information on the regulation of embryogenesis in maize and determined, for example, that a interaction exists between endosperm and embryo during seed development (Sheridan and Neuffer, 1982), that embryo development can be blocked at a variety of different stages, that the arrest of development can imply necrosis or not and can be associated to morphological alterations (Vernoud et al., 2005).

The determination of sporogenic fate late during development, the differentiation of gametes within multicellular gametophytes, and the distinction of the two female gametes involved in double fertilization, are not only under genetic control but also under epigenetic control (Baroux et al., 2011; Gutierrez-Marcos and Dickinson, 2012). This phenomenon occurs when gene expression is controlled by changes in the

structure of chromatin without changing the DNA sequence (Fujimoto et al., 2012).

Epigenetic mechanisms, such as DNA methylation, regulation of transposons via small RNAs, and histone modifications, all represent effective ways of controlling the epigenetic status of plant gametes, regulating in this way the inheritance and gene expression during plant reproduction and development (Migicovsky and Kovalchuk, 2012).

DNA methylation is a well known epigenetic modification and a major component of the gene silencing machinery in plants. DNA methylation refers to an addition of a methyl group at the fifth carbon position of a cytosine ring, and in plants it is observed not only in the symmetric CG context but also in sequence contexts of CHG and CHH (where H is A, C, or T) (Cokus et al., 2008; Law and Jacobsen, 2010). DNA methylation patterns are established by two different DNA methyltransferase activities: *de novo* activity that transfers a methyl group to completely unmethylated double stranded DNA, and maintenance activity that methylates cytosine in proximity with methylcytosine on the complementary strand (Kapoor et al., 2005).

In plants, DNA methylation in the CG context is maintained

during DNA replication by MET1 (METHYLTRANSFERASE 1), while non-CG contexts are maintained by DRM2 (DOMAINS REARRANGED METHYLTRANSFERASE2) and CMT3 (CHROMOMETHYLASE 3) (Law and Jacobsen 2010; Saze, 2008). The process of *de novo* DNA methylation is triggered by 24-nt siRNAs produced by the RNAi (RNA interference) pathway, termed RdDM (RNA-directed DNA methylation) (Matzke et al., 2009). Two plant specific RNA polymerases, Pol IV and Pol V, RDR2 (RNA-DEPENDENT RNA POLYMERASE 2), DCL3 (DICER-LIKE 3), and AGO4 (ARGONAUTE 4) proteins function in this RNAi pathway (Matzke et al., 2009; Haag and Pikaard, 2011), forming an effector complex which directs DRM2 for *de novo* methylation of target genomic sequences (He et al., 2009).

DNA methylation appears to function mainly to protect the plant genome by suppressing the activity of transposons and other repetitive sequences and it also regulates gene expression in response to changes during development or in response to environmental stimuli (Martienssen and Colot, 2001; Chan et al., 2005; He et al., 2011). Methylation content varies widely between plants, from about 5% of total cytosines in *A. thaliana* to more than 20% in wheat germ (Leutwiler et al., 1984). This

is largely attributable to differences in repetitive DNA content among species, which is the major target of DNA methylation (Gehring and Henikoff, 2007).

The level and pattern of 5-meC are highly dynamic and they are determined by two processes: DNA methylation and demethylation. In fact, DNA demethylation may be needed to activate specific genes or to reset the epigenetic state of the genome during development or in response to environmental perturbations (Zhu, 2009).

Demethylation of DNA can be passive or active. Passive DNA demethylation occurs when maintenance methyltransferases are inactive during the cell cycle following DNA replication, which results in a retention of the unmethylated state of the newly synthesized strand. Active DNA demethylation involves one or more enzymes and can occur independently of DNA replication. The first enzyme in the active demethylation pathway has been referred to as the demethylase (Zhu, 2009). Demethylation has emerged as an important mechanism in flowering plants for shaping methylation patterns, crucial in genome regulation and plant development (Gehring et al., 2009a). DNA demethylation prevents the spreading of DNA methylation from repetitive sequences and protects genes from

deleterious methylation (Zhu, 2009). In this way, plants enjoy a robust methylation defense system that silences transposable elements without negatively affecting nearby genes (Gehring et al., 2009a). Nevertheless, active DNA demethylation is also important for keeping transposons in a dynamic state, that is not completely silenced. In this way the plant epigenome is maintained plastic and the plant can respond efficiently to environmental challenges during adaptation (Zhu, 2009).

Active DNA demethylation is involved in two processes in angiosperms: gene imprinting during reproduction and maintaining normal methylation patterns throughout the plant (Gehring and Henikoff, 2008). Imprinting is the differential expression of the alleles of a gene depending on whether they are inherited from the male or female parent. Imprinting regulates a number of genes essential for normal development and in plants the endosperm is the site where imprinting is observed (Gehring et al., 2004, 2006). The exact number of imprinted genes in plants is unknown, but recent analysis has discovered that more than 200 genes that appear to show imprinting (Gehring et al., 2011; Hsieh et al., 2011; Wolff et al., 2011). For imprinted plant genes, the methylated inactive state is the default state, and their expression in the endosperm

is the consequence of DNA active demethylation occurring in the female gametophyte before fertilization (Gehring et al., 2006; Zhu et al., 2009).

1.5 DNA demethylases in plants

In plants, a subfamily of DNA glycosylases which can remove the methylation mark through active DNA demethylation has been identified (Gong et al., 2002; Gehring et al., 2006). These demetylases are DNA glycosylases/lyases of the DEMETER (DME) family, which is unique to plants and consists of four proteins: DEMETER (DME), DEMETER-LIKE 2 (DML2), DML3, and DML1 or REPRESSOR OF SILENCING1 (ROS1) (Agius et al., 2006; Gehring et al., 2006; Morales- Ruiz et al., 2006; Penterman et al., 2007a).

These proteins are bifunctional DNA glycosylases because they not only recognize and remove 5-meC from double-stranded DNA, but also show lyase activity, which nicks double-stranded DNA at an abasic site. This mechanism, known as base excision repair (BER), normally functions to repair damaged and mispaired bases and uniquely in plants it is also required for active DNA demethylation (Gehring et al.,

2009b; Zhu, 2009; Law and Jacobsen, 2010).

DML1, DML2 and DML3 are expressed in vegetative tissues (Gong et al., 2002; Penterman et al., 2007b; Ortega-Galisteo et al., 2008) and they protect genes from potentially deleterious methylation (Penterman et al., 2007b; Zhu et al., 2007). The *dml1 dml2 dml3* triple mutant has no overt morphological phenotype, and results in increased methylation at limited loci without affecting the global methylation status (Penterman et al., 2007a). Some loci are exclusively demethylated by a particular DML and others demethylated redundantly by multiple DML enzymes (Penterman et al., 2007b). DNA demethylation by DME occurs during reproductive development and is required for genomic imprinting and seed viability (Choi et al., 2002; Gehring et al., 2006).

DME DNA glycosylases/lyases are large polypeptides with significant sequence similarity to base excision DNA repair proteins in the HhH-GPD superfamily (Nash et al., 1996), widespread in all three domains of life (bacteria, archaea and eukaryotes). Members of the DME family are unusually large (1100–2000 amino acids) compared with typical DNA glycosylases (200–400 amino acids long (Denver et al., 2003). DME glycosylases/lyases have three distinct domains, the

glycosylase domain, domain A and B, all required for 5mC excision activity (Mok et al., 2010). The glycosylase domain of DME contains a helix– hairpin–helix (HhH) motif and a glycine/proline-rich loop with a conserved aspartic acid (GPD), also present in both prokariotic and eukariotic DNA glycosylases. In contrast to most other members of the HhH glycosylase superfamily, DME family members contain two additional conserved domains, domain A and domain B, flanking the central glycosylase domain. The function of these domains is still unknown, but the domain A seems to be required for nonspecific DNA binding (Mok et al., 2010).

The DME family is highly conserved in diverse plant species, with homologs also present in mosses and unicellular green algae. This suggests that active demethylation through excision of 5-meC may have appeared early during plant evolution (Roldan-Arjona and Ariza, 2009).

1.6 DEMETER: a DNA glycosylase/lyase involved in seed development

The largest gene for DME family glycosylases, DEMETER (DME) was initially identified by mutations that cause

maternal effects on seed viability in *A. thaliana* (Choi et al., 2002). Either self-pollinating heterozygous DME/*dme* plants or pollinating them with wild type pollen, a 1:1 ratio of viable: inviable seeds is obtained, and all the viable seeds are wild type. Inheritance of a *dme* mutant allele by the female gametophyte results in embryo and endosperm abortion even when a wild type paternal *DME* allele is inherited. Thus, seed viability depends only upon the presence of a wild type maternal *DME* allele, and the paternal allele is expendable (Choi et al., 2002). In *A. thaliana*, homozygous *dme* plants generate normal rosette leaves, an inflorescence, and produced siliques containing nearly all (98%) aborted seeds, with enlarged endosperm and aborted embryos (Choi et al., 2002) (Fig. 2.5).

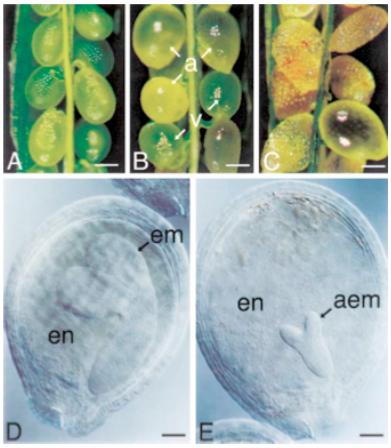

Fig. 2.5: *A. thaliana dme* mutants. A, wild type silique ; B, heterozygous *DME/dme* silique; C, homozygous *dme* silique; D, viable seed obtained from silique in B; E, aborted seed obtained from silique in B. Scale bars: 0.5 mm (A–C) and 0.1 mm (D and E). a, aborted seed; aem, aborted embryo; em, embryo; en, endosperm; v, viable seed. (Choi et al., 2002).

DME is expressed in the homodiploid central cell of the female gametophyte before fertilization, where it promotes an extensive demethylation of the maternal genome (Hsieh et al., 2009, 2011), activating both genes and transposable elements (Gehring et al., 2006, 2009a). After double fertilization the maternal alleles can be expressed throughout endosperm development, whereas the paternal alleles still cannot be expressed because of the lack of DME in the endosperm (Gehring et al., 2004). This condition allows the establishment of the imprinting, with an endosperm inheriting two parental genomes with differential DNA methylation (maternal hypomethylated, paternal hypermethylated) (Bauer and Fischer, 2011).

Since imprinting takes place in the endosperm, a tissue that supports embryo growth during seed development and seedling germination, imprinted genes have a crucial role in plant development (Gehring et al., 2009a). Five imprinted genes regulated by DME activity have been subject of intense study in *A. thaliana*: *FLOWERING WAGENINGEN* (*FWA*), *MEDEA* (*MEA*), *FERTILIZATION INDEPENDENT SEED 2* (*FIS2*) and *MATERNALLY EXPRESSED PAB C-TERMINAL* (*MPC*) are expressed maternally and are silent paternally, whereas

PHERES1 (*PHE1*) is oppositely imprinted (Gehring et al., 2009a). These genes are all involved in transcriptional regulation (Grossniklaus et al., 1998; Vielle-Calzada et al., 1999; Luo et al., 2000; Soppe et al., 2000; Köhler et al., 2003b; Kinoshita et al., 2004; Köhler et al., 2005; Jullien et al., 2006). The FWA and PHE1 proteins are both transcription factors (homeodomain and MADS domain, respectively), while MEA and FIS2 are members of Polycomb Repressive Complex 2 (PRC2), which inhibits expression of target genes in endosperm, including *PHE1* (Gehring et al., 2009a). Mutations in the imprinted *MEA*, *FIS2, MPC* genes, include endosperm overproliferation and seed abortion when ovules are fertilized, ectopic division of the central cell in unfertilized ovules and a variety of effects on seeds, including seed abortion, reduced seed size, and abnormal embryo and endosperm morphology (Ohad et al., 1996; Chaudhury et al., 1997; Tiwari et al., 2008). These mutants phenotype confirm that parental imprinting has significant effects on seed development, growth and viability (Gehring et al., 2004). Also in maize a gene whose imprinting in the endosperm seems to act in a similar manner, has been identified (Gutierrez-Marcos et al., 2006; Hermon et al., 2007). *FERTILIZATION INDEPENDENT ENDOSPERM 1* (*FIE1*) is

less methylated in the central cell compared with the egg cell and sperm cell and after fertilization (Gutierrez-Marcos et al., 2006).

However, DNA demethylation is not targeted to imprinted genes, but it is genome wide and that could result in widespread activation of TEs and other siRNA loci in the endosperm. TEs, if reactivated, have the ability to cause unfavorable mutations (Lisch, 2009). During gametogenesis and seed development in plants, it is very important to keep transposons inactive to maintain genome stability in gamete and embryo and to ensure the accuracy of genetic information during the life cycle (He et al., 2011).

Plants seem to have developed a mechanism of defense against TEs and protection of the embryo during development. Through DME demethylation loci for siRNAs production are activated in the endosperm and the newly created siRNAs can be transported to the egg cell and later to the embryo to reinforce TE silencing through RdDM pathway. This mechanism benefits the embryo by reinforcing repetitive DNA silencing, and the genomic danger imposed by a possible TE reactivation would be confined to the endosperm (Hsieh et al., 2011; Ibarra et al., 2012).

A similar siRNA silencing effect acts in pollen, where DME is active and demethylates genes and transposons in the genome of the vegetative cell (Schoft et al., 2011). TE reactivation allows for siRNA production that is shuttled to the two sperm cells to reinforced TE silencing through RdDM pathway (Slotkin et al., 2009). The vegetative cell genome does not participate in double fertilization. Hence, DME activity in the vegetative cell, unlike its activity in the central cell, does not regulate gene imprinting in the endosperm (Schoft et al., 2011). The accessory cells and tissues such as the vegetative cell, central cell, and endosperm do not contribute genetically to the next generation, so the transient transposon activation is likely to carry a fairly low cost. Thus, the plant can afford to "sacrifice" these terminal tissues and cells to obtain in return the repression of TE expression and the maintainance of genome stability in sperm cell and embryo (Johnson and Bender, 2009; Slotkin et al., 2009; LeTrionnaire and Twell, 2010; Mosher and Melnyk, 2010).

The important role of DME in controlling the described siRNAs pathway has been demonstrated in a recent study (Hsieh et al., 2009), where through a genome-wide epigenetic analysis all the sequence contexts (CG, CHG and CHH) in *A.*

thaliana endosperm and embryo were compared.

As expected, because DME is a demethylase acting in the central cell, a genome-wide demethylation was found in the endosperm compared to the embryo and an increased DNA methylation level was detected in *dme* mutant endosperm (Gehring et al., 2009a, Hsieh et al., 2009). However, the unexpected result was that only methylation in CG context is increased in *dme* mutants, while levels of methylation in CHG and CHH contexts were reduced compared to wild type endosperm (Hsieh et al., 2009). The explanation is that the removal of DNA methylation by DME activates expression of siRNAs, which in turn utilize the RdDM pathway for the *de novo* non-CG methylation. Thus, in the *dme* mutant, there is higher CG methylation and less siRNA activation, resulting in a reduction of both RdDM activity and non-CG methylation.

Most of the knowledge about DNA methylation in plant seeds is derived from *A. thaliana*, while less is known in other plants, like monocots. Monocots and dicots diverged about 150 million years ago (Hedges et al., 2006) and since processes involving genetic conflict tend to evolve rapidly (Swanson and Vacquier, 2002), methylation dynamics in monocot seeds may be quite different. A recent genome-wide study in rice showed

a global reduction of the DNA methylation level in rice endosperm compared to the embryo, as seen in *A. thaliana* (Hsieh et al., 2009). Nevertheless, in contrast to *A. thaliana*, where a global CG demethylation is detected in the endosperm (Hsieh et al., 2009), CG methylation of most loci is unchanged in rice endosperm, with hypomethylation restricted only to specific domains, corresponding to genes precursors of glutelin and starch syntetizing enzymes (Zemach et al., 2010). On the other hand, non-CG methylation in rice endosperm is reduced throughout the genome, while in *A. thaliana* the methylation in these contexts is reinforced by siRNAs activity. To conclude, this wild type rice endosperm methylation pattern, with globally reduced non-CG methylation and local CG hypomethylation, resemble that of *A. thaliana* with a mutation in the DEMETER (DME) DNA glycosylase (Hsieh et al., 2009), leading the authors to speculate about the lack of DME in monocots (Zemach et al., 2010).

Although the mechanism of demethylation in monocots seems to be quite different compared to *A.thaliana*, it is been shown that a major reduction of DNA methylation occurs also in the endosperm of rice and maize (Lauria et al., 2004; Zemach et al., 2010). Other features are shared between monocots and

eudicots. In fact, short TEs hypermethylated at CHH sites in rice embryo suggest that demethylation functions to immunize the embryo against TEs through small RNAs (Zemach et al., 2010). Furthermore, a number of monocot imprinted genes apparently activated by selective maternal demethylation have been identified (Lauria et al., 2004; Gutierrez-Marcos et al., 2006; Hermon et al., 2007; Jahnke and Scholten, 2009), but the mechanism and the enzymes responsible for imprinting and DNA demethylation in monocots are still unknown and further investigation is needed.

1.7 Aim of this work

This work aims to gain a better understanding of the genetic mechanisms involved in gametogenesis and embryogenesis in maize. For this reason, the presence and the role of *A. thaliana DEMETER* (*DME*) homologues is here investigated in maize. In *A. thaliana*, this gene is known to encode a demethylase which is active in the central cell of the female gametophyte before fertilization and it is necessary for embryo and seed viability.

Although the lack of DME in monocots has been speculated

(Zemach et al., 2010), recent findings leave open the question of whether DME is actually absent in these plants.

The aim of this work is to identify and characterize *DME* homologues in maize in order to better understand the genetic mechanisms occurring in the female gametophyte and how they affect seed development.

2. MATERIALS AND METHODS

2.1 Plant material

To study the maize seed development, *Zea mays* L. plants of the inbred line B73 were used. A morphological analysis was performed in order to identify different stages of development during gametogenesis. Unfertilized ears from wild type B73 plants were collected to study the morphology of the gametophyte.

Furthermore, to investigate the role of *DME* homologues in maize, the expression pattern of these genes was analyzed in: 1. three different stages of ovule development from unfertilized ears, to verify the expression in the mature gametophyte; 2. embryo and endosperm from 20 DAP kernels, as control because *A. thaliana DME* is not expressed after fertilization; 3. leaf, radicle and coleoptile from seedlings, as second control since *A. thaliana DME* expression is not detected in vegetative tissues.

Also, to perform a functional analysis of *DME* homologues in maize, mutant plants were studied.

Seeds with transposon insertions were obtained from UniformMu and Mu-Illumina databases (see Chapter I, paragraph 2.4), while seeds with a point mutation, originally derived from an EMS mutagenesis population, were kindly given to me by Dr. Wei Zhang from Dr. Joachim Messing's Lab, Waksman Institute of Microbiology, Rutgers University (USA). Unfertilized florets, 20 DAP and 40 DAP kernels from homozygous mutant plants and B73 wild type plants were used for a morphological analysis to verify the presence of defects in gametophyte and embryo development in the mutants. Plants were grown in the research fields and greenhouse of the University of Milan and the Waksman Institute of Microbiology, Rutgers University (USA).

2.2 Sequence analysis

To identify putative *DME* genes in maize, the DME protein sequence of *A. thaliana* (At5g04560) was used as reference sequence in BLASTP analysis performed at Phytozome (www.phytozome.net), MaizeGDB (www.maizegdb.org) and NCBI (http://www.ncbi.nlm.nih.gov/). Two genes encoding DME homologues in maize were found: GRMZM2G123587

and GRMZM2G422464. In this work we renamed these *DME* sequences as *ZmDME1* and *ZmDME2*, respectively.

In order to evaluate the protein structure and the presence of conserved motifs, ZmDME1 and ZmDME2 sequences were analyzed with *A. thaliana* DME and other two monocot DMEs of *S. bicolor* and *O. sativa.* by using MEME, a motif-based sequence analysis tool (Timothy et al., 2009).

2.3 Phylogeny

A total of 43 homologous proteins to ZmDME1 and ZmDME2 detected in eudicots (*Arabidopsis thaliana*, *Arabidopsis lyrata*, *Carica papaya*, *Cucumis sativus*, *Glycine max*, *Populus trichocarpa*, *Ricinus communis*, *Vitis vinifera*) and monocots (*Brachypodium distachyon*, *Oryza sativa*, *Sorghum bicolor*) and moss (DMLs of *Phsycomitrella patens*), were used for phylogenetic analysis. Two *Phsycomitrella patens* DMLs amino acid sequences were used as outgroup. Conserved domains of the indicated glycosylase proteins were aligned using the ClustalW algorithm in BIOEDIT version 7.1.3 (Hall, 1999) and adjusted manually. Bayesian phylogenetic analysis using MrBayes 3.2.1 (Huelsenbeck and Ronquist, 2001) was

performed. Two independent Markov chain Monte Carlo (MCMC) runs of four chains using the default Poisson model were started from independent random trees, and were carried through a total of 1,500,000 generations, with trees sampled every 100th generation. Convergence was confirmed by checking that the standard deviations of split frequencies were <0.01 and at this point the analysis was stopped. The 25% of the first stored trees from each run was discarded and the remaining trees were used to construct the consensus tree.
Final tree was checked and graphically presented using FigTree v1.4.0 (http://tree.bio.ed.ac.uk/software/figtree/).

2.4 Genotyping

In order to study the role and function of *DME* homologues in maize, mutants were investigated.
Two transposon insertions in *ZmDME2* gene were found in UniformMu and Mu-Illumina databases and seeds were obtained from the seed stock. Plants were genotyped using primers Zma464ill1/EoMumix3 and Zma 464Mu3/MuTIR6 (Table 2.1) to verify the presence of the insertions as described in Chapter I, paragraph 2.2.

Seeds with a point mutation in *ZmDME1* gene were also obtained. These seeds, derived from a self-crossed *Zmdme1*/B73 population were planted and plants of the F2 population were genotyped using primers dng-102F and dng-102R (Table 2.1).

Primer	Sequence (5'-3')	Gene	T annealing
dng-102F	GGGACACACAGCCATCAATATCTGGAG	GRMZM2G123587	65°C
dng-102R	TGGTTATGGCCCTCCTGACTGGAAGTA		
dng-102seq	GCATGCAAAAGGATGAGACCAGAGA		
Zma464illF1	CACCCGACTTTGAGCTAGGAGGTA	GRMZM2G422464	65°C
Zma464illR1	GCGCGGCATTTCTGGTTTGAGTTG		
Zma464MuF3	TGCAATTCATGTCCAATGAGAGCTG		
Zma464MuR3	GGAACACCTAAAGAGGTGGGTGCAG		
EoMumix3	EoMu1: GCCTCCATTTCGTCGAATCCC	MuIllumina transposon insertion	65°C
	EoMu2: GCCTCTATTTCGTCGAATCCG		
MuTIR6	AGAGAAGCCAACGCCAWCGCCTCYATTTCGTC	UniformMu transposon insertion	65°C

Table 2.1: Primers used to verify the presence of the insertions and the point mutation.

PCR products were then sent for sequencing to GenScript or Genewiz, as described in Chapter I, paragraph 2.2.5. To verify the presence of the insertions in *ZmDME2* gene, PCR products were sent for sequencing using both forward and reverse primers. To verify the presence of the point mutation in *ZmDME1*, PCR products were sent for sequencing using primer dng102-seq (Table 2.1).

2.5 Morphological analysis

A morphological analysis was performed in order to: 1. identify different stages of development during gametogenesis in maize; 2. verify the presence of defects in the gametophyte and embryo of mutant plants.

Unfertilized florets and 20 DAP embryos from fertilized ears were collected from B73 wild type plants and homozygous *Zmdme1* mutant plants and they were processed as described in paragraphs 2.5.1 and 2.5.2.

40 DAP kernels from B73 wild type ears and *Zmdme1* mutant ears were collected and dissected under a stereo microscope (Leica M205C) to examine the phenotype.

2.5.1 Sample treatment

All the plant tissues used for morphological analysis were dissected and fixed using FAA (3.7% formaldehyde, 5% acetic acid and 50% ethanol). The obtained tissues were immersed in cold fixative and kept in vials on ice under vacuum to pull the air out of the tissue. After vacuuming, the fixative was replaced in vials with fresh fixative and they were fixed overnight at 4°C.

Subsequently, samples were dehydrated in a graded ethanol series (80%, 90%, 95% and 100%). Tissues were then embedded in wax, sectioned at the microtome and mounted on slides as described in Chapter I paragraphs 2.5.2 and 2.5.3.

In the case of samples used for *in situ* hybridization experiment, the 8 µm sections were mounted on Probe on Plus Slides (Fisher Scientific). If the tissues were used for a simple morphological analysis, sections were mounted on regular slides (VWR).

2.5.2 Histological analysis

For histological analysis, slides were arranged in a metal rack and were treated twice with 100% Histoclear (National Diagnostics, Atlanta, GA, USA) to remove wax and hydrated twice with 100% ethanol. Slides were then dried under vacuum, added into a coplin jar and stained in a staining solution. Three different staining solutions were used: Toluidine Blue (0.1%), Acridine Orange (0.5%) and DAPI (1µg/µl). Toluidine Blue is a dye with high affinity for acidic components and it was used to stain nuclei and cell walls in the tissue slices. Acridine Orange is a nucleic acid selective fluorescent dye, used to test the quality of RNA preservation in our samples. DAPI (4',6-diamidino-2-phenylindole) is a fluorescent stain that binds to A-T rich regions in DNA and it was used to stain the nuclei in the tissues analyzed.

After staining in a staining solution, slides were rinsed with water and dried overnight on the slide warmer. Few drops of Permount (Fisher Scientific) were used to mount the slides with coverslips.

Plant sections were then observed on the light microscope (ZEISS Axiophot D1 and Leica DM5500B), using UV light in case of Acridine Orange and DAPI staining.

2.6 Expression analysis

To investigate the role of *ZmDME1* and *ZmDME2*, the expression pattern of these genes was investigated through RT-PCR analysis, Real Time PCR analysis and *in situ* hybridization analysis.

2.6.1 RNA extraction

In order to study gene expression through RT-PCR and Real Time PCR, RNA was extracted from unfertilized ovules at three different stages of development, embryo and endosperm from 20 DAP kernels and three vegetative tissues (leaf, radicle and coleoptile).
RNeasy Plant Mini Kit (Qiagen) was used for RNA extraction, according to manifacturer's instructions.

2.6.2 RNA retrotranscription

Retrotrascription was performed using the Enhanced Avian HS RT-PCR Kit (Sigma-Aldrich), according to manufacturer's instructions. This step allowed to convert RNA into its DNA complement through the use of a reverse transcriptase. Thus, the first strand cDNA was ready for PCR amplification.

2.6.3 Primers

Primers to amplify *ZmDME1* and *ZmDME2* were designed in coding regions of these genes (Table 2.2). Due to the high similarity of *ZmDME1* and *ZmDME2*, primers were designed in regions showing polymorphisms between the two genes, in order to specifically amplify one gene or the other.

The primer pair Zma2DMEint-F/Zma2DME-R was used to amplify approximately 250 bp of the gene *ZmDME1*, while the primer pair Zma464-F/R was used to amplify approximately 200 bp of *ZmDME2,* using cDNA as template.

Primers were designed using Primer3 (v.0.4.0) (Untergrasser et al., 2012), GeneFisher2 (Giegerich et al., 1996) and Operon Oligo Analysis Tool (http://www.operon.com/tools/oligo-analysis-tool.aspx).

Reverse primers Zma2DME-R and Zma464-R with a T7 promoter at the 5' end were used to synthetized the antisense probe for the *in situ* hybridization (Table 2.2).

ZmACT-F/R primer pair (Gutiérrez-Marcos et al., 2006) was used to amplify actin gene as positive control in the RT-PCR and Real-Time PCR. ZmES1-F ZmES1-R and ZmES1R-T7 were used to amplify *ZmES1* and synthetize the antisense probe

for this gene (Cordts et al., 2001), used as positive control in the *in situ* hybridization (Table 2.2).

Primer	Sequence (5'-3')	Gene	T annealing
Zma2DMEint-F	CATTGGGGTTGGGGTGGT	GRMZM2G123587 (*ZmDME1*)	63°C
Zma2DME-R	CACGTCTAGCTGGCAGAT		
Zma2DME-RT7	TAATACGACTCACTATAGGGC ACGTCTAGCTGGCAGAT		
Zma464-F	TGCTGGAGCACATACAGA	GRMZM2G422464 (*ZmDME2*)	63°C
Zma464-R	CAGGTGCAGGAAGAGCA		
Zma464-RT7	TAATACGACTCACTATAGGGC AGGTGCAGGAAGAGCA		
ZmES1-F	CCCTTGGATTGGATTGGATCG	GRMZM2G012012 (*ES1*)	59°C
ZmES1-R	GTCATTACCACCACAGACTTC		
ZmES1-RT7	TAATACGACTCACTATAGGGT CATTACCACCACAGACTTC		
ZmAct-F	CCTTCGAATGCCCAGCAATG	*ACT1*	63°C
ZmAct-R	GAGGATCTTCATTAGGTGGT		

Table 2.2: Primers used for the expression analysis

2.6.4 RT-PCR analysis

RT-PCR was performed to qualitatively detect the expression of *ZmDME1* and *ZmDME2* in reproductive tissues before and after fertilization and in vegetative tissues.

The cDNA was amplified through a standard Polymerase Chain Reaction (PCR), using the puRe Taq Ready To Go PCR

beads kit (Amersham Biosciences) and according to manufacturer's instructions. Primer pairs Zma2DMEint-F/Zma2DME-R and Zma464-F/R were used to amplify *ZmDME1* and *ZmDME2*, respectively. Primer pair ZmAct-F/R (Gutiérrez-Marcos et al., 2006) was used to amplify *ACTIN1* (*ACT1*) (accession no. NM_001155179), as positive control.

The PCR reaction was performed using a standard thermal cycling profile. The amplified product was checked running a 1.5% agarose/TAE buffer gel stained with ethidium bromide, later visualized at UV light.

PCR products were then excised from agarose gel, purified and quantified. Sequencing was performed at Macrogen Inc. Korea.

2.6.5 Real Time PCR analysis

To better investigate the expression pattern of *ZmDME1* and *ZmDME2*, a Real Time PCR analysis was carried out. In addition to a qualitatively detection of gene expression, this analysis allowed also to quantitatively measure the expression level in the different tissues. The amplification was performed using cDNA from reproductive tissues before and after fertilization and from vegetative tissues.

Real time PCR was performed using the SsoFast EvaGreen®

Supermix with Low ROX kit (BIO RAD), according to manufacturer's instructions. Standard Real Time PCR cycling conditions were used. Three technical replications were performed for each sample to assess the reproducibility, and the mean of the three replications was used to calculate relative expression quantification.

The amplification curve was generated after analyzing the raw data, and the cycle threshold (Ct) value was calculated. Primer pairs Zma2DMEint-F/Zma2DME-R and Zma464-F/R were used to detect the level of expression of *ZmDME1* and *ZmDME2*, respectively. The expression level of maize *ACTIN1* (*ACT1*) (accession no. NM_001155179), amplified with primer pair ZmAct-F/R (Gutiérrez-Marcos et al., 2006) was used as an internal control. The sample with the lowest level of expression was arbitrarily chosen as internal calibrator. The relative expression level of target genes in different samples was calculated using $2^{-\Delta\Delta Ct}$ method (Livak and Schmittgen, 2001), defined as:

$\Delta\Delta Ct = \Delta Ct(sample) - \Delta Ct(calibrator)$

where:

$\Delta Ct(sample) = Ct(gene,sample) - Ct(actin,sample)$

$\Delta Ct(calibrator) = Ct(gene,calibrator) - Ct(actin,calibrator)$

2.6.6 *in situ* hybridization analysis

in situ hybridization analysis was performed in order to localize the expression of *ZmDME1* and *ZmDME2* genes in the mature female gametophyte.

Probe synthesis

cDNA from mature ovules was PCR amplified using Zma2DMEint-F/Zma2DME-R, Zma464-F/R and ZmES1-F ZmES1-R primer pairs, were purified and inserted into a pGEM®-T vector.

The cloning was performed using pGEM®-T and pGEM®-T Easy Vector Systems kit (Promega), according to manufacturer's instructions.

The amount of cDNA used in the reaction was based on a 3:1 insert:vector molar ratio.

JM109 High Efficiency *E.coli* Competent Cells were the transformed with the T4 ligation reactions through heat-shock at 42°C. SOC medium was then added to the tubes containing the transformed cells and tubes were incubated at 37°C. Cells were plated onto LB/ampicillin/IPTG/X-Gal plates and incubated overnight at 37°C. Recombinant clones were identified by white/blue color screening. Transformed cells

from the plates were added to a tube containing liquid LB medium and ampicillin and incubated overnight at 37°C with shaking. 100% glycerol was then added and the stock was stored at -80°C. A colony PCR was performed to check the transformation of the cells.

Plasmid DNA was then isolated from culture of *E.coli* in LB medium using the QIAprep Spin Miniprep Kit (Qiagen), according to manufacturer's instructions.

Isolated DNA was amplified using primers Zma2DMEint-F/Zma2DME-RT7, Zma464-F/RT7, ZmES1-F/RT7 (Table 2.2), conveniently designed for incorporating a T7 promoter into the PCR product. The T7 sequence is required by RNA polymerase to start the transcription. Reverse primers were used to ensure a proper direction of RNA transcription, so that an antisense RNA probe complementary to the mRNA of interest was obtained. The PCR product was run on an agarose gel, gel purified and quantified using a Mass Ladder.

The transcription of the RNA probe was performed using the DIG RNA Labeling Kit (SP6/T7) (Boehringer Mannheim). Using this kit, DNA was transcribed with T7 RNA polymerase in presence of digoxigenin-UTP. Thus, three two DIG-labeled

RNA probes were obtained, complementary to the mRNA transcripts of the target genes *ZmDME1*, *ZmDME2* and *ZmES1*.

in situ hybridization

The labeled RNA probes were then used to hybridize the target mRNA sequences within a sample. Slides with ovules containing mature gametophyte were used for the hybridization. RNA probes were detected by using an antibody-phosphatase conjugate which binds the DIG-labeled probes, resulting in luminescence reaction.

In situ hybridization was performed as described in Chapter I, paragraph 2.5.5. Slides were then visualized at the microscope (ZEISS Axiophot D1).

The probes were therefore used to detect the expression of *ZmDME1* and *ZmDME2* in the mature gametophyte.

ZmES1 gene was used as positive control to verify whether the experiment was successful. *ZmES1* expression is observed in egg cell, synergids, central cell and in the zygote until 18 hours after fertilization (Cordts et al., 2001).

3. RESULTS

3.1 Sequence analysis

Using the DME amino acid sequence of *Arabidopsis thaliana* (At5g4560.2) as query sequence, two maize DME homologues sequences were identified in GenBank database by the BLASTP program. The genes, GRMZM2G123587 and GRMZM2G422464, encoding for DME homologous proteins were re-named as *ZmDME1* and *ZmDME2*, respectively. The *ZmDME1* locus is on chromosome 5 (161,861,555-161,907,984) and the gene consists of 46430 bp including 16 exons (Fig. 2.6). *ZmDME2* locus is on chromosome 4 (218,137,641-218,155,614) and the gene consists of 17972 bp, including 17 exons (Fig. 2.6).

ZmDME1 encodes a protein of 1906 amino acids, while *ZmDME2* encodes a protein of 1904 amino acids. These two proteins share an 82% of identity.

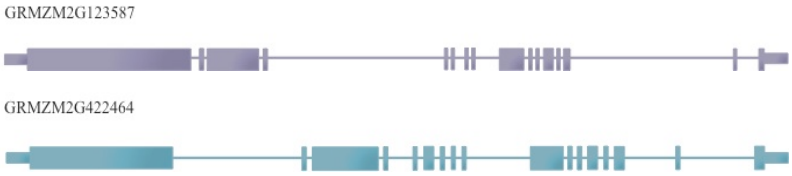

Fig. 2.6: Schematic representation of GRMZM2G123587 (*ZmDME1*) and GRMZM2G422464 (*ZmDME2*) genes.

These protein sequences revealed the highest homology to *A. thaliana* DME, with a similarity of 64% for ZmDME1 and 67% for ZmDME2. In both cases the similarity was higher to *A. thaliana* DME than other *A. thaliana* DMLs (62% identity with DML1, 58-55% identity with DML2 and 48-43% identity with DML3).

Domain analysis of ZmDME1 and ZmDME2 included the DME of *A. thaliana*, and two putative DME of monocots: Sb04g019820 of *Sorghum bicolor* and LOC_Os01g11900.1 of *Oryza sativa.* Results described in figure 2.7 suggest well-conserved regions of DME proteins among eudicots and monocots. All the amino acid sequences contain a glycosylase domain, present in all the DNA glycosylases, and the domains A and B, characteristic of all DNA demethylases within the DME family (Mok et al., 2010).

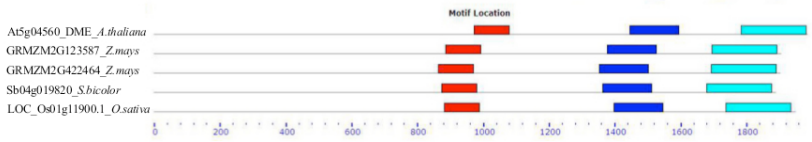

Fig. 2.7: Conserved domain in DME homologues from different plant species. *A. thaliana* DME (AT5G04560), *Z. mays* ZmDME1 (GRMZM2G123587) and ZmDME2 (GRMZM2G422464), *S. bicolor* homologue (Sb04g019820) and *O. Sativa* homologue (LOC_Os01g11900.1) were analyzed. Red, domain A; Blue, Glycosylase domain; Light blue, domain B.

A phylogenetic analysis of 43 DME and DMLs homologous proteins from 12 species (8 eudicots and 4 monocots) was performed to investigate the evolutionary relationships of these proteins among angiosperms (Fig. 2.8). The resulting phylogenetic tree, rooted using 2 moss sequences (*Physcomitrella patens*), estimates a well-supported (100%) monocot clade comprising two lineages (both supported at 100%). One of these lineages includes the *Zea mays* ZmDME1 and ZmDME2, closely related to each other, and the other monocot species *Sorghum bicolor* Sb04g019820 and Sb08g008620, *Oryza sativa* LOC_Os02g29230.1 and LOC_Os01g11900.1 and *Brachypodium distachyon* Bradi3g43690 and Bradi4g08870. The monocot clade is sister to a clade containing two well-supported (100%) eudicot lineages, one representing DME orthologues and the other one representing DML1 orthologues. ZmDME1 and ZmDME2 are situated in a clade separated from the *A. thaliana* DME/DMLs proteins. In fact, homologues of monocots and eudicots are grouped in different clades, possibly indicating a divergent evolution of these proteins in angiosperms. Interestingly, ZmDME1 and ZmDME2 lineage includes the rice protein LOC_Os01g11900.1 (ROS1a), which is known to play

analogous roles to those of DME in *A. thaliana* (Ono et al., 2012).

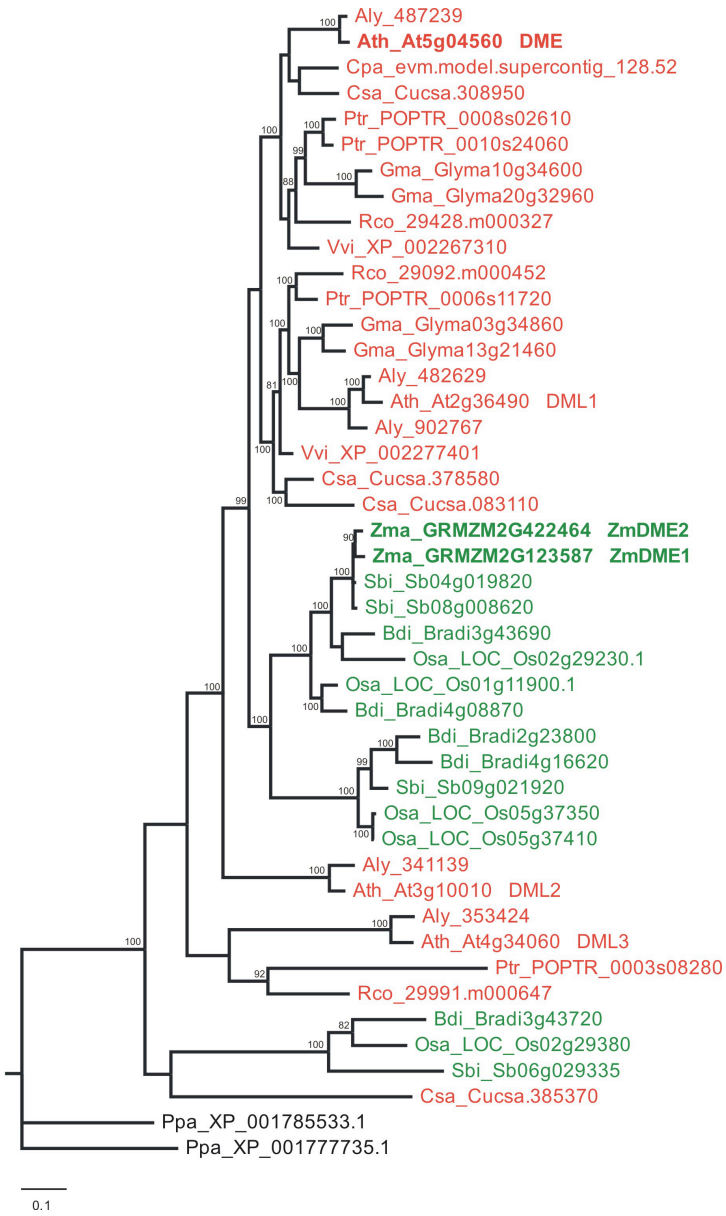

Fig. 2.8: Phylogenetic analysis of the DME/DMLs glycosylase family. A phylogenetic tree based on conserved domains of glycosylase proteins, with basal land plant (moss) proteins as outgroup. Posterior probability values are shown for key nodes. Values lower than 80% are not shown. Monocot, eudicot and moss proteins are colored green, red and black, respectively. Aly, *Arabidopsis lyrata*; Ath, *Arabidopsis thaliana*; Bdi, *Brachypodium distachyon*; Cpa, *Carica papaya*; Csa, *Cucumis sativus*; Gma, *Glycine max*; Osa, *Oryza sativa*; Ppa, *Physcomitrella patens*; Ptr, *Populus trichocarpa*; Rco, *Ricinus communis*; Sbi, *Sorghum bicolor*; Vvi, *Vitis vinifera*; Zma, *Zea mays*. In bold, *A. thaliana* DME and *Z. mays* ZmDME1 and ZmDME2. Scale bar indicates 0.1 substitutions per site.

3.2 Morphological analysis

In order to analyze the expression of the genes *ZmDME1* and *ZmDME2*, a morphological study of the development of the female gametophyte was first necessary.

Since it is known that in *A. thaliana DME* is expressed in central cell of the female gametophyte before fertilization (Choi et al., 2002), it was crucial to distinguish all the different stages of maize gametophyte development in order to identify the stage of interest.

The first step was to find a correlation between the stage of gametophyte development and the external morphology of the female inflorescence and florets. In order to do that, the silk length was used as external morphological feature to obtain a developmental index for embryo sac development along the

length of the ear, as shown in Huang and Sheridan (1994). The development of the embryo sacs in the ovules corresponds with silk development in the ear in which a gradient of developmental pattern reveals that ovule development progresses from the base to the top of the ear (Huang and Sheridan, 1994).

Immature ears were divided transversely into three equal sections, and in each section the silk lengths were measured before manually dissecting and microscopically analyzing the ovules.

Three main stages of ear and gametophyte development were considered (Fig. 4):

1. florets with a range of silk length from 0 to 0.6 cm. In this phase the megagametophyte was not present yet, in fact according to Huang and Sheridan (1994), the ovules contain megasporocytes in meiosis or megaspores.

2. florets with a range of silk length from 0.7 to 1.2 cm. In this phase the megagametophyte became visible. According to Huang and Sheridan (1994), the ovules

contain megagametophyte with eight nuclei.

3. florets with a range of silk length from 1.3 to 2.5 cm. In this phase the embryo sac was still visible and well defined in its structures. In fact, Huang and Sheridan (1994) describe this stage with ovules containing a mature embryo sac with more than three antipodal cells.

Thus, these results were consistent with the stages of the gametophyte development described in Huang and Sheridan (1994) and this morphological analysis allowed to identify the phase of interest, i.e. the mature embryo sac before fertilization.

This developmental stage was characterized by the presence of the egg cell, the synergids, the antipodals and the central cell, consisting of two polar nuclei (Fig. 2.9). The presence of the central cell was crucial in this study in order to investigate the expression of *ZmDME1* and *ZmDME2*.

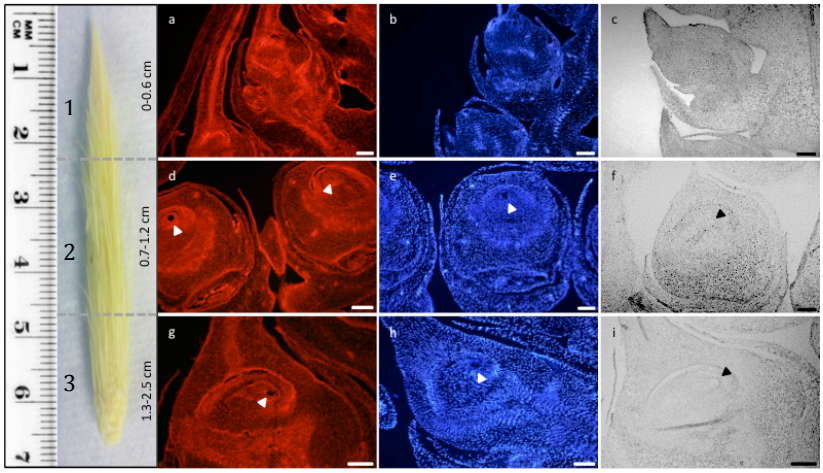

Fig. 2.9: Three main stages of ear and gametophyte development. The correlation between the stage of gametophyte development and the silk length is shown. Stage 1, in florets with silks ranging from 0-0.6 cm the megagametophyte is not formed (a, b, c). Stage 2, in florets with silks ranging from 0.7-1.2 cm the megagametophyte is visible (d, e, f). Stage 3, in florets with silks ranging from 1.3 to 2.5 cm the megagametophyte is visible and its structure well defined (g, h, i). Florets stained with acridine orange under a fluorescent microscope (a, d, g). Florets stained with DAPI under a fluorescent microscope (b, e, h). Florets visualized under brightfield microscope (c, f, i). Arrowheads indicate the megagametophyte. Scale bars: 100 µm.

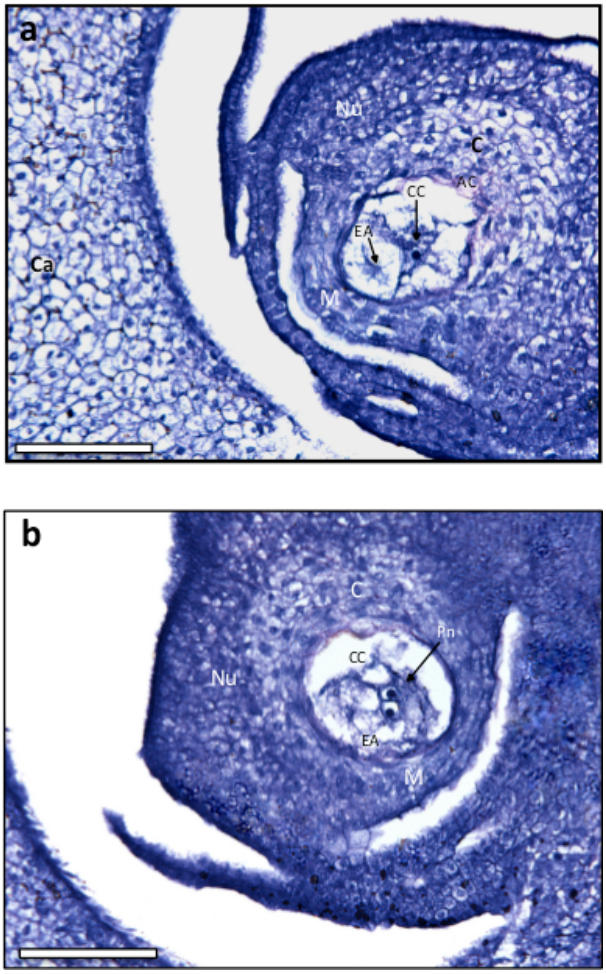

Fig. 2.10 a, b: The mature megagametophyte. The female gametophyte is deeply embedded in the maternal tissues of the ovule. The central cell is highly vacuolated and it consists in two polar nuclei in contact with each other (b). AC, antipodal cells; C, chalazal region; Ca, carpel; CC, central cell; EA, egg apparatus; M, micropylar region; Nu, nucellus; Pn, polar nuclei. Scale bars: 100 µm.

In figure 2.10 a mature embryo sac is shown. The female gametophyte is deeply embedded in the maternal tissues of the ovule. The egg apparatus and the central cell are strongly polarized, and especially central cell is highly vacuolated. The central cell consists in two polar nuclei, which remain in contact (Fig. 2.10), but they do not fuse until after fertilization (Kiesselbach, 1949; Evans and Grossniklaus, 2008).
The antipodal cells proliferate and consist of a cluster of up to 40 cells. The nucellus cells most closely adjacent to the embryo sac are compressed or collapsed (Fig. 2.10).

3.3 Gene expression analysis

Expression of *ZmDME1* and *ZmDME2* was found in a variety of tissues (Fig. 2.11): ovules at different stages of development, embryo, endosperm, leaf, radicle and coleoptile. Both gene transcripts were detected by RT-PCR in florets of unfertilized ears at all the three stages of development described in paragraph 3.2. We underline that in *A. thaliana DME* is not expressed after fertilization and in vegetative tissues (Choi et al., 2002; Hsieh et al., 2009, 2011), while *ZmDME1* and *ZmDME2* transcripts were found in embryo and endosperm and

also in several vegetative tissues, i.e. leaf, radicle and coleoptile (Fig. 2.11).

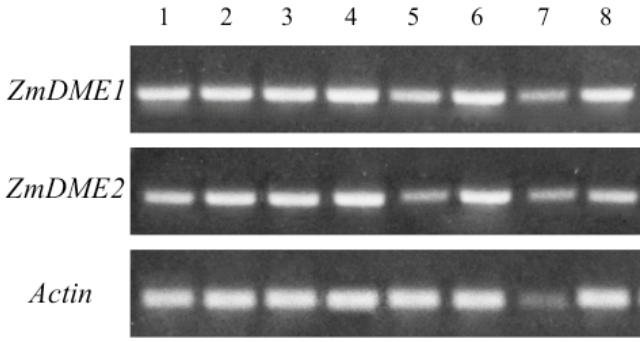

Fig. 2.11: Expression of *ZmDME1* and *ZmDME2* detected by RT-PCR analysis in the following tissues: 1, ovules from florets with silks of 0.4 cm; 2, ovules from florets with silks of 1 cm; 3, ovules from florets with silks of 2.5 cm; 4, embryo 20 DAP; 5, endosperm; 6, leaf; 7, radicle; 8, coleoptile. *Actin*, used ad control.

In order to quantify the gene expression in the different tissues, a Real Time PCR was performed on the same samples used for the RT-PCR. Results confirmed that *ZmDME1* and *ZmDME2* genes were expressed in all the tissues analyzed (Fig. 2.12), and in particular the lowest expression in both cases was found in the endosperm, which was arbitrarily chosen as calibrator for the relative quantification of the gene expression.

ZmDME1 gene was expressed at all different stages of ovules.

At the stages 1, 2 and 3 of ovules development, *ZmDME1* was expressed at a level 77 (± 3.29), 127 (± 3.18) and 90 (± 3.30) greater than the endosperm, respectively. An increase in the expression from stage 1 to stage 2 and a decrease from stage 2 to stage 3 were observed. Furthermore, the gene expression was found also in the embryo at a level 13.6 (± 3.19) greater than the calibrator. However after fertilization (embryo and endosperm) *ZmDME1* expression was lower than in the ovule at all its developmental stages. The highest level of *ZmDME1* expression was found in the coleoptile, followed by the radicle with a level 170 (± 3.20) and 120 (± 3.38) greater than the endosperm, respectively. *ZmDME1* was expressed at a lower level in the leaf, only 8 (± 3.45) greater than the calibrator (Fig. 2.12). *ZmDME2* showed an overall lower level of expression compared to *ZmDME1*. Also in this case, gene expression was found in all the developmental stages of the ovule. At stages 1, 2 and 3, *ZmDME2* was expressed at a level 27 (± 2.31), 25.5 (± 2.49) and 43.5 (± 2.38) greater than the endosperm, respectively. An increased level of expression from stage 2 to stage 3 was observed. In the embryo the gene was expressed 4.7 (± 2.28) more than the calibrator, but after fertilization the level was lower than in the ovule at all the three stages of

development. The highest level of *ZmDME2* expression was found in the coleoptile (53 ± 2.23), followed by the radicle (40 ± 3.29), while the other vegetative stage, the leaf, showed a lower level of expression (1.4 ± 2.37) (Fig. 2.12).

Thus, the expression of both genes was found at all the stages of ovule development, also in ovules where the gametophyte was not formed yet. Furthermore, the expression was detected also after fertilization in the embryo and endosperm. Interestingly, the expression was found in vegetative tissues, and in radicle and coleoptile it was higher than in reproductive tissues (Fig. 2.12).

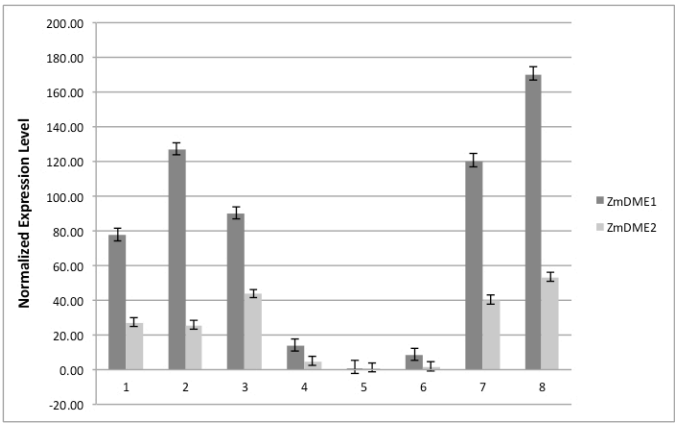

Fig. 2.12: Expression levels of *ZmDME1* and *ZmDME2* detected by real time PCR in the following tissues: 1, ovules from florets with silks of 0.4 cm; 2, ovules from florets with silks of 1 cm; 3, ovules from florets with silks of 2.5 cm; 4, embryo 20 DAP; 5, endosperm; 6, leaf; 7, radicle; 8, coleoptile. Expression levels were normalized with the maize actin (*ACT1*) gene expression. Error bars represent the SD (n=3).

3.4 Localization of gene expression in the mature gametophyte

To gain a better understanding of the expression pattern of *ZmDME1* and *ZmDME2*, *in situ* hybridization was performed on ovules at maturity (Fig. 2.13). This analysis was carried out to determine in which cells of the mature gametophyte the selected genes are expressed. Slices from ovules containing mature female gametophytes were examined and the stage of interest was previously identified through morphological analysis. Using specific probes for *ZmDME1* (Fig. 2.13 a, b, c) and *ZmDME2* (Fig. 2.13 d, e, f), gene expression was localized in the tissue.

The results showed the same localization in the embryo sac of the transcripts of the two genes. In both cases, a strong signal was detected in the central cell, the antipodal cells, the egg apparatus and also in the nucellus cells around the embryo sac and at the boundary between integuments and nucellus. Since ovule slices used were 8 μm thick, not every slice went through a female reproductive cell, so it was not possible to identify synergids and egg cell and discriminate the expression between these cells. These results showed that both *ZmDME1* and *ZmDME2* gene expression is not restricted to the central cell

and it is found in different cells of the embryo sac and tissues surrounding it (Fig. 2.13).

In the control samples, hybridized with the probe for *ZmES1* gene, the expression was detected in the egg apparatus and the central cell, as reported in Cordts et al. (2001).

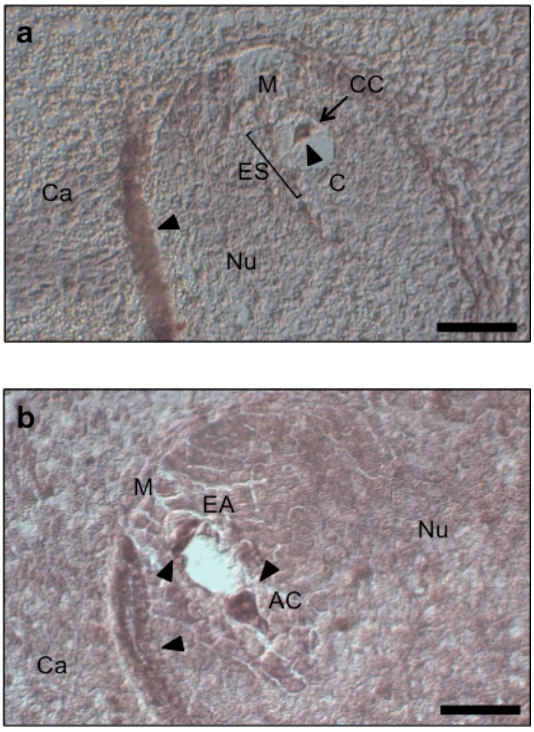

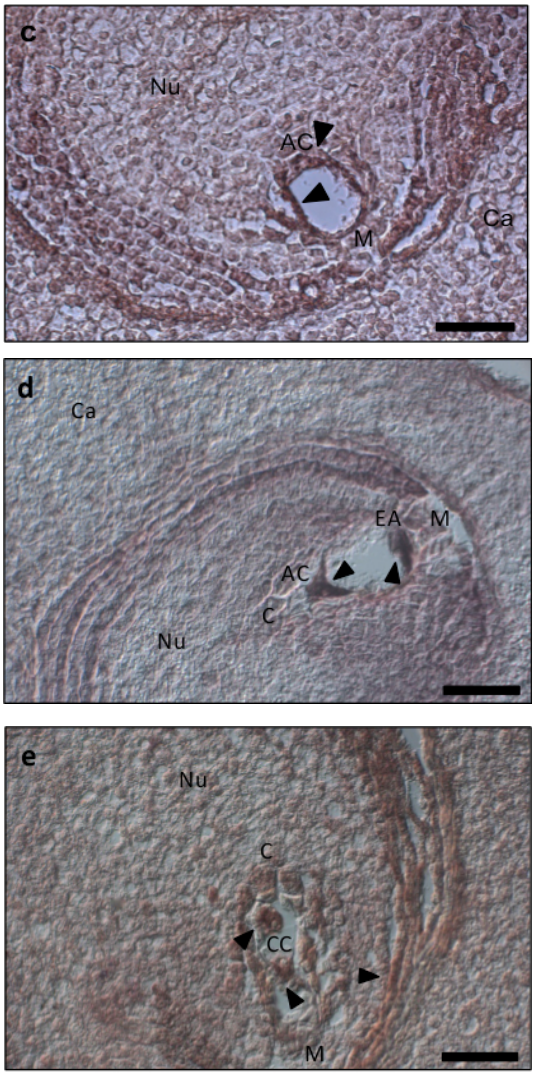
c
Nu
AC
M
Ca
d
Ca
EA
M
AC
C
Nu
e
Nu
C
CC
M

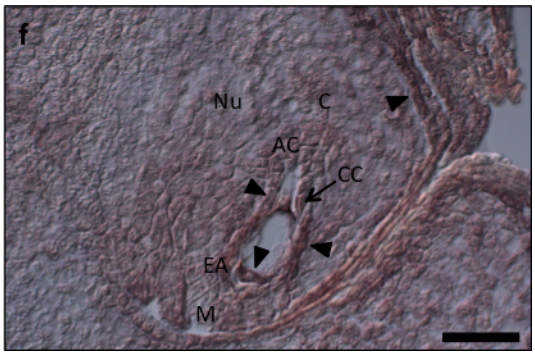

Fig. 2.13: *in situ* hybridization in the mature ovule. Specific probes were used to localized the expression of *ZmDME1* (a, b, c) and *ZmDME2* (d, e, f). Signal is detected in the central cell (a, e, f), the antipodal cells (b, c, d) and the egg apparatus (b, d, f). Arrowheads point to the regions where gene expression is detected. Signal is found also in the nucellus cells around the embryo sac and at the boundary between integuments and nucellus. AC, antipodal cells; C, chalazal region; Ca, carpel; CC, central cell; EA, egg apparatus; ES, embryo sac; M, micropylar region; Nu, nucellus. Scale bars: 50 μm.

3.5 Investigation of *Zmdme1* and *Zmdme2* mutants

In order to better investigate the role of *ZmDME1* and *ZmDME2* and their homology to *DME* of *A. thaliana*, a functional study using mutant plants was performed.

Seeds from a self crossed population (*Zmdme1*/B73) carrying a point mutation in the coding region of the gene *ZmDME1* (GRMZM2G123587) were planted (Fig. 2.14). The mutation

consists in a cytosine (CCT) replaced by a thymine (CTT). This substitution represents a non-synonymous mutation, resulting in a codon that codes for a different amino acid, where a Proline is replaced by a Leucine. The amino acid change occurs in a non-domain region of the protein.

Plants were genotyped and sequenced to verify the presence of the mutation (Table 2.4). Heterozygous and homozygous mutant plants were found in the segregant population. All the plants showed no vegetative and reproductive defects, developing normal male and female inflorescences. Also, these plants were self-crossed and the fertilized ears had all normal-shaped seeds.

Furthermore, using UniformMu and Mu-Illumina databases, two transposon insertions (UFMu-04319 and Mu-illumina_249179.3) in an intronic region of the gene *ZmDME2* (GRMZM2G422464) were found (Fig. 2.14). Seed stocks for both the insertions were available and seeds were planted. Plants were genotyped and sequenced to verify the presence of the insertions (Table 2.3 and 2.4). No homozygous plants for any of the two insertions were found. Heterozygous plants were found and they exhibited no overt morphological phenotypes during the vegetative and reproductive phases

(Table 2.3 and 2.4). These plants were self-crossed and they produced ears having all normal-shaped seeds.

The morphological analysis of the gametophyte and embryo in mutant plants was performed using homozygous mutants for *ZmDME1* gene. Since the two insertions found in *ZmDME2* were both in an intronic region, it was unlikely to identify a mutant phenotype. Thus, effects of mutations in *ZmDME2* gene on gametophyte and embryo development, were not investigated.

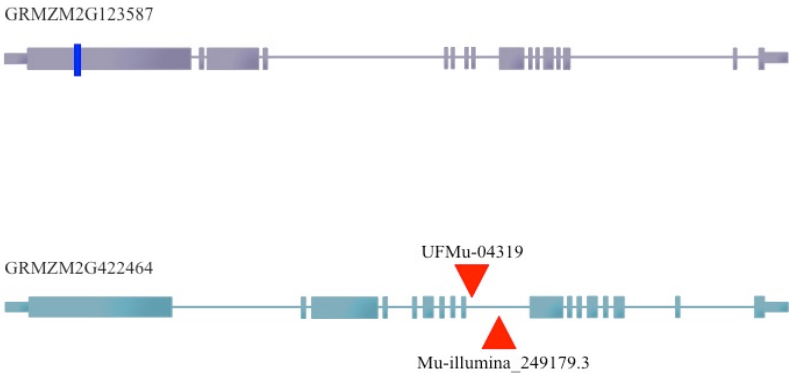

Fig. 2.14: Schematic representation of GRMZM2G123587 (*ZmDME1*) and GRMZM2G422464 (*ZmDME2*) genes. Position of the point mutation (blue bar) in *ZmDME1* and positions of the two transposon insertions (red arrowheads) in *ZmDME2* are indicated.

	Genotype			
	A	**B**	**C**	**Tot #**
Mu-illumina_249179.3	0	4	10	14
UFMu-04319	0	4	7	11

Table 2.3. Seeds ordered from UniformMu and Mu-Illumina databases carried the transposon insertions UFMu-04319 and Mu-illumina_249179.3. Plants were grown in the greenhouse at the Waksman Institute, Rutgers Univ, USA and in the winter nursery in Hawaii. Plants were genotyped to verify the presence of the insertions: A, plants homozygous for the insertion; B, Plants heterozygous for the insertion; C, wild type plants; Tot #, total number of plants.

	Genotype			
	A	**B**	**C**	**Tot #**
Mu-illumina_249179.3/+ x +/+	0	5	5	10
UFMu-04319/+ x +/+	0	33	36	69
Zmdme1/+ x *Zmdme1*/+	2	6	4	12

Table 2.4. Progeny genotype of plants heterozygous for the insertions in table 2.3, back-crossed with wild type plants (+/+) and genotype of an F2 population obtained by self-crossing heterozygous plants for the point mutation *zmdme1*. Plants were grown in the field at the Waksman Institute, Rutgers Univ. USA. Plants were genotyped to verify the presence of the insertion and point mutation: A, plants homozygous for the insertion/mutation; B, Plants heterozygous for the insertion/mutation; C, wild type plants; Tot #, total number of plants.

3.6 Morphological analysis of *Zmdme1* mutants during gametogenesis and embryogenesis

A morphological analysis on *Zmdme1* mutants was performed in order to investigate the phenotype and verify the similarity with *A. thaliana dme* mutant phenotype. Since DME is active in the central cell of the female gametophyte and *dme* mutants are affected in embryo development, the morphology during both gametogenesis and embryogenesis was studied. Different stages of development were detected and compared to B73 wild type plants.

Images of the embryo sac at different phases of gametogenesis showed that *Zmdme1* mutant went through a normal development of the female gametophyte. The functional megaspore underwent three rounds of nuclear divisions (Fig. 2.15 a, b), giving rise to a mature gametophyte (Fig. 2.15 c) which did not show any difference when compared to a wild type embryo sac (Fig. 2.10).

Morphological analysis of a 20 DAP embryo showed a normal development during embryogenesis, when compared to a wild type embryo. The embryo was fully differentiated with a central axis terminating at the basal end by the primary root, protected by the coleorhiza, and at the other hand by the stem

tip, with few short internodes and leaf primordia surrounded by the coleoptile (Fig. 2.16).

The phenotype of mature kernels (40 DAP) was also analyzed. Seeds were dissected and visualized under the stereo microscope. This study confirmed the previous results of the morphological analysis, showing an embryo not affected in its development. In fact, the embryo was fully differentiated and its basal/apical axis and the scutellum were visible. Also the endosperm was normally formed (Fig. 2.17).

These results revealed no defects in the development of *Zmdme1* mutants during gametogenesis and embryogenesis, allowing the formation of normal and viable seeds. Thus, *Zmdme1* mutant did not show a phenotype similar to *dme* of *A. thaliana*, whose seeds are not viable, with enlarged endosperm and aborted embryos (Choi et al., 2002).

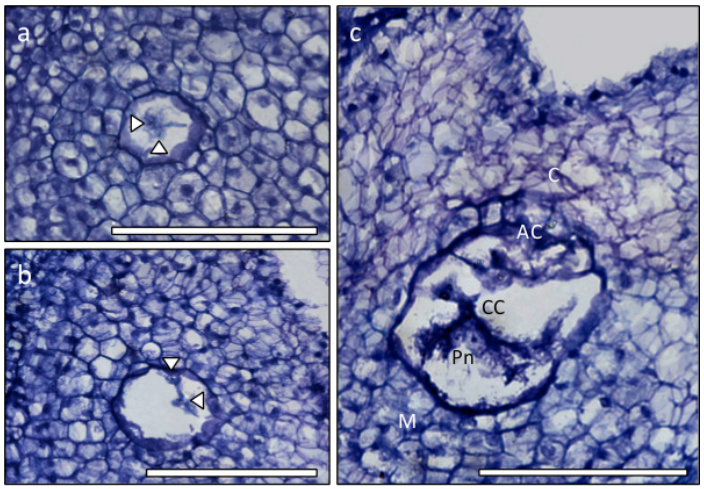

Fig. 2.15: *Zmdme1* mutant gametophyte. a, two nuclei dividing to form four; b, four-nucleate stage; c, mature gametophyte. AC, antipodal cells; C, chalazal region; CC, central cell; M, micropylar region; Pn, polar nuclei. Arrowheads indicate nuclei during mitosis and at the four-nucleate stage. Scale bars: 100 µm

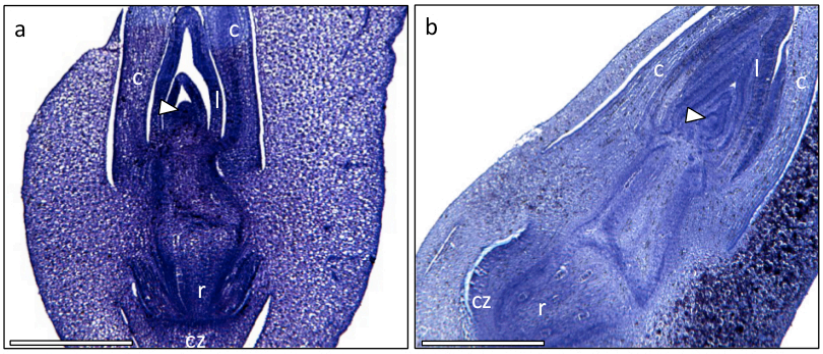

Fig. 2.16: Embryo 20 DAP. a, *Zmdme1* mutant embryo; b, wild type embryo. Indicated in the image: c, coleoptile; cz, coleorhiza; l, leaf primordia; r, radicle. The arrowhead points to the SAM. Scale bar: 100 µm

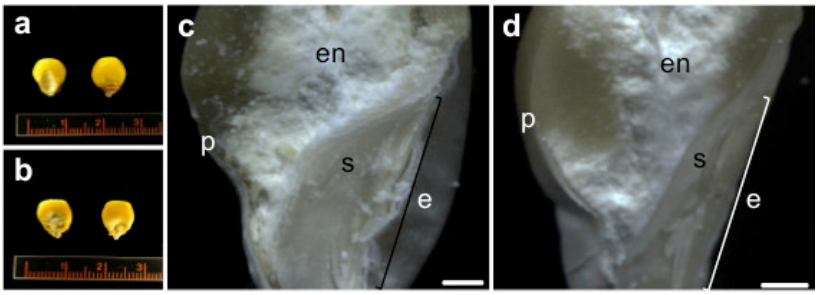

Fig. 2.17: Mature kernels. The phenotype of mature kernels shows that *Zmdme1* embryo is not affected in its development. In: a, *Zmdme1* kernels; b, wild type B73 kernels; c, dissected *Zmdme1* kernel; d, dissected wild type B73 kernel. e, embryo; en, endosperm; p, pericarp; s, scutellum. Scale bars: 1 mm.

4. DISCUSSION

Several genes expressed in the female gametophyte and embryo are known to regulate seed development (Tzafrir et al., 2003; Drews et al., 2008; José-Estanyol et al., 2009; Shen et al., 2013). Many of these genes are regulated by epigenetic mechanisms, such as DNA methylation and demethylation (Gehring et al., 2009; Ikeda, 2012). In *A. thaliana*, DEMETER (DME) is a DNA glycosylase/lyase, active in the central cell of the female gametophyte before fertilization. This enzyme is capable to activate the expression of maternal alleles through DNA active demethylation, leading to maternal allele-specific expression of imprinted genes in the endosperm (Choi et al., 2002; Gehring et al., 2006, 2009a). The function of this enzyme is also supported by the extensive DNA demethylation found in endosperm genome (Hsieh et al., 2009). Nevertheless, in monocots this mechanism seems to be different. In fact, a study in rice revealed that the endosperm is locally hypomethylated and the methylation pattern resembles the one of *dme A. thaliana* mutant, leading the author to conclude that monocots lack DME orthologues (Zemach et al., 2010).

In order to shed light on the mechanisms of DNA demethylation and imprinting in monocots, our research

focused on the identification and characterization of putative *DME* homologues in maize.

In this work, two homologues to the *A. thaliana DME* were identified in maize: *ZmDME1* and *ZmDME2*. The proteins encoded by these genes showed a conserved structure characteristic of the *A. thaliana* DME family and a high homology with *A. thaliana* DME. These results were also supported by a phylogenetic analysis, which revealed that these enzymes are highly conserved between monocots and eudicots, suggesting that DNA demethylation may have a common evolutionary origin among angiosperms. The expression of *DME* in *A. thaliana* is found in the central cell of the female gametophyte before fertilization and rapidly ceases after fertilization to allow the establishment of the imprinting in the endosperm (Choi et al., 2002; Gehring et al., 2006). In order to verify whereas the sequence similarity of ZmDME1 and ZmDME2 with DME corresponds to a functional similarity of the genes, expression analyses were carried out.

To investigate the expression of *ZmDME1* and *ZmDME2* in different stages of gametophyte development and, in particular in the mature gametophyte, a morphological study was performed.

Even though maize represents a model organism in plant biology and genetics, there is little known about a morphological correlation between florets external traits and the correspondent developmental phases of the gametophyte.

The morphological analysis allowed to find this correlation, using the silk length as external morphological feature to obtain a developmental index for embryo sac development along the length of the ear. Three main developmental stages of the ovule were identified: immature ovule where the gametophyte was not formed yet; ovule where a eight-nucleate mature gametophyte was present; ovule with a mature gametophyte at a later stage of development.

Thus, this analysis was crucial for the identification of the mature gametophyte in maize, characterized by the presence of the egg apparatus, the antipodal cells and the central cell, and it was essential to distinguish the different stages of gametophyte development where gene expression was studied.

Results from RT-PCR and Real Time PCR showed that *ZmDME1* and *ZmDME2* genes are expressed in ovules containing a mature gametophyte. Interestingly, a lower gene expression was also detected in the first stage of ovule development, when the gametophyte was not formed yet.

Furthermore, *ZmDME1* and *ZmDME2* expression was detected also in embryo and endosperm and in vegetative tissues. Relative quantification through Real Time PCR showed a peak of expression of the two genes in the coleoptile and in the radicle. The high expression in the coleoptile and in the radicle might be related to the presence of proliferating cells regions in these tissues.

These findings reveal that *ZmDME1* and *ZmDME2* are broadly expressed when compared to *DME* in *A. thaliana*, where the expression is detected in the central cell of the female gametophyte and rapidly ceases after fertilization (Choi et al., 2002; Hsieh et al., 2009, 2011).

An *in situ* hybridization performed on ovules containing mature female gametophytes showed that also *ZmDME1* and *ZmDME2* transcripts are detected in the central cell in maize.

Although some authors speculate about the lack of DME in monocots (Zemach et al., 2010), differentially methylated regions (DMRs) showing a pattern of maternal hypomethylation and paternal hypermethylation were recently identified in maize (Waters et al., 2011; Zhang et al., 2011). As in *A. thaliana*, some of the maize imprinted genes exhibit endosperm-preferred expression such that expression is low in

all tissues except for endosperm. These genes are highly enriched for DMRs, suggesting that DNA methylation may play an important role in regulating expression and imprinting in maize as well (Waters et al., 2011).

Very recently, further evidence that DNA demethylation may act in monocots endosperm has been reported in Wen et al. (2012), where the authors show that DME homologues in *Triticum aestivum* regulate the amounts of gliadins and glutenin family members in the endosperm. The genes encoding these proteins are known to be endosperm preferred genes, apparently activated by DNA demethylation (Zemach et al., 2010; Wen et al., 2012), suggesting that the same mechanism may act in monocots.

Thus, if the functional homology of *ZmDME1* and *ZmDME2* is confirmed, the enzymes encoded by these genes may be able to promote DNA demethylation and activate the imprinted genes in order to facilitate normal seed development in maize.

ZmDME1 and *ZmDME2* expression was also found in the antipodal cells, the egg apparatus and also in the nucellus cells around the embryo sac and at the boundary between integuments and nucellus. This further confirms the broader expression pattern of these genes compared to *A. thaliana*

DME. Nevertheless, the molecular mechanisms of *ZmDME1* and *ZmDME2* function in these cells remain to be elucidated.

The *ZmDME1* and *ZmDME2* expression pattern seems to be consistent with recent findings (Ono et al., 2012), where a DNA glycosylase in rice, ROS1a (Os01g11900), has been characterized. The authors show that ROS1a exerts effects comparable to those of DME in *A. thaliana*. *DME* maternal allele is essential for seed viability, in fact the inheritance of a *dme* mutant allele by the female gametophyte in *A thaliana* results in embryo and endosperm abortion even when a wild type paternal *DME* allele is inherited (Choi et al., 2002).

In rice, even in the presence of the wild type paternal *ROS1a* allele, the maternal *ros1a* allele causes failure of early-stage endosperm development, resulting in incomplete embryo development. Even though these maternal allele-specific defects in endosperm development imply that ROS1a and DME play some analogous role, also the expression pattern of *ROS1a* shows some differences from the *A. thaliana* one. In fact, *ROS1a* expression is also found in reproductive tissues after fertilization and in vegetative tissues.

Moreover, analyzing the gametophyte, the authors show that *ROS1a* is expressed in the central cell, and also in antipodal

cells and egg apparatus.

ROS1a, *ZmDME1* and *ZmDME2* share a similar expression pattern and interestingly proteins encoded by these genes are situated in the same clade of the phylogenetic tree, leading to the hypothesis that also in maize these proteins may play roles analogous to those of DME in *A. thaliana*.

As shown in the phylogenetic tree (Fig. 2.8), ZmDME1 and ZmDME2 are closely related to the DNA demethylases of DME family, suggesting that these proteins have a common evolutionary origin among angiosperms. ZmDME1 and ZMDME2 are situated in a clade including only monocot species and their separation from the *A. thaliana* DME/DMLs clade might be due to a divergent evolution of these proteins between monocots and eudicots.

After the separation between monocots and eudicots, occurred 150 mya (Hedges et al., 2006), DME enzymes in monocots may have acquired different functions, and because of their broader expression pattern, they could have further roles in plant development.

Zmdme1 homozygous plants were used to investigate whereas *ZmDME1* exert roles comparable to *DME*. In *A. thaliana*, homozygous *dme* plants produce aborted seeds, with enlarged

endosperm and aborted embryos (Choi et al., 2002).

Zmdme1 homozygous plants showed no defects in vegetative and reproductive phases and ears carried all normal-shaped seeds. In rice, ROS1a/*ros1a* plants are phenotypically indistinguishable from wild type plants during the vegetative phase. These plants produce equal number of normal–shaped and deformed seeds, with the null *ros1a* allele co-segregating with the deformed seed phenotype. In the deformed seeds the endosperm fails to develop and the embryos display variable morphologies, ranging from severely defective embryos with no distinctive organs to less severe phenotype with defects in shoot and root meristems or the formation of multiple meristems (Ono et al., 2012). The morphological analysis of *Zmdme1* mutants during gametophyte and embryo development revealed no defects during gametogenesis and embryogenesis, giving rise to normal mature gametophytes and fully differentiated embryos.

Nevertheless, the lack of a mutant phenotype in *Zmdme1* plants can be explained by the fact that the point mutation in the coding region of *ZmDME1* gene might not have caused any malfunctions in the protein, since it does not occur in one of the conserved domains. Also, because of the high homology

between *ZmDME1* and *ZmDME2*, these two genes are likely redundant and they may play the same role during plant development. Thus, the role of *ZmDME1* gene in the mutants, could have been played by its homologue.

A further functional analysis creating new mutant alleles for both *ZmDME1* and *ZmDME2* genes is needed in order to clarify the role of these genes in maize seed development.

In conclusion, even though the lack of DME orthologues in monocots has been previously hypothesized (Zemach et al., 2010), localized DNA hypomethylation in the maize central cell (Gutierrez-Marcos et al., 2006) and on maternal genome in the endosperm (Gutierrez-Marcos et al., 2006; Waters et al., 2011; Zhang et al., 2011) have been reported, leading to the hypothesis that a similar mechanism takes place in monocot gametophyte.

Therefore, it is still an open possibility that ZmDME1 and ZmDME2 proteins may be responsible for active demethylation of the maternal endosperm genome in maize, taking part in the genetic and epigenetic mechanisms involved in seed development.

REFERENCES

Agius F, Kapoor A, Zhu JK. 2006. Role of the *Arabidopsis* DNA glycosylase/lyase ROS1 in active DNA demethylation. *Proceedings of the National Academy of Sciences* USA **103**, 11796–11801.

Apuya NR, Yadegari R, Fischer RL, Harada JJ, Goldberg RB. 2002. *RASPBERRY3* gene encodes a novel protein important for embryo development. *Plant Physiology* **129**, 691–705.

Baroux C, Raissig MT, Grossniklaus U. 2011. Epigenetic regulation and reprogramming during gamete formation in plants. *Current Opinion in Genetics & Development* **21**, 124-133.

Barrell PJ, Grossniklaus U. 2005. Confocal microscopy of whole ovules for analysis of reproductive development*:* The *elongate1* mutant affects meiosis II. *Plant Journal* **43**, 309-320.

Bauer JM, Fischer RL. 2011. Genome demethylation and imprinting in the endosperm. *Current Opinion in Plant Biology* **14,** 1-6

Chan SW, Henderson IR, Jacobsen SE. 2005. Gardening the genome: DNA methylation in *Arabidopsis thaliana. Nature Reviews Genetics* **6**, 351–60.

Chaudhury AM, Ming L, Miller C, Craig S, Dennis ES, Peacock WJ. 1997. Fertilization-independent seed development in *Arabidopsis thaliana. Proceedings of the National Academy of Sciences, USA* **94**, 4223–4228.

Choi Y, Gehring M, Johnson L, Hannon M, Harada JJ, Goldberg RB, Jacobsen SE, Fischer RL. 2002. DEMETER, a DNA glycosylase domain protein, is required for endosperm gene imprinting and seed viability in *Arabidopsis. Cell* **110**, 33–42.

Clark JK, Sheridan WF. 1991. Isolation and characterization of 51 embryo-specific mutations of maize. *The Plant Cell* **3**, 935–951.

Coe EH. 2001. The origins of maize genetics. *Nature Reviews Genetics* **2**, 898-905.

Cokus SJ, Feng S, Zhang X, Chen Z, Merriman B, Haudenschild CD, Pradhan S, Nelson SF, Pellegrini M, Jacobsen SE. 2008. Shotgun bisulphite sequencing of the *Arabidopsis* genome reveals DNA methylation patterning. *Nature* **452***,* 215–219.

Cordts S, Bantin J, Wittich PE, Kranz E, Lörz H, Dresselhaus T. 2001. *ZmES* genes encode peptides with structural homology to defensins and are specifically expressed in the female gametophyte of maize. *The Plant Journal* **25** (1), 103-114

Cove DJ, Knight CD. 1993. The moss *Physcomitrella patens***,** a model system with potential for the study of plant reproduction. *The Plant Cell* **5,** 1483-1488.

Denver DR, Swenson SL, Lynch M. 2003. An evolutionary analysis of the helix-hairpin-helix superfamily of DNA repair glycosylases. *Molecular Biology Evolution* **20,** 1603–1611.

Diboll AG, Larson DA. 1966. An electron microscopic study of the mature megagametophyte in *Zea mays. American Journal of Botany* **53,** 391-402.

Ding YH, Liu NY, Tang ZS, Liu J, Yang WC. 2006. *Arabidopsis GLUTAMINE-RICH PROTEIN23* is essential for early embryogenesis and encodes a novel nuclear PPR motif protein that interacts with RNA polymerase II subunit III. *The Plant Cell* **18,** 815–830.

Doelling JH, Yan N, Kurepa J, Walker J, Vierstra RD. 2001. The ubiquitin-specific protease UBP14 is essential for early embryo

development in *Arabidopsis thaliana*. *Plant Journal* **27,** 393–405.

Drews GN, Lee D, Christensen CA. 1998. Genetic analysis of the female gametophyte development and function. *The Plant Cell* **10**, 5-17.

Dumas C, Mogensen HL. 1993. Gametes and fertilization: maize as a model system for experimental embryogenesis in flowering plants. *The Plant Cell* **5,** 1337–1348.

Eastmond PJ, van Dijken AJ, Spielman M, Kerr A, Tissier AF, Dickinson HG, Jones JD, Smeekens SC, Graham IA. 2002. Trehalose-6- phosphate synthase 1, which catalyses the first step in trehalose synthesis, is essential for *Arabidopsis* embryo maturation. *Plant Journal* **29**, 225–235.

Evans MM, Grossniklaus U. 2008. The maize megagametophyte. In: Bennetzen J, Hake S, Handbook of maize: Its Biology. *Springer New York, US*, 79-104.

Fu S, Meeley R, Scanlon MJ. 2002. *empty pericarp2* encodes a negative regulator of the heat shock response and is required for maize embryogenesis. *The Plant Cell* **14**, 3119–3132.

Fu S, Scanlon MJ. 2004. Clonal analysis of EMPTY PERICARP2 reveals non redundant functions of the duplicated HEAT SHOCK FACTOR BINDING PROTEINs during maize shoot development. *Genetics* **167,** 1381–1394.

Fujimoto R, Sasaki T, Ishikawa R, Osabe K, Kawanabe T, Dennis ES. 2012. Molecular mechanisms of epigenetic variation in plants. *International Journal of Molecular Sciences* **13**, 9900-9922.

Gager Stuart C. 1907. An account of the glands in the endosperm of Zea mays. *Bullettin of Torrey Botanical Club* **34,** 125-134.

Gehring M, Henikoff S.2007. DNA methylation dynamics in plant genomes. *Biochimica et Biophysica Acta* **1769**, 276-286.

Gehring M, Bubb KL, Henikoff S. 2009a. Extensive demethylation of repetitive elements during seed development underlies gene imprinting. *Science* **324**,1447–51.

Gehring M, Choi Y, Fischer RL. 2004. Imprinting and seed development. *Plant Cell* **16**, S203–S213.

Gehring M, Henikoff S. 2008. DNA methylation and demethylation in *Arabidopsis*. The Arabidopsis Book, 6:e01002

Gehring M, Huh JH, Hsieh TF, Penterman J, Choi Y, Harada JJ, Goldberg RB, Fischer RL. 2006. DETEMER DNA glycosylase establishes *MEDEA* polycomb gene self-imprinting by allele-specific demethylation. *Cell* **124**, 495–506.

Gehring M, Missirian V, Henikoff S. 2011. Genomic analysis of parent-of-origin allelic expression in *Arabidopsis thaliana* seeds. *PLoS ONE* **6**, e23687.

Gehring M, Reik W, Henikoff S. 2009b. DNA demethylation by DNA repair. *Trends in Genetics* **25,** 82–90.

Giegerich R, Meyer F and Schleiermacher C. 1996. GeneFisher-Software support for the detection of postulated genes. *Proceedings of International Conference on Intelligent Systems for Molecular Biology* **4**, 68-77

Gong Z, Morales-Ruiz T, Ariza RR, Rolda´ n-Arjona T, David L, Zhu J-K. 2002. *ROS1*, a repressor of transcriptional gene silencing in *Arabidopsis*, encodes a DNA glycosylase/lyase. *Cell* **111**, 803–814.

Grossniklaus U, Vielle-Calzada J-P, Hoeppner MA, Gagliano W. 1998. Maternal control of embryogenesis by *MEDEA,* a Polycomb

group gene in *Arabidopsis. Science* **280,** 446–450.

Guignard L. 1901. La double fecondation dans le mais. *Journal de Botanique* **15**, 37-50.

Guitton AE, Page DR, Chambrier P, Lionnet C, Faure JE, Grossniklaus U, Berger F. 2004. Identification of new members of Fertilisation Independent Seed Polycomb Group pathway involved in the control of seed development in *Arabidopsis thaliana. Development* **131**, 2971–2981.

Gutierrez-Marcos JF, Costa LM, Dal Pra' M, Scholten S, Kranz E, etal. 2006. Epigenetic asymmetry of imprinted genes in plant gametes. *Nature Genetics* **38,** 876–878.

Gutierrez-Marcos JF, Dickinson HG. 2012. Epigenetic reprogramming in plant reproductive lineages. *Plant & Cell Physiology* **53** (5), 817-823.

Haag JR, Pikaard CS. 2011. Multisubunit RNA polymerases IV and V: Purveyors of non-coding RNA for plant gene silencing. *Nature Reviews Molecular Cell Biology* **12***,* 483–492.

Hall TA. 1999. BioEdit: a user-friendly biological sequence alignment editor and analysis program for Windows 95/98/NT. *Nucleic Acids Symposium Series* **41**, 95-98.

Harz CO. 1885. Zea. Landwirtschaftliche Samenkunde. pp.1237-1243.

He G, Elling AA, Deng XW. 2011. The epigenome and plant development. *The Annual Review of Plant Biology* **62**, 411-435.

He XJ, Hsu YF, Zhu S, Wierzbicki A, Pontes O, Pikaard CS, Liu HL, Wang CS, Jin H, Zhu J. 2009. An effector of RNA-directed

DNA methylation in *Arabidopsis* is an ARGONAUTE 4- and RNA-binding protein. *Cell* **137**, 498–508.

Hedges SB, Dudley J, Kumar S. 2006. TimeTree: A public knowledge-base of divergence times among organisms. *Bioinformatics* **22,** 2971–2972 .

Hermon P, Srilunchang KO, Zou J, Dresselhaus T, Danilevskaya ON. 2007. Activation of the imprinted Polycomb Group *Fie1* gene in maize endosperm requires demethylation of the maternal allele. *Plant Molecular Biology* **64,** 387–395.

Hsieh TF, Ibarra CA, Silva P, Zemach A, Eshed-Williams L, et al. 2009. Genome-wide demethylation of *Arabidopsis* endosperm. *Science* **324**, 1451–54

Hsieh TF, Shin J, Uzawa R, Silva P, Cohen S, Bauer M, Hashimoto M, Kirkbride R, Harada J,Zilberman D, Fischer R. 2011. Regulation of imprinting gene expression in *Arabidopsis* endosperm. *Proceedings of the National Academy Sciences USA* **108**, 1755–1762.

Huang BQ, Russell SD. 1992. Female germ unit: Organization, isolation, and function. *International Review of Cytology* **140**, 233–292.

Huang BQ, and Sheridan WF. 1994. Female gametophyte development in maize: microtubular organization and embryo sac polarity. *Plant Cell* **6**, 845-861.

Huelsenbeck JP and Ronquist F. 2001. MRBAYES: Bayesian inference of phylogenetic trees. *Bioinformatics* **17** (8), 754-755.

Ibarra CA, Feng X, Schoft VK et al. 2012. Active DNA demethylation in plant companion cells reinforces transposon methylation in gametes. *Science* **337**, 1360-1364.

Ikeda Y. 2012. Plant imprinted genes identified by genome-wide approaches and their regulatory mechanisms. *Plant and Cell Physiology* **53** (5), 809-816.

Jahnke S, Scholten S. 2009. Epigenetic resetting of a gene imprinted in plant embryos. *Current Biology* **19**, 1677–1681.

Johnson MA, Bender J. 2009. Reprogramming the epigenome during germline and seed development. *Genome Biology* **10**, 232.

José-Estanyol M, Lopez-Ribera I, Bastida M, Jarhmann T, Sanchez-Pons N, Becerra C, Vicient CM, Puigdomenech P. 2009. Genetic, molecular and cellular approaches to the analysis of maize embryo development. *The International Journal of Developmental Biology*. **53**, 1649-1654.

Jullien PE, Kinoshita T, Ohad N, Berger F. 2006. Maintenance of DNA methylation during the *Arabidopsis* life cycle is essential for parental imprinting. *Plant Cell* **18,** 1360–1372.

Kapoor A, Agius F, Zhu JK. 2005. Preventing transcriptional gene silencing by active DNA demethylation. *FEBS Letters* **579**, 5889–98

Kiesselbach TA. 1949. The Structure and Reproduction of Corn. Univ. Nebraska Coll. Agric., *Agricultural Experiment Station Research Bullettin* **161,** 1-96.

Kinoshita T, Miura A, Choi Y, Kinoshita Y, Cao X, Jacobsen SE, Fischer RL, Kakutani T. 2004. Of one-way control of *FWA* imprinting in *Arabidopsis* endosperm by DNA methylation. *Science* **303,** 521–523.

Kiyosue T, Ohad N, Yadegari R, Hannon M, Dinneny J, Wells D, Katz A, Margossian L, Harada JJ, Goldberg RB, Fischer RL. 1999. Control of fertilization-independent endosperm development by the

MEDEA polycomb gene in *Arabidopsis*. *Proceedings of the National of Academy of Sciences, USA* **96**, 4186–4191.

Köhler C, Page DR, Gagliardini V, Grossniklaus U. 2005. The *Arabidopsis thaliana* MEDEA Polycomb group protein controls expression of *PHERES1* by parental imprinting. *Nature Genetics* **37,** 28–30.

Köhler C, Hennig L, Spillane C, Pien S, Gruissem W, Grossniklaus U. 2003. The Polycomb-group protein MEDEA regulates seed development by controlling expression of the MADS-box gene *PHERES1*. *Genes & Development* **17,** 1540–1553.

Köhler C, Hennig L, Bouveret R, Gheyselinck J, Grossniklaus U, Gruissem W. 2003. *Arabidopsis* MSI1 is a component of the MEA/FIE polycomb group complex and required for seed development. *Embo Journal* **22**, 4804–4814.

Lauria M, Rupe M, Guo M, Kranz E, Pirona R, Viotti A, Lund G. 2004. Extensive maternal DNA hypomethylation in the endosperm of *Zea mays*. *Plant Cell* **16,** 510–522.

Law JA, Jacobsen SE. 2010. Establishing, maintaining and modifying DNA methylation patterns in plants and animals. *Nature Reviews Genetics* **11**, 204–220.

Le Trionnaire G,Twell D. 2010. Small RNAs in angiosperm gametophytes: from epigenetics to gamete, development. *Genes & Development* **24**, 1081–1085 .

Leutwiler LS, Hough-Evans BR, Meyerowitz EM. 1984. The DNA of *Arabidopsis thaliana*, *Molecular Genetics and Genomics* **194**, 15–23.

Lisch D. 2009. Epigenetic regulation of transposable elements in plants. *Annual Review of Plant Biology* **60**, 43-66.

Livak KJ, Schmittgen TD. 2001. Analysis of relative gene expression data using real-time quantitative PCR and the 2−ΔΔCt method. *Methods* **25**, 402–408.

Luo M, Bilodeau P, Dennis ES, Peacock WJ, Chaudhury A. 2000. Expression and parent-of-origin effects for *FIS2, MEA,* and *FIE* in the endosperm and embryo of developing *Arabidopsis* seeds. *Proceedings of the National Academy of Sciences USA* **97,** 10637–10642.

Luo M, Bilodeau P, Koltunow A, Dennis ES, Peacock WJ, Chaudhury AM. 1999. Genes controlling fertilization-independent seed development in *Arabidopsis thaliana. Proceedings of the National Academy of Sciences, USA* **96,** 296–301.

Migicovsky Z, Kovalchuk I. 2012. Epigenetic modifications during angiosperm gametogenesis. *Frontiers in Plant Science*. **3**: doi: 10.3389/fpls.2012.00020.

Maheshwari P**.** 1950. An introduction to the embryology of angiosperms (New York: McGraw-Hill).

Mansfield SG, Briarty LG, Erni S. 1990. Early embryogenesis in *Arabidopsis thaliana*. I. The mature embryo sac. *Canadian Journal of Botany* **69**, 447-460.

Martienssen RA, Colot V. 2001. DNA methylation and epigenetic inheritance in plants and filamentous fungi. *Science* **293**, 1070–74.

Matzke M, Kanno T, Daxinger L, Huettel B, Matzke AJM. 2009. RNA-mediated chromatin-based silencing in plants. *Current Opinion in Cell Biology* **21***,* 367–376.

Mok YG, Uzawa R, Lee J, Weiner GM, Eichman BF, Fischer RL, Huh JH. 2010. Domain structure of the DEMETER 5-methylcytosine

DNA glycosylase. *Proceedings of the National Academy of Sciences USA* **107** (45), 19225-19230.

Morales-Ruiz T, Ortega-Galisteo AP, Ponferrada-Marin MI, Martinez- Macias MI, Ariza RR, Roldan-Arjona T. 2006. *DEMETER* and *REPRESSOR OF SILENCING1* encode 5-methylcytosine DNA glycosylases. *Proceedings of the National Academy of Sciences USA* **103,** 6853–6858.

Mosher RA, Melnyk CW. 2010. siRNAs and DNA methylation: seedy epigenetics. *Trends in Plant Science* **15,** 204–210.

Nash HM, Bruner SD, Scharer OD, Kawate T, Addona TA, Spooner E, Lane WS, Verdine GL. 1996. Cloning of a yeast 8-oxoguanine DNA glycosylase reveals the existence of a base-excision DNA-repair protein superfamily. *Current Biology* **6,** 968–980.

Neuffer MG, Sheridan WF. 1980. Defective kernel mutants of maize. I. Genetic and lethality studies. *Genetics* **95,** 929–944.

Ohad N, Margossian L, Hsu YC, Williams C, Repetti P, Fischer RL. 1996. A mutation that allows endosperm development without fertilization. *Proceedings of the National Academy Sciences USA* **93,** 5319–5324.

Ohad N, Yadegari R, Margossian L, Hannon M, Michaeli D, Harada JJ, Goldberg RB, Fischer RL. 1999. Mutations in *FIE*, a WD polycomb group gene, allow endosperm development without fertilization. *The Plant Cell* **11**, 407–416.

Ono A, Yamaguchi K, Fukada-Tanaka S, Terada R, Mitsui T, Iida S. 2012. A null mutation of *ROS1a* for DNA demethylation in rice is not transmittable to progeny. *Plant Journal* **71**(4), 564–574.

Opsahl-Ferstad HG, Le Deunff E, Dumas C, Rogowsky PM. 1997. *ZmEsr*, a novel endosperm-specific gene expressed in a restricted

region around the maize embryo. *Plant Journal* **12,** 235–246.

Ortega-Galisteo AP, Morales-Ruiz T, Ariza RR, Rolda´ n-Arjona, T. 2008. *Arabidopsis* DEMETER-LIKE proteins DML2 and DML3 are required for appropriate distribution of DNA methylation marks. *Plant Molecular Biology* **67,** 671–681.

Penterman J, Uzawa R, Fischer RL. 2007a. Genetic interactions between DNA demethylation and methylation in *Arabidopsis*. *Plant Physiology* **145**, 1549-1557.

Penterman J, Zilberman D, Huh JH, Ballinger T, Henikoff S, Fischer RL. 2007b. DNA demethylation in the *Arabidopsis* genome. *Proceedings of the National Academy of Sciences USA* **104**, 6752–6757.

Portereiko MF, Lloyd A, Steffen JG, Punwani JA, Otsuga D, Drews GN. 2006. *AGL80* is required for central cell and endosperm development in *Arabidopsis*. *The Plant Cell* **18**,1862-1872.

Randolph LF. 1936. Developmental morphology of the caryopsis in maize. *Journal of Agricultural Research* **53,** 881-916.

Reiser L, Fisher RL. 1993. The ovule and the embryo sac. *The Plant Cell* **5,** 1291-1301.

Roldan-Arjona T, Ariza RR. 2009. DNA demethylation. In Grosjean H. (ed.), DNA and RNA modification enzymes: comparative structure, mechanism, functions, cellular interactions and evolution. *Landes Bioscience,* Austin, TX, pp. 149–161.

Rowlee WW, Doherty MW. 1898. The histology of the embryo of Indian corn. *Bullettin of Torrey Botanical Club* **25,** 311-315.

Russell SD. 1979. Fine structure of megagametophyte development in *Zea mays. Canadian Journal of Botany* **57,** 1093-1110.

Russell SD. 1993. The egg cell: development and role in fertilization and early embryogenesis. *The Plant Cell* **5,** 1349-1359.

Saze H. 2008. Epigenetic memory transmission through mitosis and meiosis in plants. *Seminars in Cell Developmental Biology* **19,** 527–536.

Schoft, V.K., Chumak, N., Choi, Y. et al. 2011. Function of DEMETER DNA glycosylase in the *Arabidopsis thaliana* male gametophyte. *Proceedings of the National Academy of Sciences USA* **108**, 8042–8047.

Shen Y, Li C, McCarty DR, Meeley R, Tan B. 2013. *Embryo defective12* encodes the plastid initiation factor 3 and is essential for embryogenesis in maize. *The Plant Journal* **74**, 792-804.

Sheridan WF, Neuffer MG. 1980. Defective kernel mutants of maize II. Morphological and embryo culture studies. *Genetics* **95**, 945–960.

Sheridan WF, Neuffer MG. 1982. Maize developmental mutants. Embryos unable to form leaf primordia. *Journal of Heredity* **73,** 318-329.

Slotkin RK, Vaughn M, Borges F, Tanurdzic M, Becker JD, Feijo JA, Martienssen RA. 2009. Epigenetic reprogramming and small RNA silencing of transposable elements in pollen. *Cell* **136,** 461-472.

Soppe WJJ, Jacobsen SE, Alonso-Blanco C, Jackson JP, Kakutani T, Koornneef M, Peeters AJM. 2000. The late flowering phenotype of *fwa* mutants is caused by gain-of-function epigenetic alleles of a homeodomain gene. *Molecular Cell* **6,** 791–802.

Springer PS, McCombie WR, Sundaresan V, Martienssen RA. 1995. Gene trap tagging of PROLIFERA, an essential MCM2-3-5-like

gene in *Arabidopsis*. *Science* **268,** 877–880.

Swanson WJ, Vacquier VD. 2002. The rapid evolution of reproductive proteins. *Nature Reviews Genetics* ***3,***137–144.

Thompson RD, Hueros G, Becker HA, Maitz M. 2001. Development and functions of seed transfer cells. *Plant Science* **160,** 775–783.

Timothy L. Bailey, Mikael Bodén, Fabian A. Buske, Martin Frith, Charles E. Grant, Luca Clementi, Jingyuan Ren, Wilfred W. Li, William S. Noble. 2009. MEME SUITE: tools for motif discovery and searching. *Nucleic Acids Research* **37**, W202-W208.

Tiwari S, Schulz R, Ikeda Y, Dytham L, Bravo J, et al. 2008. *MATERNALLY EXPRESSED PAB C-TERMINAL*, a novel imprinted gene in *Arabidopsis,* encodes the conserved C-terminal domain of polyadenylate binding proteins. *Plant Cell* **20**, 2387-2398.

True Rodnet H. 1893. On the development of the caryopsis. *Botanical Gazette* **18,** 212-226.

Tzafrir I, Dickerman A, Brazhnik O, Nguyen Q, Mcelver J, Frye C, Patton D, Meinke D. 2003. The *Arabidopsis* seed genes project. *Nucleic Acids Reearch* **31**, 90-93.

Untergrasser A, Cutcutache I, Koressaar T, Ye J, Faircloth BC, Remm M, Rozen SG. 2012 Primer3 - new capabilities and interfaces. *Nucleic Acids Research* **40**(15), e115.

Uwer U, Willmitzer L, Altmann T. 1998. Inactivation of a glycyl-tRNA synthetase leads to an arrest in plant embryo development. *The Plant Cell* **10**, 1277–1294.

Vernoud V, Hajduch M, Khaled AS, Depege N, Rogowsky MP. 2005. Maize embryogenesis. *Maydica* **50,** 469-484.

Vielle-Calzada JP, Thomas J, Spillane C, Coluccio A, Hoeppner MA, Grossniklaus U. 1999. Maintenance of genomic imprinting at the *Arabidopsis medea* locus requires zygotic *DDM1* activity. *Genes & Development* **13,** 2971–2982.

Vollbrecht E, Hake S. 1995. Deficiency analysis of female gametogenesis in maize. *Developmental Genetics* **16**, 44-63.

Vroemen CW, Mordhorst AP, Albrecht C, Kwaaitaal MA, de Vries SC. 2003. The *CUP-SHAPED COTYLEDON3* gene is required for boundary and shoot meristem formation in *Arabidopsis*. *The Plant Cell* **15,** 1563-1577.

Waters AJ, Makarevitch I, Eichten SR, Swanson-Wagner RA, Yeh C, Xu W, Schnable PS, Vaughn MW, Gehring M, Springer NM. 2011. Parent-of-origin effects on gene expression and DNA methylation in the maize endosperm. *Plant Cell* **23**(12), 4221-4233.

Weatherwax P. 1930. The endosperm of *Zea* and *Coix*. *American Journal of Botany* **17**, 371-380.

Webb MC, Gunning BES. 1990. Embryo sac development in *Arabidopsis thaliana*: Megasporogenesis, including the microtubular cytoskeleton. *Sexual Plant Reproduction* **3,** 244-256.

Wen S, Wen N, Pang J, et al. 2012. Structural genes of wheat and barley 5-methylcytosine DNA glycosylases and their potential applications for human health. *Proceedings of the National Academy of Sciences USA* **109** (50), 20543–20548.

Willemse MTM, Van Went JL. 1984. The female gametophyte. In embryology of angiosperms, B.M. Johri, ed (Berlin: Springer-Verlag), pp. 159–196.

Wolff P, Weinhofer I, Seguin J, Roszak P, Beisel C, Donoghue M, Spillane C, Nordborg M, Rehmseier M, Kohler C. 2011. High-

resolution analysis of parent-of-origin allelic expression in the *Arabidopsis* endosperm. *PLoS Genetetics* **7**, e1002126.

Yadegari R, Drews GN. 2004. Female gametophyte development. *The Plant Cell* **16**, S133-S141.

Zemach, A., Kim, M.Y., Silva, P., Rodrigues, J.A., Dotson, B., Brooks, M.D. and Zilberman, D. 2010 Local DNA hypomethylation activates genes in rice endosperm. *Proceedings of the National Academy of Sciences USA* **107**, 18729-18734.

Zhang M, Zhao H, Xie S, Chen J, Xu Y, Wang K, Zhao H, Guan H, Hu X, Jiao Y, Song W, Lai J. 2011. Extensive, clustered parental imprinting of protein-coding and noncoding RNAs in developing maize endosperm. *Proceedings of the National Academy of Sciences USA* doi: 10.1073/pnas.1112186108

Zhu J, Kapoor A, Sridhar VV, Agius F, Zhu JK. 2007. The DNA glycosylase/lyase ROS1 functions in pruning DNA methylation patterns in *Arabidopsis*. *Current Biology* **17,** 54–59.

Zhu JK. 2009. Active DNA demethylation mediated by DNA glycosylases. *Annual Review of Genetics* **43,** 143–166.

ACKNOWLEDGMENTS

I would like to express my gratitude to my supervisor, Dr. Massimo Labra, whose support, help and advice were of utmost importance during these years.

I am also particularly thankful to Dr. Andrea Gallavotti for giving me the opportunity to work in his lab during the last year. I am really grateful for his assistance and for all the things he taught me. His expertise considerably added to my graduate experience.